CHARACTERIZATION OF COMPONENTS INVOLVED IN TOMATO INNATE IMMUNITY AGAINST BACTERIAL SPECK DISEASE

A Dissertation

Presented to the Faculty of the Graduate School

of Cornell University

in Partial Fulfillment of the Requirements for the Degree of

Doctor of Philosophy

by

Simon Schwizer

January 2017

CHARACTERIZATION OF COMPONENTS INVOLVED IN TOMATO INNATE IMMUNITY AGAINST BACTERIAL SPECK DISEASE

Simon Schwizer, Ph.D.

Cornell University 2017

The Pti1 kinase was identified from a reverse genetic screen as contributing to pattern-triggered immunity (PTI) against the bacterial speck pathogen *Pseudomonas syringae* pv. *tomato* (*Pst*). This was unexpected because Pti1 was originally identified as an interactor of the Pto kinase that confers effector-triggered immunity to *Pst* strains secreting either of the type III effectors AvrPto or AvrPtoB. A hairpin-Pti1 (hpPti1) construct was developed and used to generate stable transgenic tomato lines with reduced expression of *Pti1*. These hpPti1 plants were more susceptible to infection with *Pst* strains lacking both AvrPto and AvrPtoB and had reduced transcript accumulation of PTI-associated genes compared to wild-type plants. The hpPti1 plants produced less reactive oxygen species (ROS), but showed no difference in mitogen-activated protein kinase (MAPK) activation in response to two flagellin-derived peptides. Synthetic *Pti1* genes designed to avoid silencing were transiently expressed in hpPti1 plants and restored the ability of the plants to produce wild-type levels of ROS. This work identifies a new component of PTI in tomato which, because it affects ROS production but not MAPK signaling, appears to act early in the immune response. We speculate that Pti1 was identified originally as a Pto interactor because it may interact with a Pto-like kinase that plays a role in PTI.

We identified several putative receptors in tomato that consist of extracellular

This dissertation was completed in August 2016.

malectin-like domains and intracellular kinase domains that show high similarity to Pto. Interestingly, the starting sequence of Pto and some of its family members is conserved in two of the identified malectin-like proteins, Mal1 and Mal2, at approximately the beginning of their kinase domains and is not found in any other predicted tomato protein. Silencing the orthologs of *Mal1* and *Mal2* in *Nicotiana benthamiana* resulted in compromised induction of immune responses and thus increased susceptibility to *Pst* infection. We found that AvrPtoB interacts with the kinase domains of both Mal1 and Mal2 and we speculate that these putative receptors are targeted by AvrPtoB to suppress plant immunity. Furthermore, we propose that Pto evolved from the kinase domain of either Mal1 or Mal2 (or a progenitor protein) to sense the presence of AvrPtoB inside the plant cell and induce robust defense responses.

We describe a rapid method to detect two major forms of fatty acylation, N-myristoylation and S-acylation, of candidate proteins using alkyne fatty acid analogs coupled with click chemistry. We applied our approach to confirm and decisively demonstrate that AvrPto, Pto, and the FLS2 receptor all undergo plant-mediated fatty acylation. In addition to providing a means to readily determine fatty acylation, particularly myristoylation, of candidate proteins, this method is amenable to a variety of expression systems. We demonstrate this using both Arabidopsis protoplasts and stable transgenic Arabidopsis plants and we leverage Agrobacterium-mediated transient expression in *Nicotiana benthamiana* leaves as a means for high-throughput evaluation of candidate proteins. The metabolic labeling approach leveraging alkyne fatty acid analogs and click chemistry described here has the potential to provide mechanistic details of the molecular tactics used at the host plasma membrane in the battle between plants and pathogens.

BIOGRAPHICAL SKETCH

Simon Schwizer received his Master of Science in Plant Sciences from the University of Zurich in Switzerland where he worked in the laboratory of Dr. Beat Keller on the characterization of barley *Mla* genes that confer resistance to barley powdery mildew. Following the completion of his degree, Simon worked as a research assistant at the Sainsbury Laboratory in Norwich, United Kingdom under the supervision of Dr. Sophien Kamoun to study the ability of *Phytophthora infestans* effector proteins to suppress plant immune responses. He then moved to the United States and joined the laboratory of Dr. Gregory Martin at the Boyce Thompson Institute in Ithaca, New York to work as a research assistant and help further characterize the *Pseudomonas syringae* effector protein AvrPtoB. Simon decided to continue his research under the supervision of Dr. Martin and pursue a Doctor of Philosophy at Cornell University. His work focused on elucidating the function of a tomato kinase involved in resistance to *P. syringae* and identifying putative receptor proteins that seem to be targeted by one of its effectors.

ACKNOWLEDGMENTS

I would like to thank my advisor Dr. Gregory Martin for giving me the opportunity to work in his laboratory and supervising my research over these past years. I am grateful to Dr. Alan Collmer and Dr. Michael Mazourek for serving on my special committee and for their help and advice. I am thankful to Dr. Johannes Mathieu for being my mentor during my first year in the Martin laboratory and teaching me the skills needed to successfully pursue my research interests. I would also like to thank the numerous other members of the Martin laboratory for their help, collaboration, and company over the years.

CONTENTS

CHAPTER 1

STRATEGIES TO IMPROVE THE GENETIC DISEASE RESISTANCE OF CROP PLANTS

1.1 Introduction

Green plants are the primary producers of energy that sustain all animal life on earth. As the human population is increasing in the coming decades we will need to produce an ever growing amount of food. In addition, as living standards in many developing countries increase meat consumption will rise. This will require increased production of grains because feeding grain to animals and consuming the meat is much less efficient than consuming the grain directly. Arable land is limited because not all land is suitable for agricultural use and climate change with its accompanying changes in temperature and rainfall will affect the suitability of many regions. To produce sufficient (and cheap) food for the high living standards we have come to expect crops are grown in large-scale monocultures which enables efficient mechanized planting and harvesting. This modern agriculture depends on fertilizers and pesticides because intense farming depletes soil of nutrients and large fields of genetically uniform crops are susceptible to diseases. Nitrogen and phosphorus are the two main components in fertilizers. Nitrogen production is very energy intensive and phosphorus availability on earth is limited, making fertilizers a precious commodity. Chemical pesticides on the other hand can be harmful to farmers, consumers, and the environment. Therefore, there is not only a growing need to increase the amount of food produced, but to do so in a sustainable way that minimizes the impact on our environment. One portion of the larger problem can be addressed by reducing crop losses due to plant diseases while minimizing the use of potentially harmful agrochemicals. This goal is best achieved using a

combination of cultural practices and genetic resistance that protects crop plants from potentially devastating diseases.

Traditionally, resistance breeding has involved introgression of major resistance (R) genes that confer complete protection against specific pathogen strains. Most R genes encode nucleotide-binding leucine-rich repeat proteins that either directly or indirectly recognize secreted pathogen proteins called effectors (Dodds & Rathjen, 2010). These effectors are virulence factors that in the absence of cognate R genes interfere with plant immune functions, enabling disease and thus increase pathogen fitness (Dou & Zhou, 2012). The presence of R genes exerts a strong evolutionary pressure on the pathogen to evade recognition, thereby becoming virulent again (McDonald & Linde, 2002). This leads to boom-and-bust cycles where a new R gene is introduced and is rapidly adopted on a large scale because of its beneficial effects, temporarily reducing the occurrence of the disease. But sooner or later a pathogen strain evolves that evades or otherwise overcomes the resistance, thus giving it an enormous fitness advantage which leads to the rapid spread of that strain, rendering the R gene useless (McDonald & Linde, 2002). This arms race between plant and pathogen is illustrated by allelic series of R genes that have been described in some plants species. Examples in crop plants include the barley *Mla* locus which contains at least 28 full-length alleles that can recognize different isolates of the barley powdery mildew pathogen *Blumeria graminis* f. sp. *hordei* and appear to be under diversifying selection (Seeholzer et al., 2010). Another example is the flax L locus with 12 cloned alleles that confer resistance to isolates of the flax rust pathogen *Melampsora lini* carrying cognate effector genes (Ellis et al., 2007). In natural populations of the model plant *Arabidopsis thaliana* the highly polymorphic *RPP13* locus confers resistance to isolates of the oomycete pathogen *Hyaloperonospora arabidopsidis* (Rose et al.,

2004). The pathogen population contains the matching *ATR13* locus that encodes an allelic series of effector proteins and both loci are under diversifying selection as expected for an arms race scenario in which the pathogen accumulates mutations in its effector protein to evade recognition and the plant responds with corresponding mutations in the R protein to maintain pathogen recognition (Allen et al., 2004; Rose et al., 2004; Coates & Beynon, 2010).

To prolong the useful lifespan of an R gene or even prevent its bust various strategies have been proposed, such as stacking multiple R genes in a single cultivar, producing near-isogenic lines that vary only in the R gene and employ them in a spatial and/or temporal rotation, or growing mixtures of these near-isogenic lines to create a heterogeneous R gene population in an otherwise homogeneous crop field (McDonald & Linde, 2002). The aim with these different strategies is to either force the pathogen to simultaneously evolve evasive mutations in its effectors to multiple R proteins, which is far less likely than an evasive mutation to only one R protein, or present the pathogen population with changing evolutionary pressures, thereby reducing the chances that a given R gene will be overcome (McDonald & Linde, 2002).

Different approaches exist that may provide more durable disease resistance but are more difficult to transfer into elite breeding lines or may not provide complete resistance against certain pathogen isolates like major R genes. Quantitative resistance loci (QRLs) can provide durable resistance to multiple isolates of a pathogen but because they consist of multiple genes with additive effects that may be spread over several chromosomes they are more difficult to combine into an elite breeding line (Poland et al., 2009). A single gene that is part of a QRL may not provide full resistance but it can significantly reduce disease severity. The *Lr34* gene from wheat conferring resistance to the wheat leaf rust pathogen *Puccinia*

triticina was cloned a few years ago and found to encode an ABC transporter that presumably functions in delivering antimicrobial compounds into the extracellular space (Krattinger et al., 2009). Even though *lr34* mutant lines are not completely susceptible and the *Lr34* gene therefore only confers partial resistance, the effect is significant. Many wheat varieties worldwide contain *Lr34* and the resistance it confers has been durable in the field for over 50 years (Krattinger et al., 2009). In addition to leaf rust, *Lr34* also confers partial resistance to isolates of the stripe rust pathogen *P. striiformis* and to *B. graminis* f. sp. *tritici* (McIntosh, 1992; Singh, 1992; Spielmeyer et al., 2005), thus providing an important source of partial resistance to multiple important wheat pathogens (Krattinger et al., 2009).

A different approach that was proposed is the use of so-called susceptibility (S) genes which encode proteins that aid in disease establishment and pathogen proliferation (Gust et al., 2010; Gawehns et al., 2012). These genes (or proteins) serve regular functions in plant life but are exploited by the pathogen to promote disease. A classic example is the *Mlo* gene in barley which encodes a plasma membrane protein that modulates vesicle-associated processes and might be required for haustoria formation of barley powdery mildew (Büschges et al., 1997; Panstruga, 2005). The *mlo* mutation has been used in barley cultivars in the field for close to 40 years and has provided durable powdery mildew resistance (Jorgensen, 1992). One of the disadvantages of the S gene approach is that mutating important plant genes can have negative effects. While the *mlo* mutation provides resistance to powdery mildew, an obligate biotrophic pathogen, it also enhances susceptibility to the hemibiotrophic rice blast pathogen *Magnaporthe grisea* and the necrotrophic fungus *Bipolaris sorokiniana*, which causes leaf spot blotch disease (Jarosch et al., 1999; Kumar et al., 2001). Therefore, whether the use of the *mlo* mutation is advisable depends on the predominant pathogens in a given region and it should

be avoided in areas where rice is grown in close proximity.

Another example of plant proteins that promote disease susceptibility are the SWEET sucrose efflux carriers that export sucrose assimilated in leaf mesophyll cells from phloem parenchyma cells into the phloem apoplasm, a key step for subsequent phloem loading (Chen et al., 2010; Chen, 2014). Biotrophic and hemibiotrophic pathogens depend on living plant tissue for reproduction and sucrose availability in the apoplast might represent an important energy source for bacterial pathogens. In rice, *OsSWEET11* is induced by the transcriptional activator-like (TAL) effector PthXo1 from *Xanthomonas oryzae* pv. *oryzae* (*Xoo*) which binds to the promoter region of *OsSWEET11* and causes its expression in mesophyll cells (Chu et al., 2006; Yang et al., 2006; Yuan et al., 2009). It is thought that expression of this gene, which is required for *Xoo* growth (Yang et al., 2006; Yuan et al., 2009), leads to export of sucrose into the apoplastic space surrounding the mesophyll cells, creating a more hospitable environment for *Xoo* proliferation (Chen, 2014). Similarly, *OsSWEET14* is induced by the TAL effectors AvrXa7 and PthXo3 to support *Xoo* growth (Antony et al., 2010; Chen et al., 2010). Because *SWEET* genes serve important roles in sucrose transport, loss-of-function mutations would likely affect plant growth and development and have negative consequences on crop yield. Given that the promoter binding sites of TAL effectors can be predicted (Boch et al., 2009), those promoter regions can be modified to abolish effector binding and thus prevent transcriptional activation of the target gene (Schornack et al., 2013). Indeed, the binding sites of AvrXa7 and PthXo3 in the *OsSWEET14* promoter were mutated, resulting in rice plants resistant to *Xoo* infection (Li et al., 2012).

In addition to possible negative effects, *S* genes are difficult to identify because of their recessive nature and potential functional redundancy. It was suggested

that pathogen effectors could be used as molecular probes to identify virulence targets that are modified by the pathogen to promote disease (Gawehns et al., 2012). Given that plant pathogens contain dozens (bacteria) to hundreds (fungi and oomycetes) effector proteins and that only a comparatively small number of effector targets has been identified (Dou & Zhou, 2012; Macho & Zipfel, 2015), this approach is likely only feasible for a limited number of problematic diseases. As mentioned earlier, null mutations in identified *S* genes might have deleterious effects and it might be necessary to engineer the protein under investigation so that it can no longer be modified by the effector but still fulfill its function in the required plant processes.

These different approaches, employing *R* genes, introgressing QRLs, and taking advantage of *S* genes, have in common that they usually confer resistance to only specific pathogen species, sometimes only certain strains or isolates. Therefore it is often only feasible to breed for resistance to the most important and devastating diseases, leaving crops vulnerable to various other pests that require repeated pesticide application. An alternative strategy is to employ plasma membrane-localized pattern recognition receptors (PRRs) that can detect conserved microbe-associated molecular patterns such as components of the bacterial flagellum or the fungal cell wall (Zipfel, 2014). Some of the best-studied examples are FLS2 from Arabidopsis which recognizes a portion of flagellin, an important flagellum building block, and CERK1/CEBiP from Arabidopsis and rice which bind chitin oligomers that comprise the cell wall in fungi (Kaku et al., 2006; Miya et al., 2007; Boller & Felix, 2009). Numerous of these receptors exist in a single plant species which together make most plants resistant to most potential pathogens. While some receptors such as FLS2 are evolutionary ancient and widely conserved in the plant kingdom (Boller & Felix, 2009), others are specific to certain plant families.

The EFR receptor that is able to sense the presence of bacterial elongation factor Tu is found only in the brassica family and it is thought to have evolved more recently (Zipfel et al., 2006; Li et al., 2009). Transfer of EFR from the model plant Arabidopsis to members of the solanaceae family enhanced the resistance of those plants to different bacterial pathogens (Lacombe et al., 2010). For example, tomato plants expressing *EFR* were more resistant to the bacterial wilt pathogen *Ralstonia solanacearum* (Lacombe et al., 2010). Even though genetically modified crop plants are poorly accepted by the public, this approach of moving PRRs from other plant families into important crop species has the potential to significantly enhance broad-spectrum disease resistance.

Research in recent years has revealed that PRR activation and regulation mechanisms are complex processes that carefully modulate defense signaling (Macho & Zipfel, 2014). PRRs exist in receptor complexes at the plasma membrane that consist of various proteins. For example, it was found that in Arabidopsis FLS2 associates with BAK1, which functions as a co-receptor and is required for full flagellin-induced pattern-triggered immunity (PTI) (Chinchilla et al., 2007). Both FLS2 and BAK1 have extracellular leucine-rich repeat (LRR) domains that function in protein-protein interactions, but whereas FLS2 contains 28 such repeats, BAK1 contains only four LRRs (Boller & Felix, 2009). Because of this truncated binding domain it was thought that BAK1 functions in a regulatory role. Recent work showed that binding of flg22 (the flagellin peptide capable of inducing defense responses in many plants) to FLS2 leads to rapid FLS2-BAK1 heterodimer formation (Schulze et al., 2010). Co-crystallization of the extracellular domains of the two proteins bound to flg22 revealed that the peptide is bound by both receptor domains and thus stabilizes the heterodimer (Sun et al., 2013). Following flg22 binding and association of the two receptors, the intracellular kinase

domains of FLS2 and BAK1 are phosphorylated, which activates downstream signaling (Schulze et al., 2010).

However, this process involves several accessory proteins, chief among them BIK1. BIK1 is a receptor-like cytoplasmic kinase (RLCK) that constitutively associates with the FLS2 receptor complex (Lu et al., 2010; Zhang et al., 2010). Dimerization of FLS2 and BAK1 leads to phosphorylation of BIK1 by BAK1 and BIK1 phosphorylates FLS2 and BAK1 in turn, followed by disassociation of BIK1 from the receptor complex (Lu et al., 2010; Zhang et al., 2010). Other RLCKs of the PBS1-like family (to which BIK1 belongs) such as PBL1 are also part of the receptor complex and serve a role in defense signaling (Zhang et al., 2010; Liu et al., 2013). Two hallmark responses of PRR-mediated defense are a rapid oxidative burst, commonly referred to as production of reactive oxygen species (ROS), and phosphorylation of mitogen-activated protein kinase (MAPK) cascades (Boller & Felix, 2009). BIK1 was found to serve an important role in ROS production by phosphorylating the NADPH oxidase RBOHD responsible for the oxidative burst in Arabidopsis upon release from the FLS2-BAK1 receptor complex and thus contributing to its activation (Kadota et al., 2014). How PRR activation leads to MAPK phosphorylation and subsequent gene expression changes is still unknown, but it is not dependent on BIK1 (Feng et al., 2012).

The activation of PRRs needs to be carefully controlled and the defense signaling switched off after initiation of the PTI response. Considering the importance of phosphorylation in PTI activation, it is not surprising that the phosphatase KAPP was found to associate with FLS2, presumably keeping the receptor in an inactive state through dephosphorylation (Gómez-Gómez et al., 2001). KAPP and other phosphatases are either inactivated or dissociate from the receptor complex upon ligand binding, thus enabling phosphorylation and activation of the

various signaling partners (Macho & Zipfel, 2014). Furthermore, receptors with bound ligands need to be removed from the plasma membrane and replaced with newly synthesized proteins capable of detecting further danger signals. Thus, after FLS2 binds flg22 it is internalized through endocytosis and degraded (Robatzek et al., 2006). This degradation is mediated by the E3 ubiquitin ligases PUB12 and PUB13 that constitutively associate with BAK1 and are phosphorylated by the co-receptor upon flg22 binding, leading to polyubiquitination and subsequent degradation of FLS2 (Lu et al., 2011). Interestingly, only FLS2 is ubiquitinated and degraded whereas BAK1 seems to stay at the plasma membrane (Lu et al., 2011). This might be because BAK1 functions as a co-receptor for other PRRs such as EFR (Roux et al., 2011). In addition, BAK1 is required for the function of PEPR1 and PEPR2 that sense endogenous danger signals and are thought to amplify PTI responses (Roux et al., 2011; Zipfel, 2013). BAK1 is also necessary for non-defense signaling as it functions as a co-receptor for the brassinosteroid receptor BRI1 that regulates growth and development in response to this plant hormone (Li et al., 2002; Belkhadir & Chory, 2006).

The straightforward transfer of EFR into other plant species shows that we need not necessarily fully understand the intricacies of PRR activation and regulation in order to employ this strategy for increased disease resistance. However, a better understanding of the complexity of PTI initiation at the plasma membrane should enhance our ability to take full advantage of this approach. In order to sustain modern agriculture while minimizing pesticide use, we need to improve the genetic resistance of our crops. In addition to traditional resistance breeding, this can be best achieved by studying the molecular mechanisms by which agronomically important pathogens cause disease and developing strategies that maximize the effectiveness and durability of the introduced genetic resistance.

Bacterial speck disease of tomato (*Solanum lycopersicum*) caused by the bacterial pathogen *Pseudomonas syringae* pv. *tomato* (*Pst*) is a model system to study the molecular interaction between plants and pathogens (Pedley & Martin, 2003; Martin, 2012). Bacterial speck is favored by cool and wet conditions and *Pst* infection results in necrotic lesions on leaves and fruits, reduces growth and yield of tomato plants, and affects the marketability of the fruits (Pedley & Martin, 2003). The bacteria are splash dispersed and enter the leaves and other plant parts through stomata and wounds where they multiply in the apoplastic space, ultimately leading to manifestation of disease symptoms (Melotto et al., 2008).

Bacterial speck is controlled through cultural practices, application of preventative copper formulations, and limited genetic resistance that has been introgressed mostly into processing tomatoes (Pedley & Martin, 2003). As such, studying the molecular interaction between tomato and *Pst* not only provides important information on the basic functions of plant defense and bacterial virulence mechanisms, but the knowledge can be applied to breed varieties of both fresh market and processing tomatoes with improved resistance to this persistent disease.

The main source of genetic resistance to bacterial speck is provided by the *Pto* locus, which was introgressed into commercial cultivars from the wild tomato relative *S. pimpinellifolium* (Pedley & Martin, 2003). Pto is a serine/threonine protein kinase that together with the nucleotide-binding leucine-rich repeat protein Prf confers robust resistance to *Pst* strains secreting either of the type III effector proteins AvrPto or AvrPtoB (referred to as race 0 strains). While the recognition of these effectors by Pto and Prf has been intensively studied, much less is known about downstream signaling after the initial recognition events (Pedley & Martin, 2003).

While Pto-based resistance is effective against race 0 strains such as the widely-

studied model strain DC3000 and the more prevalent strain JL1065, the most commonly found strains are T1 and T1-like that are not recognized by Pto/Prf (referred to as race 1 strains) (Cai et al., 2011; Thapa et al., 2015). These strains either do not have AvrPto and AvrPtoB, the effectors do not accumulate, or they have mutations that prevent binding to and thus recognition by Pto. In the case of T1, the strain does not have *avrPto* and while *avrPtoB* is present, the corresponding protein does not accumulate (Lin et al., 2006). In recent years a highly virulent strain of T1 has been found in New York state called NYS-T1 that can result in severe outbreaks of bacterial speck and is not detected by Pto (Jones et al., 2015). The early summer of 2015 with cool and wet weather in NY presented the perfect environmental conditions for *Pst* throughout the state, resulting in widespread outbreaks of bacterial speck. In addition to the crops of growers, an experimental tomato field near Freeville, NY was devastated by bacterial speck, demonstrating that if the environmental conditions are right *Pst* can cause complete crop loss in the absence of genetic resistance. While severe outbreaks in the field are not that common, the emergence of new and highly virulent strains such as NYS-T1 that are able to evade the currently available Pto-based resistance presents a compelling case to discover additional sources of genetic resistance.

A pair of recent studies using the wild tomato relative *S. habrochaites* identified a number of QRLs that confer partial resistance against T1 and T1-like race 1 strains (Bao et al., 2015; Thapa et al., 2015). Of particular interest, the work using *S. habrochaites* accession LA2109 identified a number of receptor-like kinases that might represent novel PRRs that seem to confer resistance against diverse *P. syringae* pathovars (Bao et al., 2015). Even though these and other QRLs may not provide the same level of resistance against race 1 strains that Pto provides against race 0 strains, their identification allows breeders to generate at least partially

resistant tomato cultivars.

As mentioned earlier, PTI provides broad-spectrum disease resistance and should be effective against both race 0 and race 1 strains. Therefore, identifying novel components of the PTI machinery might open new avenues for enhanced resistance against bacterial speck. Pti1, another serine/threonine protein kinase, was originally discovered as a Pto-interacting protein and was thought to function downstream of Pto and mediate resistance signaling in response to AvrPto (Zhou et al., 1995). The work presented in this dissertation provides evidence that Pti1 instead functions in immunity triggered by flagellin perception. Specifically, Pti1 contributes to ROS production in response to flagellin-derived peptides and enhances resistance of tomato plants to *Pst* strains lacking AvrPto and AvrPtoB. Furthermore, the Pti1 kinase might interact with and function downstream of two putative cell-surface receptors identified over the course of this work. While the exact function of Pti1 and the role of the putative receptors is still unknown, this work reveals new details about the molecular interaction between tomato and *Pst* and might lead to tomato varieties with enhanced resistance to bacterial speck.

1.2 Bibliography

Allen, R. L., Bittner-Eddy, P. D., Grenville-Briggs, L. J., Meitz, J. C., Rehmany, A. P., Rose, L. E., & Beynon, J. L. (2004). Host-parasite coevolutionary conflict between *Arabidopsis* and downy mildew. *Science*, *306*(5703), 1957–1960.

Antony, G., Zhou, J., Huang, S., Li, T., Liu, B., White, F., & Yang, B. (2010). Rice *xa13* recessive resistance to bacterial blight is defeated by induction of the disease susceptibility gene *Os-11N3*. *Plant Cell*, *22*(11), 3864–3876.

Bao, Z., Meng, F., Strickler, S. R., Dunham, D. M., Munkvold, K. R., & Martin, G. B. (2015). Identification of a candidate gene in *Solanum habrochaites* for resistance to a race 1 strain of P*seudomonas syringae* pv. *tomato*. *The Plant Genome*, *8*(3).

Belkhadir, Y., & Chory, J. (2006). Brassinosteroid signaling: a paradigm for steroid hormone signaling from the cell surface. *Science*, *314*(5804), 1410–1411.

Boch, J., Scholze, H., Schornack, S., Landgraf, A., Hahn, S., Kay, S., Lahaye, T., Nickstadt, A., & Bonas, U. (2009). Breaking the code of DNA binding specificity of TAL-type III effectors. *Science*, *326*(5959), 1509–1512.

Boller, T., & Felix, G. (2009). A renaissance of elicitors: perception of microbe-associated molecular patterns and danger signals by pattern-recognition receptors. *Annu Rev Plant Biol*, *60*(1), 379–406.

Büschges, R., Hollricher, K., Panstruga, R., Simons, G., Wolter, M., Frijters, A., van Daelen, R., van der Lee, T., Diergaarde, P., Groenendijk, J., Töpsch, S., Vos, P., Salamini, F., & Schulze-Lefert, P. (1997). The barley *Mlo* gene: a novel control element of plant pathogen resistance. *Cell*, *88*(5), 695–705.

Cai, R., Lewis, J., Yan, S., Liu, H., Clarke, C. R., Campanile, F., Almeida, N. F., Studholme, D. J., Lindeberg, M., Schneider, D., Zaccardelli, M., Setubal, J. C., Morales-Lizcano, N. P., Bernal, A., Coaker, G., Baker, C., Bender, C. L., Leman, S., & Vinatzer, B. A. (2011). The plant pathogen *Pseudomonas syringae* pv. *tomato* is genetically monomorphic and under strong selection to evade tomato immunity. *PLoS Pathog*, *7*(8), e1002130.

Chen, L.-Q. (2014). SWEET sugar transporters for phloem transport and pathogen nutrition. *New Phytol*, *201*(4), 1150–1155.

Chen, L.-Q., Hou, B.-H., Lalonde, S., Takanaga, H., Hartung, M. L., Qu, X.-Q., Guo, W.-J., Kim, J.-G., Underwood, W., Chaudhuri, B., Chermak, D., Antony, G., White, F. F., Somerville, S. C., Mudgett, M. B., & Frommer, W. B. (2010). Sugar transporters for intercellular exchange and nutrition of pathogens. *Nature*, *468*(7323), 527–532.

Chinchilla, D., Zipfel, C., Robatzek, S., Kemmerling, B., Nürnberger, T., Jones, J. D. G., Felix, G., & Boller, T. (2007). A flagellin-induced complex of the receptor FLS2 and BAK1 initiates plant defence. *Nature*, *448*(7152), 497–500.

Chu, Z., Fu, B., Yang, H., Xu, C., Li, Z., Sanchez, A., Park, Y. J., Bennetzen, J. L., Zhang, Q., & Wang, S. (2006). Targeting *xa13*, a recessive gene for bacterial blight resistance in rice. *Theor. Appl. Genet.*, *112*(3), 455–461.

Coates, M. E., & Beynon, J. L. (2010). *Hyaloperonospora arabidopsidis* as a pathogen model. *Annu Rev Phytopathol*, *48*, 329–345.

Dodds, P. N., & Rathjen, J. P. (2010). Plant immunity: towards an integrated view of plant-pathogen interactions. *Nat Rev Genet*, *11*(8), 539–548.

Dou, D., & Zhou, J.-M. (2012). Phytopathogen effectors subverting host immunity: different foes, similar battleground. *Cell Host Microbe*, *12*(4), 484–495.

Ellis, J. G., Dodds, P. N., & Lawrence, G. J. (2007). Flax rust resistance gene specificity is based on direct resistance-avirulence protein interactions. *Annu Rev Phytopathol*, *45*, 289–306.

Feng, F., Yang, F., Rong, W., Wu, X., Zhang, J., Chen, S., He, C., & Zhou, J.-M. (2012). A *Xanthomonas* uridine 5'-monophosphate transferase inhibits plant immune kinases. *Nature*, *485*(7396), 114–118.

Gawehns, F., Cornelissen, B. J. C., & Takken, F. L. W. (2012). The potential of effector-target genes in breeding for plant innate immunity. *Microb Biotechnol*, *6*(3), 223–229.

Gómez-Gómez, L., Bauer, Z., & Boller, T. (2001). Both the extracellular leucine-rich repeat domain and the kinase activity of FLS2 are required for flagellin binding and signaling in Arabidopsis. *Plant Cell*, *13*(5), 1155–1163.

Gust, A. A., Brunner, F., & Nürnberger, T. (2010). Biotechnological concepts for improving plant innate immunity. *Curr Opin Biotechnol*, *21*(2), 204–210.

Jarosch, B., Kogel, K.-H., & Schaffrath, U. (1999). The ambivalence of the barley *Mlo* locus: mutations conferring resistance against powdery mildew (*Blumeria graminis* f. sp. *hordei*) enhance susceptibility to the rice blast fungus *Magnaporthe grisea*. *Mol Plant Microbe Interact*, *12*(6), 508–514.

Jones, L. A., Saha, S., Collmer, A., Smart, C. D., & Lindeberg, M. (2015). Genome-assisted development of a diagnostic protocol for distinguishing high virulence *Pseudomonas syringae* pv. *tomato* strains. *Plant Disease*, *99*(4), 527–534.

Jorgensen, I. H. (1992). Discovery, characterization and exploitation of Mlo powdery mildew resistance in barley. *Euphytica*, *63*(1), 141–152.

Kadota, Y., Sklenar, J., Derbyshire, P., Stransfeld, L., Asai, S., Ntoukakis, V., Jones, J. D., Shirasu, K., Menke, F., Jones, A., & Zipfel, C. (2014). Direct regulation of the NADPH oxidase RBOHD by the PRR-associated kinase BIK1 during plant immunity. *Mol Cell*, *54*(1), 1–13.

Kaku, H., Nishizawa, Y., Ishii-Minami, N., Akimoto-Tomiyama, C., Dohmae, N., Takio, K., Minami, E., & Shibuya, N. (2006). Plant cells recognize chitin fragments for defense signaling through a plasma membrane receptor. *Proc Natl Acad Sci*, *103*(29), 11086–11091.

Krattinger, S. G., Lagudah, E. S., Spielmeyer, W., Singh, R. P., Huerta-Espino, J., McFadden, H., Bossolini, E., Selter, L. L., & Keller, B. (2009). A putative ABC transporter confers durable resistance to multiple fungal pathogens in wheat. *Science*, *323*(5919), 1360–1363.

Kumar, J., Hückelhoven, R., Beckhove, U., Nagarajan, S., & Kogel, K. H. (2001). A compromised Mlo pathway affects the response of barley to the necrotrophic fungus *Bipolaris sorokiniana* (teleomorph: *Cochliobolus sativus*) and its toxins. *Phytopathology*, *91*(2), 127–133.

Lacombe, S., Rougon-Cardoso, A., Sherwood, E., Peeters, N., Dahlbeck, D., van Esse, H. P., Smoker, M., Rallapalli, G., Thomma, B. P. H. J., Staskawicz, B., Jones, J. D. G., & Zipfel, C. (2010). Interfamily transfer of a plant pattern-recognition receptor confers broad-spectrum bacterial resistance. *Nat Biotechnol*, *28*(4), 365–369.

Li, J., Wen, J., Lease, K. A., Doke, J. T., Tax, F. E., & Walker, J. C. (2002). BAK1, an *Arabidopsis* LRR receptor-like protein kinase, interacts with BRI1 and modulates brassinosteroid signaling. *Cell*, *110*(2), 213–222.

Li, J., Zhao-Hui, C., Batoux, M., Nekrasov, V., Roux, M., Chinchilla, D., Zipfel, C., & Jones, J. D. G. (2009). Specific ER quality control components required for biogenesis of the plant innate immune receptor EFR. *Proc Natl Acad Sci*, *106*(37), 15973–15978.

Li, T., Liu, B., Spalding, M. H., Weeks, D. P., & Yang, B. (2012). High-efficiency TALEN-based gene editing produces disease-resistant rice. *Nat Biotechnol*, *30*(5), 390–392.

Lin, N.-C., Abramovitch, R. B., Kim, Y.-J., & Martin, G. B. (2006). Diverse AvrPtoB homologs from several *Pseudomonas syringae* pathovars elicit Pto-dependent resistance and have similar virulence activities. *Appl. Environ. Microbiol.*, *72*(1), 702–712.

Liu, Z., Wu, Y., Yang, F., Zhang, Y., Chen, S., Xie, Q., Tian, X., & Zhou, J.-M. (2013). BIK1 interacts with PEPRs to mediate ethylene-induced immunity. *Proc Natl Acad Sci*, *110*(15), 6205–6210.

Lu, D., Lin, W., Gao, X., Wu, S., Cheng, C., Avila, J., Heese, A., Devarenne, T. P., He, P., & Shan, L. (2011). Direct ubiquitination of pattern recognition receptor FLS2 attenuates plant innate immunity. *Science*, *332*(6036), 1439–1442.

Lu, D., Wu, S., Gao, X., Zhang, Y., Shan, L., & He, P. (2010). A receptor-like cytoplasmic kinase, BIK1, associates with a flagellin receptor complex to initiate plant innate immunity. *Proc Natl Acad Sci*, *107*(1), 496–501.

Macho, A. P., & Zipfel, C. (2014). Plant PRRs and the activation of innate immune signaling. *Mol Cell*, *54*(2), 263–272.

Macho, A. P., & Zipfel, C. (2015). Targeting of plant pattern recognition receptor-triggered immunity by bacterial type-III secretion system effectors. *Curr Opin Microbiol*, *23*, 14–22.

Martin, G. B. (2012). Suppression and activation of the plant immune system by *Pseudomonas syringae* effectors AvrPto and AvrPtoB. In F. Martin, & S. Kamoun (Eds.) *Effectors in plant-microbe interactions*, (pp. 123–154). Wiley-Blackwell, Hoboken, NJ.

McDonald, B. A., & Linde, C. (2002). Pathogen population genetics, evolutionary potential, and durable resistance. *Annu Rev Phytopathol*, *40*, 349–379.

McIntosh, R. A. (1992). Close genetic linkage of genes conferring adult-plant resistance to leaf rust and stripe rust in wheat. *Plant Pathology*, *41*(5), 523–527.

Melotto, M., Underwood, W., & He, S. Y. (2008). Role of stomata in plant innate immunity and foliar bacterial diseases. *Annu Rev Phytopathol*, *46*, 101–122.

Miya, A., Albert, P., Shinya, T., Desaki, Y., Ichimura, K., Shirasu, K., Narusaka, Y., Kawakami, N., Kaku, H., & Shibuya, N. (2007). CERK1, a LysM receptor kinase, is essential for chitin elicitor signaling in *Arabidopsis*. *Proc Natl Acad Sci*, *104*(49), 19613–19618.

Panstruga, R. (2005). Serpentine plant MLO proteins as entry portals for powdery mildew fungi. *Biochem Soc Trans*, *33*(Pt 2), 389–392.

Pedley, K. F., & Martin, G. B. (2003). Molecular basis of *Pto*-mediated resistance to bacterial speck disease in tomato. *Annu Rev Phytopathol*, *41*, 215–243.

Poland, J. A., Balint-Kurti, P. J., Wisser, R. J., Pratt, R. C., & Nelson, R. J. (2009). Shades of gray: the world of quantitative disease resistance. *Trends Plant Sci*, *14*(1), 21–29.

Robatzek, S., Chinchilla, D., & Boller, T. (2006). Ligand-induced endocytosis of the pattern recognition receptor FLS2 in *Arabidopsis*. *Genes Dev*, *20*(5), 537–542.

Rose, L. E., Bittner-Eddy, P. D., Langley, C. H., Holub, E. B., Michelmore, R. W., & Beynon, J. L. (2004). The maintenance of extreme amino acid diversity at the disease resistance gene, *RPP13*, in *Arabidopsis thaliana*. *Genetics*, *166*(3), 1517–1527.

Roux, M., Schwessinger, B., Albrecht, C., Chinchilla, D., Jones, A., Holton, N., Malinovsky, F. G., Tör, M., de Vries, S., & Zipfel, C. (2011). The *Arabidopsis* leucine-rich repeat receptor-like kinases BAK1/SERK3 and BKK1/SERK4 are required for innate immunity to hemibiotrophic and biotrophic pathogens. *Plant Cell*, *23*(6), 2440–2455.

Schornack, S., Moscou, M. J., Ward, E. R., & Horvath, D. M. (2013). Engineering plant disease resistance based on TAL effectors. *Annu Rev Phytopathol*, *51*(1), 383–406.

Schulze, B., Mentzel, T., Jehle, A. K., Mueller, K., Beeler, S., Boller, T., Felix, G., & Chinchilla, D. (2010). Rapid heteromerization and phosphorylation of ligand-activated plant transmembrane receptors and their associated kinase BAK1. *J Biol Chem*, *285*(13), 9444–9451.

Seeholzer, S., Tsuchimatsu, T., Jordan, T., Bieri, S., Pajonk, S., Yang, W., Jahoor, A., Shimizu, K. K., Keller, B., & Schulze-Lefert, P. (2010). Diversity at the *Mla* powdery mildew resistance locus from cultivated barley reveals sites of positive selection. *Mol Plant Microbe Interact*, *23*(4), 497–509.

Singh, R. P. (1992). Genetic association of leaf rust resistance gene *Lr34* with adult plant resistance to stripe rust in bread wheat. *Phytopathology*, *82*(8), 835–838.

Spielmeyer, W., McIntosh, R. A., Kolmer, J., & Lagudah, E. S. (2005). Powdery mildew resistance and *Lr34/Yr18* genes for durable resistance to leaf and stripe rust cosegregate at a locus on the short arm of chromosome 7D of wheat. *Theor. Appl. Genet.*, *111*(4), 731–735.

Sun, Y., Li, L., Macho, A. P., Han, Z., Hu, Z., Zipfel, C., Zhou, J. M., & Chai, J. (2013). Structural basis for flg22-induced activation of the *Arabidopsis* FLS2-BAK1 immune complex. *Science*, *342*(6158), 624–628.

Thapa, S. P., Miyao, E. M., Michael Davis, R., & Coaker, G. (2015). Identification of QTLs controlling resistance to *Pseudomonas syringae* pv. *tomato* race 1 strains from the wild tomato, *Solanum habrochaites* LA1777. *Theor. Appl. Genet.*, *128*(4), 681–692.

Yang, B., Sugio, A., & White, F. F. (2006). *Os8N3* is a host disease-susceptibility gene for bacterial blight of rice. *Proc Natl Acad Sci*, *103*(27), 10503–10508.

Yuan, M., Chu, Z., Li, X., Xu, C., & Wang, S. (2009). Pathogen-induced expressional loss of function is the key factor in race-specific bacterial resistance conferred by a recessive *R* gene *xa13* in rice. *Plant Cell Physiol*, *50*(5), 947–955.

Zhang, J., Li, W., Xiang, T., Liu, Z., Laluk, K., Ding, X., Zou, Y., Gao, M., Zhang, X., Chen, S., Mengiste, T., Zhang, Y., & Zhou, J.-M. (2010). Receptor-like cytoplasmic kinases integrate signaling from multiple plant immune receptors and are targeted by a *Pseudomonas syringae* effector. *Cell Host Microbe*, *7*(4), 290–301.

Zhou, J., Loh, Y. T., Bressan, R. A., & Martin, G. B. (1995). The tomato gene *Pti1* encodes a serine/threonine kinase that is phosphorylated by Pto and is involved in the hypersensitive response. *Cell*, *83*(6), 925–935.

Zipfel, C. (2013). Combined roles of ethylene and endogenous peptides in regulating plant immunity and growth. *Proc Natl Acad Sci*, *110*(15), 5748–5749.

Zipfel, C. (2014). Plant pattern-recognition receptors. *Trends Immunol*, *35*(7), 345–351.

Zipfel, C., Kunze, G., Chinchilla, D., Caniard, A., Jones, J. D. G., Boller, T., & Felix, G. (2006). Perception of the bacterial PAMP EF-Tu by the receptor EFR restricts *Agrobacterium*-mediated transformation. *Cell*, *125*(4), 749–760.

CHAPTER 2

THE TOMATO KINASE PTI1 CONTRIBUTES TO PRODUCTION OF REACTIVE OXYGEN SPECIES IN RESPONSE TO TWO FLAGELLIN-DERIVED PEPTIDES AND PROMOTES RESISTANCE TO *PSEUDOMONAS SYRINGAE* INFECTION

2.1 Summary

The Pti1 kinase was identified from a reverse genetic screen as contributing to pattern-triggered immunity (PTI) against *Pseudomonas syringae* pv. *tomato* (*Pst*). This was unexpected because Pti1 was originally identified as an interactor of the Pto kinase and was implicated in effector-triggered immunity. The tomato genome has two *Pti1* genes, referred to as *Pti1a* and *Pti1b*. A hairpin-Pti1 (hpPti1) construct was developed and used to generate two independent stable transgenic tomato lines, which had reduced transcript abundance of *Pti1a* and *Pti1b*. These hpPti1 plants developed more severe disease symptoms in response to *Pst* infection, supported higher bacterial populations, and had reduced transcript accumulation of PTI-associated genes compared to wild-type plants. The hpPti1 plants produced less reactive oxygen species (ROS), but showed no difference in mitogen-activated protein kinase (MAPK) activation in response to two flagellin-derived peptides. Synthetic *Pti1a* and *Pti1b* genes designed to avoid silencing were transiently expressed in hpPti1 plants and restored the ability of the plants to produce wild-type levels of ROS. Our results identify a new component of PTI in tomato which, because it affects ROS production but not MAPK signaling, appears to act early in the immune response. We speculate that Pti1 was identified originally as a Pto interactor because it may interact with a Pto-like kinase that plays a role in PTI.

This chapter was written by Simon Schwizer, Diane Dunham, Christine Kraus, Yi Zheng, Marina Pombo, Zhangjun Fei, Suma Chakravarthy, and Gregory Martin.

2.2 Introduction

Bacterial speck disease of tomato (*Solanum lycopersicum*) is caused by interaction with pathogenic strains of *Pseudomonas syringae* pv. *tomato* (*Pst*). This disease is a persistent problem on tomato where cool, moist conditions prevail and symptoms occur on leaves, stems, and fruits, reducing plant growth and causing significant losses in yield and marketability of fresh market tomatoes (Young et al., 1986; Jones, 1991; Pedley & Martin, 2003). Control of bacterial speck disease is achieved mainly through cultural practices, preventative copper formulations, and in the case of processing tomatoes, with genetic resistance (Pedley & Martin, 2003). To minimize crop losses and reduce the use of pesticides it is important to advance our understanding of the molecular basis of the host defense response to *Pst* and other important pathogens (Dangl et al., 2013).

The interaction of tomato and *Pst* has emerged as a powerful model system for investigating the plant immune system in an important vegetable crop. *Pst* is experimentally tractable and amenable to genetic manipulations, allowing for both addition and deletion of genes (Preston, 2000; Kvitko et al., 2007). Furthermore, culturing, plant inoculations, measurement of pathogen growth, and monitoring of disease symptoms are easily accomplished with *Pst* (Lin & Martin, 2005; Nguyen et al., 2010a). DC3000 is a widely-used *Pst* strain because its genome sequence is available and, in addition to tomato, it is able to infect and cause disease symptoms on the model plant *Arabidopsis thaliana* (Whalen et al., 1991; Buell et al., 2003). Tomato has good experimental tractability and is amenable to disease and immunity assays as well as transient gene expression and gene silencing approaches (Liu et al., 2002; Burch-Smith et al., 2004; Nguyen et al., 2010a). The available tomato genome sequence greatly aids the development of RNA interference and CRISPR knockout lines to study genes of interest (Tomato Genome Consortium, 2012).

Nicotiana benthamiana, a wild tobacco species and member of the solanaceae family, is also amenable to experimental manipulation and is a useful surrogate for tomato in many assays, especially transient gene expression and gene silencing (Goodin et al., 2008). The recent availability of a draft genome sequence for *N. benthamiana* further enhances its usefulness as a model plant (Bombarely et al., 2012). Furthermore, *Pst* DC3000 with a deleted *hopQ1-1* effector gene (Δ*hopQ1-1*) is able to infect and cause disease symptoms on *N. benthamiana* (Wei et al., 2007).

Most plants are resistant to most pathogens and disease is the exception. Plants achieve this remarkable feat by employing a sophisticated, two-layered immune system (Jones & Dangl, 2006; Dodds & Rathjen, 2010; Cook et al., 2015). The first layer of defense involves pattern recognition receptors (PRRs) located at the plasma membrane that are able to perceive extracellular microbe-associated molecular patterns (MAMPs) (Boller & Felix, 2009; Zipfel, 2014). These MAMPs are typically conserved components present in essential pathogen structures, such as the flagellin protein in the bacterial flagellum which contains two MAMPs, flg22 and flgII-28 (Felix et al., 1999; Bent & Mackey, 2007; Cai et al., 2011). One of the best-characterized PRRs is FLS2 which occurs in Arabidopsis, tomato, and other plants, and is capable of detecting flg22 (Gómez-Gómez & Boller, 2000; Chinchilla et al., 2006; Boller & Felix, 2009). FLS2, upon binding of this peptide, initiates a signaling cascade involving the co-receptor BAK1 and a number of kinases that form complexes at the plasma membrane, leading to variety of responses such as activation of mitogen-activated protein kinase (MAPK) cascades, production of reactive oxygen species (ROS), and induction of defense-related genes (Chinchilla et al., 2007; Monaghan & Zipfel, 2012). These responses, along with production of antimicrobial compounds and cell wall reinforcements, are often sufficient to halt

pathogen invasion and are collectively referred to as pattern-triggered immunity (PTI) (Zipfel et al., 2004). The flgII-28 peptide is recognized in tomato, potato, and pepper, and the gene encoding the cognate PRR, referred to as *FLS3*, was recently identified using a mapping-by-sequencing approach; the receptor was found to directly bind flgII-28 and requires BAK1 for downstream signaling (Clarke et al., 2013; Hind et al., 2016).

To overcome these defense responses and cause disease, pathogenic microbes have evolved virulence proteins ('effectors') which are often translocated into the plant cell to interfere with pathogen detection or interrupt PTI signaling (Dou & Zhou, 2012; Macho & Zipfel, 2015). Bacterial pathogens employ the type III secretion system, which acts as a molecular syringe to enable injection of a plethora of effector proteins into the plant cell (Block & Alfano, 2011; Lindeberg et al., 2012). *Pst* DC3000 contains ~30 effector proteins (Buell et al., 2003; Cunnac et al., 2009); two of these, AvrPto and AvrPtoB, are believed to be secreted early in the infection process and interfere with the FLS2 and FLS3 receptor complexes to prevent an effective induction of PTI (He et al., 2006; Shan et al., 2008; Xiang et al., 2008; Kvitko et al., 2009; **?**; Martin, 2012; Hind et al., 2016).

To defend themselves against the detrimental consequences of effectors, plants have evolved a second layer of defense involving resistance (R) proteins, which are capable of detecting the presence or action of effector proteins (Jones & Dangl, 2006; Dodds & Rathjen, 2010). In tomato, the Pto protein kinase forms a complex with the nucleotide-binding leucine-rich repeat protein Prf and has the ability to bind AvrPto or AvrPtoB (Martin et al., 1993; Salmeron et al., 1996; Mucyn et al., 2006; Xing et al., 2007; Dong et al., 2009). This interaction induces a strong defense response, referred to as effector-triggered immunity (ETI), resulting in programmed cell death (PCD) of the infected tissue and inhibition of pathogen

growth (Pedley & Martin, 2003; Jones & Dangl, 2006). It is believed that Pto evolved as a 'decoy' to mimic the kinase domains of PRRs such as FLS2 and FLS3 that are targeted by AvrPto and AvrPtoB (van der Hoorn & Kamoun, 2008; Martin, 2012). The interactions of AvrPto/AvrPtoB, Pto, and Prf have been studied extensively and several downstream signaling components have been identified, including components of MAPK cascades (Ekengren et al., 2003; del Pozo et al., 2004; Oh & Martin, 2011a). In addition, the 14-3-3 protein TFT7 was found to positively regulate the Pto/Prf response through interaction with MAPKKKα and MKK2 (Oh et al., 2010a; Oh & Martin, 2011b). More recently, RNA sequencing (RNA-Seq) analyses followed by virus-induced gene silencing (VIGS) experiments identified Epk1, a protein kinase that is required for the full response to AvrPto and AvrPtoB, although its role in the Pto pathway is yet to be determined (Pombo et al., 2014).

The Pti1 kinase was originally identified in a yeast two-hybrid screen as a Pto interactor and was implicated in ETI (Zhou et al., 1995). Overexpression of tomato *Pti1* in a stable transgenic tobacco line resulted in enhanced cell death in response to *P. syringae* pv. *tabaci* carrying *avrPto* and it was concluded that Pti1 amplifies the Pto signaling response (Zhou et al., 1995). A possible role for Pti1 in ETI was supported by the observation that Pto specifically phosphorylates Pti1 but Pti1 does not phosphorylate Pto, suggesting that Pti1 functions directly downstream of Pto (Zhou et al., 1995; Sessa et al., 1998, 2000). However, subsequent mutational analysis of Pto revealed several substitution mutants that are unable to phosphorylate Pti1 but trigger Prf-mediated cell death when overexpressed in *N. benthamiana* (Wu et al., 2004). More importantly, a transgenic tomato line overexpressing Pto^{G50S}, a variant that lacks kinase activity and does not interact with Pti1 in yeast, confers resistance to *Pst* strains expressing *avrPto* (Xiao

et al., 2003; Mathieu et al., 2014). Later work found that the response to AvrPto in tobacco differs from tomato and depends on an unidentified resistance protein (Nguyen et al., 2010b; Yeam et al., 2010). Here we describe the discovery that Pti1 appears to act early in the PTI response by inducing ROS production in response to flagellin perception, influencing the expression of defense-related genes, and enhancing resistance to *Pst*.

2.3 Materials and methods

Plant material

Nicotiana benthamiana accession Nb-1 (Bombarely et al., 2012) was grown for 4-6 weeks in a controlled environment chamber with 16 h light and 65% relative humidity with a temperature of 24°C during light and 22°C during dark periods. The hairpin-Pti1 (hpPti1) lines were generated by cloning a segment of the tomato *Pti1a* gene sequence into pHELLSGATE8 (Helliwell et al., 2002) to obtain the hpPti1 silencing construct. Tomato Rio Grande (RG)-prf3 (Salmeron et al., 1996) plants were transformed by the Center for Plant Biotechnology Research at the Boyce Thompson Institute. We obtained one single-copy line (F27-36) and one multi-copy line (F10-10) as well as two corresponding 'azygous' control lines that had lost the transgene(s) due to segregation. The hpPto line was made in the RG-PtoR background and was described previously (Pascuzzi, 2006). All tomato plants were grown in a greenhouse without supplemental light for 4-5 weeks before use in pathogen assays or RNA sequencing experiments.

Cloning

The constructs for virus-induced gene silencing (VIGS) were cloned as previously described (Rosli et al., 2013). Suitable sequences were selected using the Sol Genomics Network (SGN) VIGS tool (Fernandez-Pozo et al., 2015b) and cloned into pCR8/GW/TOPO (Invitrogen), followed by recombination into pQ11 (Liu et al., 2002) using the LR Clonase II enzyme mix (Invitrogen), and transformation into *Agrobacterium tumefaciens* GV2260 (Hellens et al., 2000). Full-length tomato *Pti1* genes were PCR-amplified and ligated into the pJLSmart Gateway entry vector (Mathieu et al., 2007) as described (Mathieu et al., 2014). Synthetic *Pti1* versions were obtained by changing the codons of the 5' gene portions to prevent binding of the hpPti1 fragment without altering the amino acid sequence. These synthetic portions were ordered from Integrated DNA Technologies and fused to the wild-type 3' sequences by PCR and cloned into pJLSmart. Cysteine-to-serine substitutions were introduced by PCR using complementary custom DNA oligonucleotides (Integrated DNA Technologies) following standard protocols. All *Pti1* constructs were recombined into the binary plant expression vectors pGWB411 or pGWB541 (Nakagawa et al., 2007) using the LR Clonase II enzyme mix to obtain C-terminal FLAG and eYFP fusions, respectively. These expression constructs were transformed into *A. tumefaciens* strains 1D1249 and GV3101 (Hellens et al., 2000; Wroblewski et al., 2005).

Cell death suppression assay

The cell death suppression assay in silenced *N. benthamiana* plants was performed as described previously (Chakravarthy et al., 2010; Rosli et al., 2013). Briefly, seedlings were syringe-infiltrated with Agrobacterium strains carrying the appropriate VIGS constructs and the assay performed 6 weeks later. Non-pathogenic

Pseudomonas fluorescens 55 (OD_{600} 0.5) was syringe-infiltrated to induce pattern-triggered immunity (PTI) responses, followed 7 h later by virulent *P. syringae* pv. *tomato* (*Pst*) DC3000 Δ*hopQ1-1* (OD_{600} 0.01) (Wei et al., 2007) in overlapping circles. Disease symptoms were monitored and scored and photographed 5 days later.

Bacterial infection assay

Four week-old tomato hpPti1 plants along with azygous and RG-prf3 controls were vacuum-infiltrated with *Pst* DC3000 Δ*avrPto* Δ*avrPtoB* (Lin & Martin, 2005) at 5 x 10^4 cfu/ml as described previously (Anderson et al., 2006; Zeng et al., 2011). Inoculated plants were kept in a controlled environment chamber and bacterial populations were assessed by taking leaf samples a few hours after infiltration and 2 days later. Plants were photographed 5 days after infiltration to document disease symptoms. The RG-PtoR F1 plants along with RG-PtoR and hpPto controls were vacuum-infiltrated with *Pst* DC3000 at 10^5 cfu/ml or 10^6 cfu/ml. Photographs were taken 3 days after infiltration.

Mitogen-activated protein kinase phosphorylation assay

Leaf discs of tomato hpPti1 and azygous control plants were floated in water for 1 h to let the wound response subside. The water was replaced by fresh water containing 10 nM flg22 (GenScript), 25 nM flgII-28 (EZBiolab), or no peptide (negative control), the leaf discs incubated for 10 min, frozen, and ground in liquid nitrogen. Whole protein was extracted using a buffer containing 10% glycerol, 25 mM Tris-HCl pH 8.0, 1 mM EDTA pH 8.0, 150 mM NaCl, 10 mM DTT (American Bioanalytical), and 0.15% IGEPAL CA-630 (Nonidet P-40; Sigma-Aldrich), with cOmplete ULTRA EDTA-free protease inhibitor (Roche Diagnostics) and PhosSTOP phosphatase inhibitor (Roche Diagnostics). Samples were incubated

for 15 min at 4°C, the supernatants collected, and boiled in Laemmli sample buffer. Gel electrophoresis and immunoblotting was performed following standard protocols. Mitogen-activated protein kinase (MAPK) phosphorylation was detected using the phospho-p44/42 MAPK (Erk1/2) antibody (anti-pMAPK, Cell Signaling) following the manufacturer's instructions.

Reactive oxygen species production assay

Production of reactive oxygen species (ROS) was measured as described previously (Chakravarthy et al., 2010; Clarke et al., 2013), with modifications. Leaf discs of tomato hpPti1 and azygous control plants were floated overnight in water in white, flat-bottom, 96-well plates (Greiner Bio-One). The water was removed 12 h later and a solution containing 100 nM flg22, 34 µg/ml luminol (Sigma-Aldrich), and 20 µg/ml horseradish peroxidase (type VI-A, Sigma-Aldrich) was added. ROS production was quantified by means of luminescence output from each well over time. Luminescence was measured using a Synergy 2 microplate reader (BioTek).

Agrobacterium-mediated transient expression

Preparation of Agrobacterium strains and plant infiltrations were performed as described previously (Mathieu et al., 2014; Kraus et al., 2016). Briefly, confirmed Agrobacterium strains were grown on lysogeny broth (LB) plates with the appropriate antibiotics for 36-48 h at 30°C. Cells were collected, suspended in infiltration buffer containing 10 mM $MgCl_2$, 10 mM MES pH 5.7, and 200 µM acetosyringone (Sigma-Aldrich), the OD_{600} for each strain adjusted to 0.3, and incubated for 1 h at room temperature. Leaves of *N. benthamiana* and tomato plants were infiltrated with needle-less syringes and the plants placed in a controlled environment chamber (see above).

Protein detection

Discs of Agrobacterium-transformed *N. benthamiana* leaf tissue were collected 2 days after agroinfiltration, frozen, and ground in liquid nitrogen. Proteins were extracted as described above, except that no phosphatase inhibitor was used for the protein extraction. FLAG-tagged proteins were detected using anti-FLAG-HRP (Sigma-Aldrich).

Fluorescence imaging

Sections of *N. benthamiana* leaves expressing *Pti1-YFP* fusions were mounted on microscopy slides 2 days after agroinfiltration and analyzed on a Leica DM5500 epi-fluorescence microscope. Images were acquired with a Retiga 2000R CCD camera (QImaging) using QCapture Pro software (QImaging).

Quantitative real-time PCR

Total RNA was extracted from *N. benthamiana* and tomato leaf tissue using Plant RNA Purification Reagent (Invitrogen) according to the manufacturer's instructions. RNA samples were additionally purified using RNeasy Mini columns (Qiagen) and the isolated RNA treated with RNase-free TURBO DNase (Ambion) following the respective manufacturers' protocols. First-strand cDNA synthesis and quantitative real-time PCR (qPCR) were performed exactly as described (Breuillin-Sessoms et al., 2015). Cycle numbers of each plant were normalized (ΔCT) to *PP2A* (Liu et al., 2012) for *N. benthamiana* and *CBL1* (Pombo et al., 2014) for tomato. Means and confidence intervals of the transformed cycle numbers ($2^{\Delta CT}$) of the biological replicates were calculated and normalized to the control plants (EC1 for *N. benthamiana*; RG-PtoR x RG-prf3 F1 and RG-PtoR for tomato).

RNA sequencing analysis

Tomato hpPti1 lines F27-36 (single hpPti1 copy) and F10-10 (multiple hpPti1 copies) along with an azygous control line were vacuum-infiltrated with *Pst* DC3000 Δ*avrPto* Δ*avrPtoB* at 5 x 10^4 cfu/ml. Tissue samples were taken 3 h and 6 h after infiltration. The treatments were repeated in three successive weeks (3 biological replicates). RNA isolation, library preparation, and RNA sequencing (RNA-Seq) analysis were performed as described previously (Rosli et al., 2013). The chosen cutoffs for differentially regulated genes were: >3 reads per kilobase of transcript per million mapped reads (RPKM) in at least one of the treatments, >1.5-fold expression change, and P <0.05. To capture the number of differentially expressed genes in the two hpPti1 lines, the 3 h and 6 h data sets were combined for each hpPti1 line and duplicate genes removed. The RNA-Seq reads for visualizing *Pti1a* and *Pti1b* silencing were taken from the 6 h data set, normalized to *CBL1* (Pombo et al., 2014), and expressed in relation to the azygous control line. The PTI 'marker genes' were visualized the same way based on the 3 h data set. The *Pti1a* and *Pti1b* expression data in response to different PTI inducers (Rosli et al., 2013) were simply visualized in graph form.

Phylogenetic analysis

Coding sequences for the *Pti1* genes from tomato and *N. benthamiana* were obtained from SGN (Fernandez-Pozo et al., 2015a). Alignment and tree construction were performed with MEGA7 (Kumar et al., 2016) with the guidance of a step-by-step protocol (Hall, 2013). Specifically, DNA sequences were aligned using the MUSCLE method (align codons, default settings). Maximum likelihood (ML) substitution models were predicted using the default settings. The phylogenetic tree was estimated using the ML method (Tamura 3-parameter model, gamma

distributed rates among sites, partial deletion of gaps/missing data, default settings otherwise). Reliability of the tree was estimated using the bootstrap method (1,000 replicates).

Gene sequences

Gene sequences are available from the SGN database (http://solgenomics.net) under the following accession numbers: *SlPti1a* (Solyc12g098980), *SlPti1b* (Solyc05g053230), *NbPti1a* (Niben101Scf01236g02003), *NbPti1b* (Niben101Scf01334g04008), *NbPti1c* (Niben101Scf01671g04002), and *NbPti1d* (Niben101Scf01820g00026). RNA-Seq reads have been deposited in the National Center for Biotechnology Information Sequence Read Archive (http://www.ncbi.nlm.nih.gov/sra) under accession number SRP076863 and analyzed data are available from the Tomato Functional Genomics Database (http://ted.bti.cornell.edu) under accession number D014.

2.4 Results

Cell death suppression assay identifies *Pti1* as contributing to PTI

We screened a collection of 129 genes encoding receptor-like cytoplasmic protein kinases to identify new components of PTI. The transcript abundance of each gene was reduced by VIGS in *N. benthamiana* and the plants were examined for altered defense responses using an assay in which PTI is induced by a non-pathogenic bacterial strain followed by overlap-infiltration of a pathogenic bacterial strain (Chakravarthy et al., 2010). If a candidate gene plays an important role in PTI, then immunity is not fully induced by the non-pathogenic strain and disease-associated cell death occurs more rapidly in the overlapping area. The *Pti1* gene was identified in this screen, which was unexpected because this gene

had previously been identified as playing a role in ETI (Zhou et al., 1995).

Inspection of the tomato genome sequence revealed that there are two *Pti1* genes which we refer to as *SlPti1a* and *SlPti1b*. The genes are 88% identical at the nucleotide level and their predicted proteins are 93% identical (Figure 2.1). *Pti1a* is the gene originally characterized as playing a role in ETI (Zhou et al., 1995). From RNA-Seq data generated previously (Rosli et al., 2013) we determined that *Pti1a* is expressed in tomato leaves though its expression is not specifically affected by inducers of PTI (it is induced in mock inoculations after 6 h compared to the initial 30 min time point, suggesting possible stress responsiveness; Figure 2.2). *Pti1b* is expressed at a basal level in leaves and its transcript abundance increased significantly in response to the MAMPs csp22 and flgII-28 as well as *P. fluorescens* (having both flg22 and flgII-28), but not in response to Agrobacterium which has a flagellin that does not trigger transcriptional change in tomato (Rosli et al., 2013). *Pti1b* transcript abundance also increased in response to inoculation with *Pst* and was reduced in the presence of the effectors AvrPto and AvrPtoB (Figure 2.2).

N. benthamiana is an allotetraploid and, as expected, we identified four *Pti1* genes in the genome sequence of this species, which we refer to as *NbPti1a*, *NbPti1b*, *NbPti1c*, and *NbPti1d* (Bombarely et al., 2012) (Figure 2.3A). To further characterize *Pti1* in *N. benthamiana* we used these gene sequences and the Sol Genomics Network (SGN) VIGS tool (Fernandez-Pozo et al., 2015b) to design two new constructs, designated NbP1 and NbP2, each of which was expected to silence all four *Pti1* genes in *N. benthamiana*. These two constructs were used for VIGS along with an NbFLS2 construct (as a positive control) and an *Escherichia coli*-derived DNA fragment (EC1; as a negative control) (Rosli et al., 2013). The cell death suppression assay was performed by inducing PTI with *P. fluorescens* (*Pf*) 55, followed 7 h later by overlap-infiltration of *Pst* DC3000 Δ*hopQ1-1* (Chakravarthy

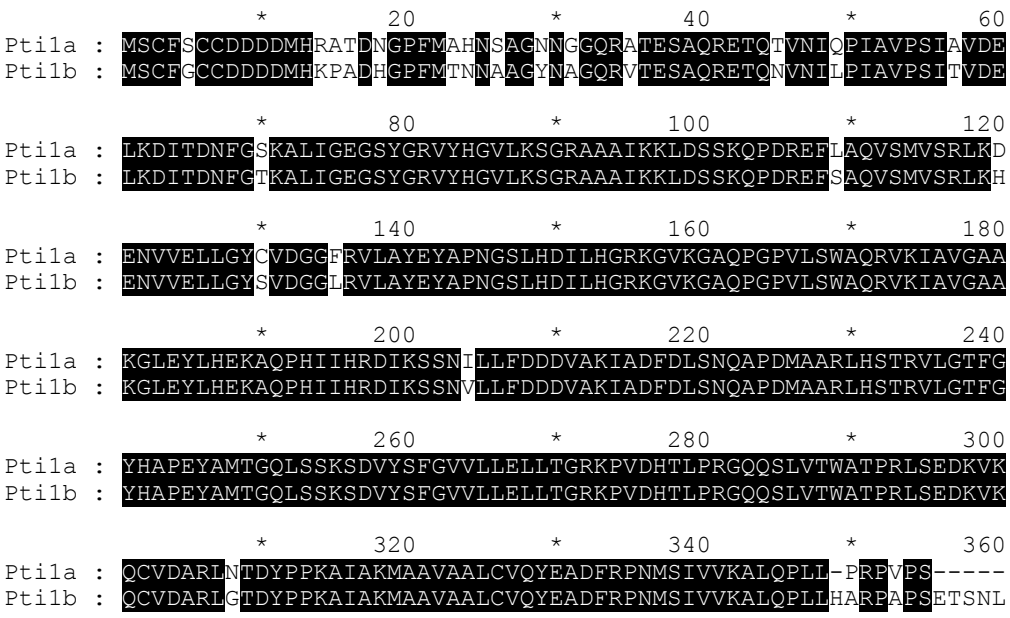

Figure 2.1. Alignment of the predicted amino acid sequences of tomato Pti1a and Pti1b. Alignment was performed with MUSCLE and visualized using GeneDoc. Identical residues are shown in black.

et al., 2010; Rosli et al., 2013). As expected, silencing of *FLS2*, which is known to diminish the response to bacterial flagellin, prevented full induction of PTI, thus resulting in increased disease-associated cell death in the overlapping area compared to EC1 control plants whose PTI response was not impaired (Figure 2.3B and 2.3C). Importantly, silencing with either NbP1 or NbP2 caused increased disease in the overlapping area compared to the negative control indicating a compromised PTI response, although the disease was less than that observed in the *FLS2*-silenced plants (Figure 2.3B and 2.3C). To evaluate the silencing efficiency of the two VIGS constructs, we performed quantitative real-time PCR (qPCR) on NbP1- and NbP2-silenced plants and found that *Pti1* transcript abundance was reduced to less than 20% of the level in the EC1 control plants (Figure 2.3D). Although our *Pti1* primers were expected to amplify transcripts of the *N. benthamiana Pti1a*, *Pti1b*, and *Pti1c* genes, sequencing of the qPCR products from the

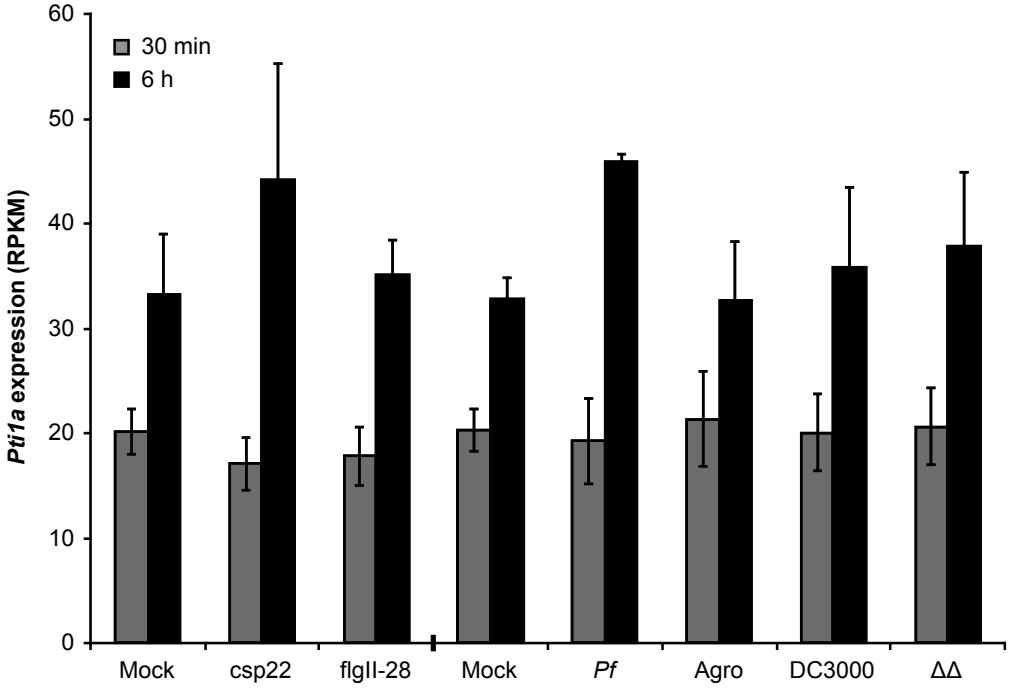
30 min
6 h
Pti1a expression (RPKM)
0
10
20
30
40
50
60
Mock
csp22
flgII-28
Mock
Pf
Agro
DC3000
ΔΔ

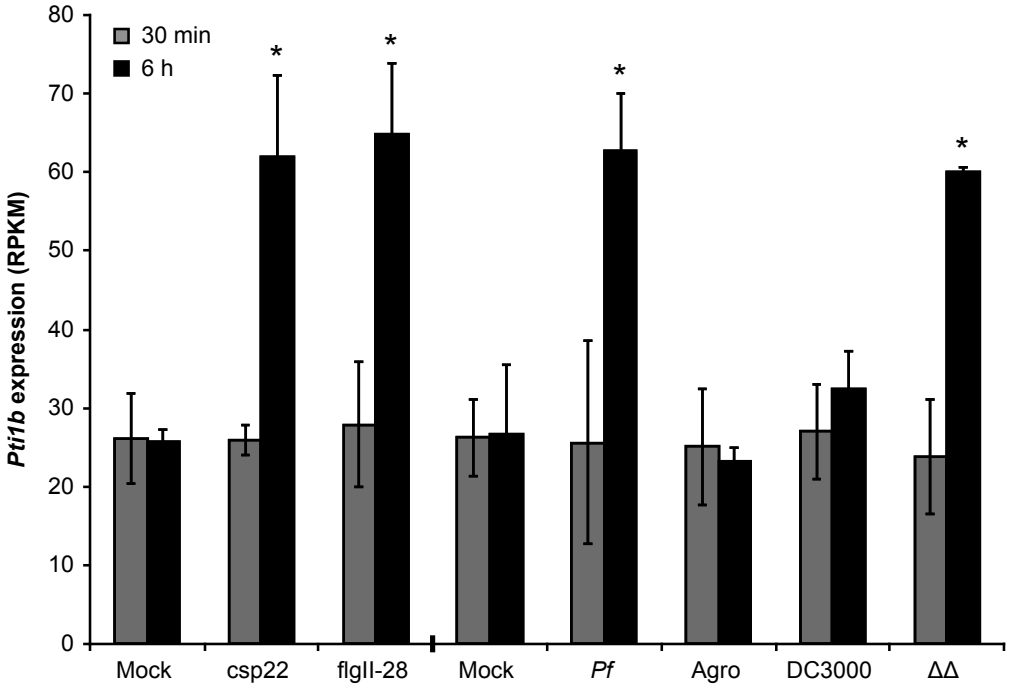
30 min
6 h
Pti1b expression (RPKM)
0
10
20
30
40
50
60
70
80
*
*
*
*
Mock
csp22
flgII-28
Mock
Pf
Agro
DC3000
ΔΔ

Figure 2.2 *(previous page).* Transcript abundance (in RPKMs), derived from RNA-Seq data, of *Pti1a* and *Pti1b* after treatment of tomato leaves with various inducers of PTI. Expression of *Pti1a* (top) or *Pti1b* (bottom) after application of the indicated peptide or bacterial strain 30 min and 6 h after treatment. csp22, 22-amino acid peptide from cold shock protein; flgII-28, 28-amino acid peptide from flagellin; *Pf*, *P. fluorescens* 55, Agro, *A. tumefaciens* GV2260; DC3000, *Pst* DC3000; ΔΔ, *Pst* DC3000 Δ*avrPto* Δ*avrPtoB*. Bars show mean ± 99% confidence interval of 3 replicates. Asterisks indicate significant differences (P <0.05, based on a false discovery rate correction) to the relevant mock treatment. Data derived from a previous study (Rosli et al., 2013).

EC1 control plants revealed only transcripts derived from *NbPti1b* and *NbPti1c*. Using previously generated RNA-Seq data (Pombo et al., 2014), we examined reads per kilobase of transcript per million mapped reads (RPKM) and discovered that both *NbPti1b* and *NbPti1c* are highly expressed in *N. benthamiana* leaves, whereas *NbPti1a* and *NbPti1d* have a much lower transcript abundance (Figure 2.3A). Based on the VIGS experiments and these expression levels we conclude that among the *Pti1* genes in *N. benthamiana*, *NbPti1b* and *NbPti1c* are the main contributors to PTI and the robust silencing of these genes likely explains the observed impact on cell death suppression in the PTI assay.

Transgenic tomato plants silenced for *Pti1a* and *Pti1b* are more susceptible to *Pst* infection.

To test whether the *Pti1* genes contribute to PTI in tomato, we developed a hairpin (hp) RNA interference (RNAi) construct designed to silence the two *Pti1* genes in this species (Figure 2.4A). The construct was used to develop two independent stable transgenic lines in the Rio Grande-prf3 background (RG-prf3; lacking a functional *Prf*) (Salmeron et al., 1996). One line has a single-copy, homozygous, hpPti1 integration (F27-36) and the other line carries multiple copies of the hpPti1

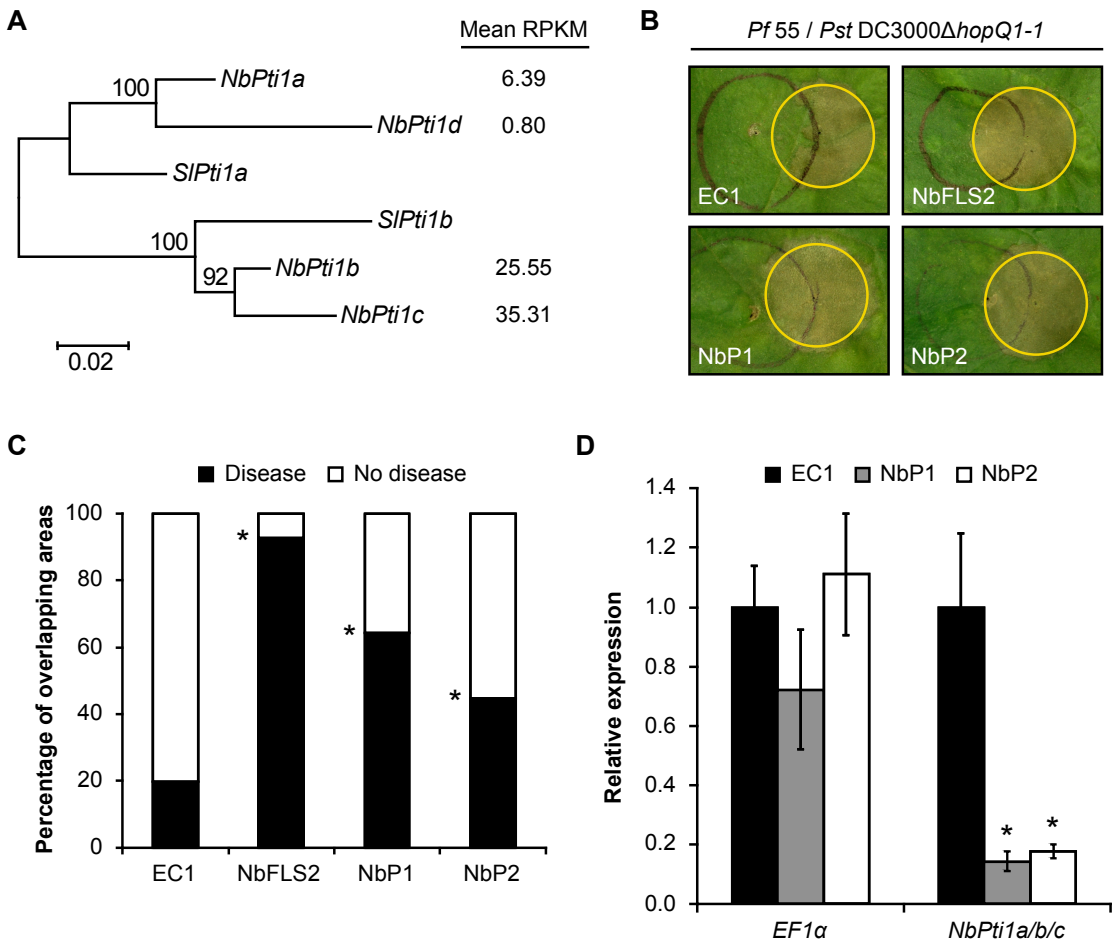

construct (F10-10). For each of these two lines we identified an 'azygous' control line that was derived from the original transformation event but which had lost the transgene(s) in subsequent generations due to segregation. To determine the degree of *Pti1* silencing and to characterize the transcriptome of these plants we performed RNA-Seq on F27-36 and F10-10 hpPti1 plants (and on one of the azygous controls) which had been inoculated 3 h or 6 h earlier with *Pst* DC3000 Δ*avrPto* Δ*avrPtoB*, a strain which has reduced virulence and is used to detect subtle changes in the host response (Lin & Martin, 2005; Kvitko et al., 2009; Rosli et al., 2013). In the hpPti1 lines, the transcript levels of *Pti1a* and *Pti1b* were reduced to about 35% and 25%, respectively, of the level in the azygous control line (Figure 2.4B; Figure 2.5A). We

Figure 2.3 ***(previous page).*** Silencing *Pti1* compromises PTI in *N. benthamiana*. **(A)** Phylogenetic tree based on nucleotide sequences showing the relationship of the four *Pti1* genes in *N. benthamiana*, *NbPti1a*, *NbPti1b*, *NbPti1c*, and *NbPti1d*, to the two *Pti1* genes in tomato, *SlPti1a* and *SlPti1b*. Bootstrap percentages are indicated at the branches. Transcript abundance (as mean RPKM from 3 replicates) for each *NbPti1* gene in mock treated *N. benthamiana* leaves is shown (Pombo et al., 2014). **(B)** *N. benthamiana* seedlings were inoculated with tobacco rattle virus-based VIGS constructs for EC1 (negative control), NbFLS2 (positive control), NbP1, or NbP2 (each construct was designed to silence all four *NbPti1* genes). Six weeks later, leaves of these plants were syringe-infiltrated with non-pathogenic *Pf* 55 (black circles) to induce PTI, followed 7 h later with disease-causing *Pst* DC3000 Δ*hopQ1-1* (yellow circles) in partially overlapping areas. Compromised induction of PTI by *Pf* 55 as a result of gene silencing leads to faster disease development in the overlapping region. Photographs of representative plants were taken 5 days after infiltration. **(C)** Quantification of disease development in silenced leaves shown in (B). Leaf circles with more than 25% of the overlapping area showing cell death were counted as having disease. For each silencing construct 7 plants were used with 2 leaves per plant and 4 circles per leaf for a total of 56 overlapping circles. Scoring was done 5 days after infiltration. Asterisks indicate significant differences compared to the EC1 control group using Fisher's exact test. P values are <0.0001 for NbFLS2, <0.0001 for NbP1, and 0.004 for NbP2. This experiment was performed twice with similar results. **(D)** qPCR assay to determine the degree of silencing of the *NbPti1* genes in *N. benthamiana* VIGS plants. The oligonucleotides were designed to detect *NbPti1a*, *NbPti1b*, and *NbPti1c*, but sequencing of the PCR products confirmed amplification of transcripts from only *NbPti1b* and *NbPti1c*. Transcript levels of *NbPti1b/c* in each plant were normalized to *PP2A* (Liu et al., 2012) and are shown in relation to the EC1 control group. *EF1a* is shown as an internal control. Each group contained 4 or 5 plants. Graph shows mean ± 95% confidence interval. Asterisks indicate significant differences compared to the control group based on a Kruskal-Wallis test followed by a Steel-Dwass post hoc test. P values are 0.0376 for NbP1 and 0.0232 for NbP2.

also inoculated plants of each hpPti1 line with *Pst* DC3000 Δ*avrPto* Δ*avrPtoB* to compare their disease symptoms and bacterial populations with azygous and RG-prf3 control plants. Severe disease symptoms were observed on hpPti1 plants compared to azygous and RG-prf3 plants which developed only moderate disease (Figure 2.4C; Figure 2.5B). The hpPti1 plants supported about three-fold higher bacterial populations compared to the azygous and RG-prf3 control plants (Figure 2.4D; Figure 2.5C). Together, these observations indicate that in tomato, one or both of the Pti1 kinases contribute to PTI acting against *Pst* DC3000 Δ*avrPto* Δ*avrPtoB*.

RNA-Seq analysis reveals overlap between genes induced by the Pti1 proteins and PTI

To gain insight into the possible roles of Pti1a and Pti1b we further analyzed our RNA-Seq data from the two hpPti1 lines treated with *Pst* DC3000 Δ*avrPto* Δ*avrPtoB* to identify genes whose transcript abundance is either reduced or increased in the absence of these kinases. We observed that more genes were affected in the multi-copy hpPti1 line (F10-10) than in the single-copy line (F27-36), possibly due to off-target silencing (Figure 2.6A). Because both hpPti1 lines showed the same degree of compromised resistance to *Pst*, we focused on the subset of genes affected in both lines. There were only 26 genes whose transcript abundance was less in both hpPti1 lines (i.e., their expression was induced in the presence of Pti1a and Pti1b), and only 11 genes whose transcript abundance was greater in both hpPti1 lines (i.e., their expression was suppressed in the presence of Pti1a and Pti1b; Figure 2.6A). Some of the genes with reduced transcript abundance have been implicated in defense responses, including the pathogenesis-related (*PR*)-*1b* gene that was recently reported to play an important role in *Pst* resistance in tomato (Chen et al., 2014b) (Figure 2.6B). To more generally investigate whether

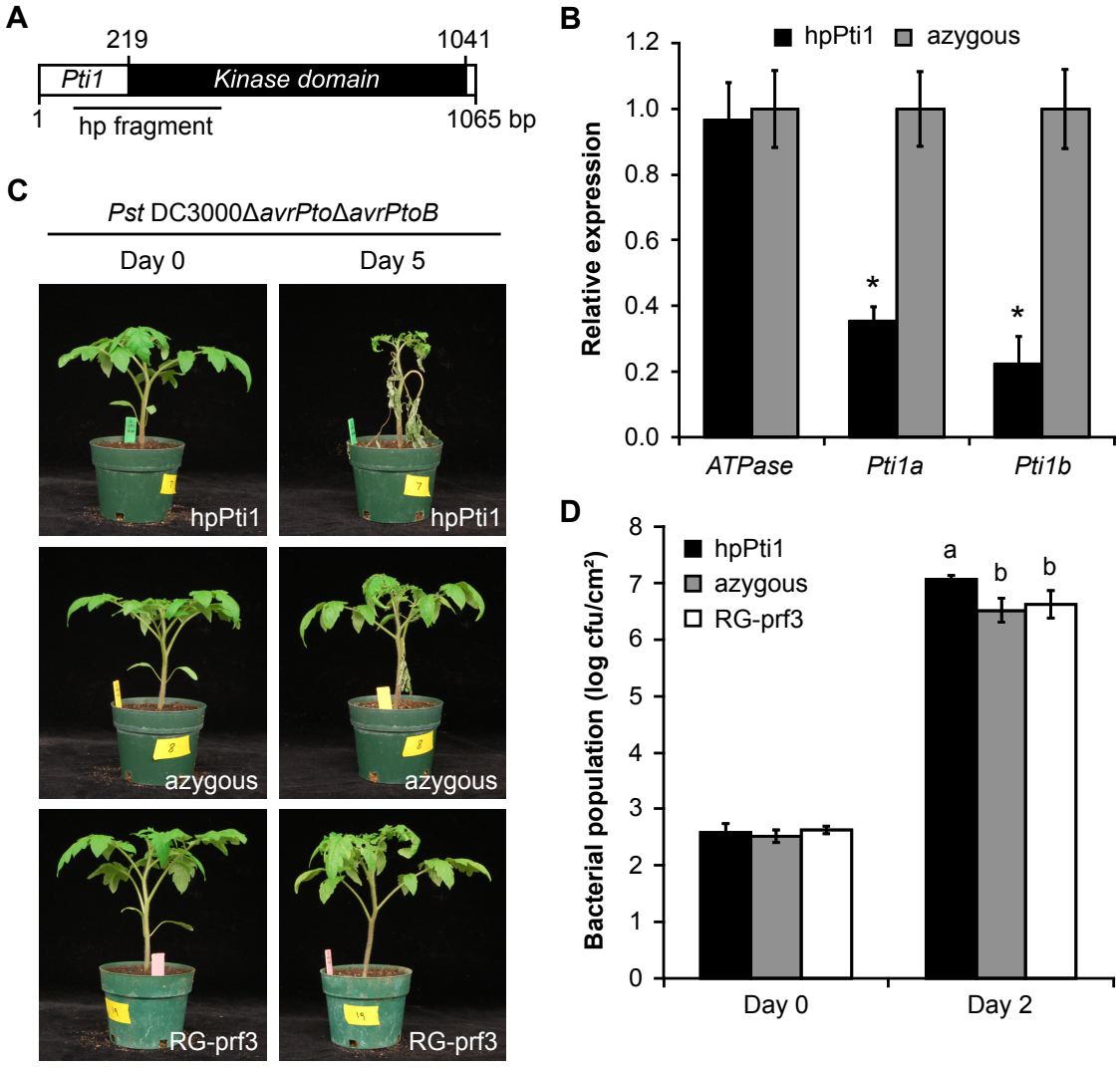

these differentially regulated genes are associated with PTI, we compared them with our previously published set of genes that are induced or suppressed after treatment with the MAMP flgII-28 (Cai et al., 2011; Rosli et al., 2013). Of the 26 genes with increased transcript abundance when the Pti1 kinases were present, 19 were also induced by flgII-28 (73%), and of the 11 genes with reduced transcript abundance none were suppressed by flgII-28; there are also 5 Pti1-suppressed genes induced by flgII-28. Gene Ontology (GO) term analysis of the 26 Pti1-induced and 11 Pti1-suppressed genes showed the former to be predominantly associated with

Figure 2.4 ***(previous page).*** Transgenic tomato plants silenced for *Pti1a* and *Pti1b* are more susceptible to infection by *Pst* DC3000 Δ*avrPto* Δ*avrPtoB*. **(A)** Schematic representation of the tomato *Pti1a* and *Pti1b* genes with the kinase domain highlighted in black. The numbers indicate nucleotide positions of the 5' and 3' ends and the location of the kinase domain. The origin of the hp fragment is shown below the gene. **(B)** Relative transcript abundance of *Pti1a* and *Pti1b* in homozygous single-copy hpPti1 plants (F27-36) compared to azygous control plants. *ATPase* is shown as a control. Transcript levels are based on RNA-Seq reads from the 6 h dataset of 3 plants per genotype normalized to *CBL1* (Pombo et al., 2014). Bars show mean ± 99% confidence interval. Asterisks indicate significant differences between hpPti1 and azygous plants. *P* values are <0.0001 for both *Pti1a* and *Pti1b* (based on a false discovery rate correction). **(C)** Four week-old transgenic hpPti1 plants (F27-36) along with azygous control plants and progenitor RG-prf3 plants were vacuum-infiltrated with 5 x 10^4 cfu/ml *Pst* DC3000 Δ*avrPto* Δ*avrPtoB* and disease symptoms monitored. Photographs of the same representative plants are shown before infiltration (Day 0) and 5 days after infiltration (Day 5). Seven plants for each genotype were tested. **(D)** Bacterial populations were determined in the plants shown in (C). Samples were taken after infiltration (Day 0) and 2 days later (Day 2). Bars show the mean ± 99% confidence interval. Different letters indicate significant differences based on a one-way ANOVA followed by Tukey's HSD post hoc test. *P* values are 0.0002 for hpPti1 vs azygous and 0.0019 for hpPti1 vs RG-prf3. This experiment was performed 4 times with similar results.

plant defense whereas the latter are associated with biosynthetic and metabolic processes (Figure 2.6C). These analyses are consistent with our disease and bacterial population assays in supporting a role for one or both of the Pti1 kinases in the PTI response to *Pst*.

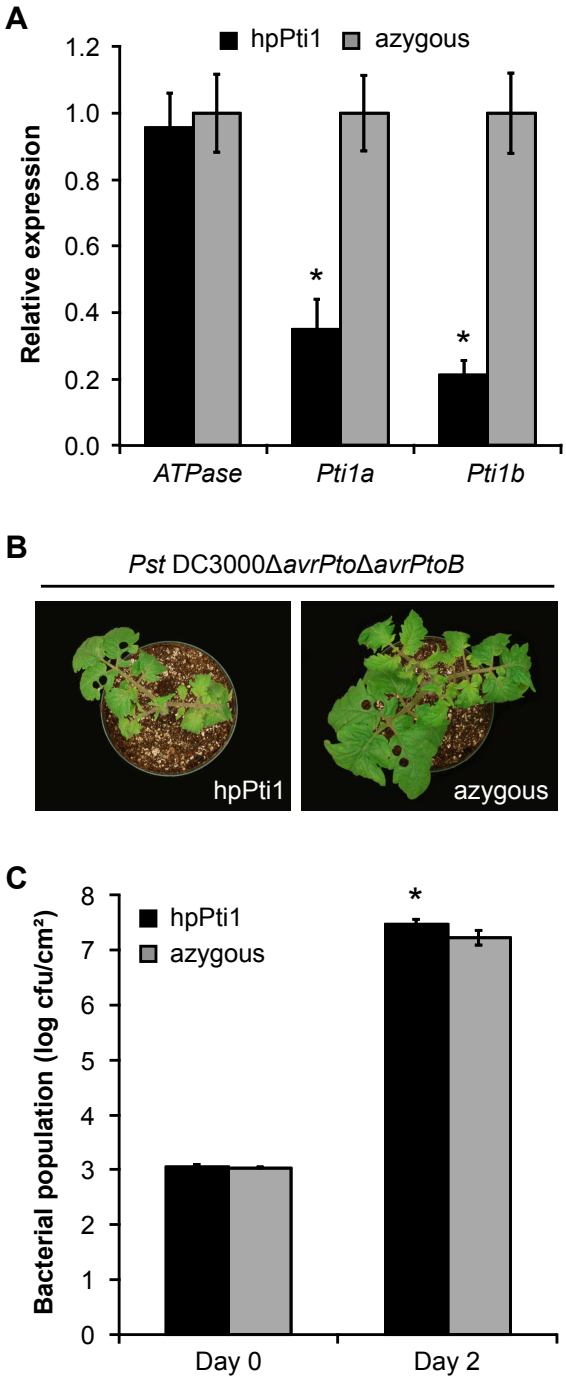
A
hpPti1
azygous
Relative expression
1.2
1.0
0.8
0.6
0.4
0.2
0.0
*
*
ATPase
Pti1a
Pti1b
B
Pst DC3000ΔavrPtoΔavrPtoB
hpPti1
azygous
C
Bacterial population (log cfu/cm²)
hpPti1
azygous
8
7
6
5
4
3
2
1
0
*
Day 0
Day 2

Figure 2.5 ***(previous page).*** The multi-copy hpPti1 line F10-10 is more susceptible to *Pst* DC3000 Δ*avrPto* Δ*avrPtoB* infection. **(A)** Relative transcript abundance of *Pti1a* and *Pti1b* in homozygous multi-copy hpPti1 plants (F10-10) compared to azygous control plants. *ATPase* is shown as a control. Transcript levels are based on RNA-Seq reads from the 6 h dataset of 3 plants per genotype normalized to *CBL1* (Pombo et al., 2014). Bars show mean ± 99% confidence interval. Asterisks indicate significant differences between hpPti1 and azygous plants. *P* values are <0.0001 for both *Pti1a* and *Pti1b* (based on a false discovery rate correction). **(B)** Four week-old transgenic hpPti1 plants (F10-10) along with azygous control plants were vacuum-infiltrated with 5 x 10^4 cfu/ml *Pst* DC3000 Δ*avrPto* Δ*avrPtoB* and disease symptoms monitored. Photographs of representative plants are shown 5 days after infiltration. Four plants for each genotype were tested. **(C)** Bacterial populations were determined in the plants shown in (B). Samples were taken after infiltration (Day 0) and 2 days later (Day 2). Bars show mean ± 99% confidence interval. The asterisk indicates a significant difference compared to the control group based on a Student's *t*-test (P =0.0217). This experiment was performed 3 times with similar results.

Silencing of *Pti1a* and *Pti1b* negatively impacts ROS production associated with PTI

Flagellin-derived peptides (i.e., flg22 and flgII-28) are important MAMPs associated with *Pst*-induced PTI in both tomato and *N. benthamiana* (Chakravarthy et al., 2010; Rosli et al., 2013) To further investigate a role of the Pti1 kinases in PTI we used two standard assays for the host response to these peptides: activation of MAPK cascades and generation of ROS (Chakravarthy et al., 2010; Nguyen et al., 2010a). Because we observed no difference in silencing efficiency or disease susceptibility between the single- and the multi-copy hpPti1 lines, we performed these assays with only the single-copy line (F27-36). To detect MAPK activation, leaf discs were incubated with either flg22, flgII-28, or water as a control and phosphorylated MAPKs were detected with an antibody. Although both

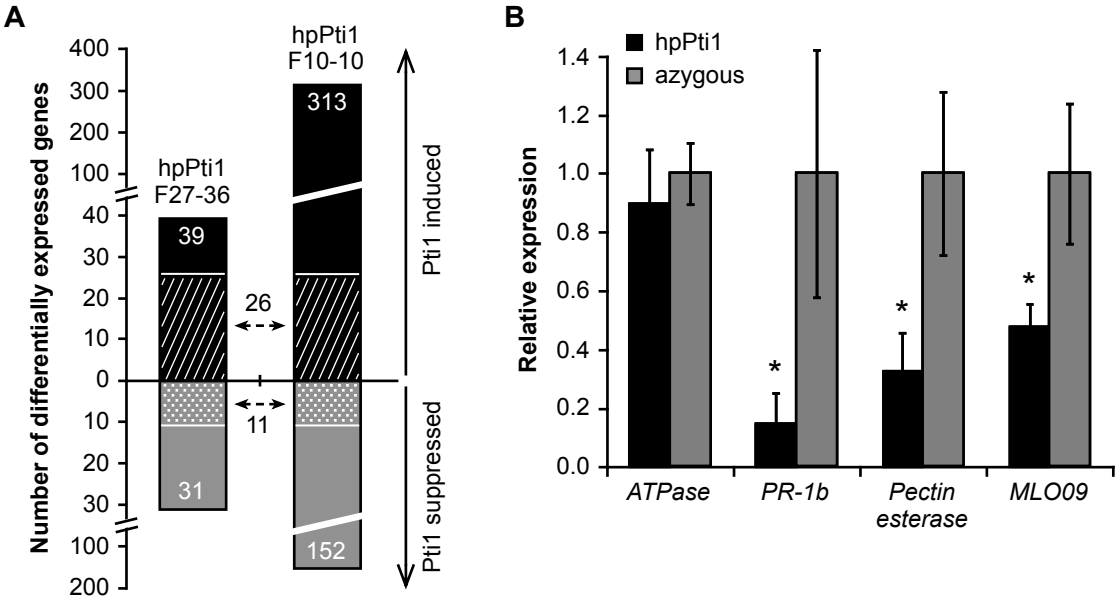

C

Group	GO term	Group %	Genome %	*P* value
Pti1 induced	Response to biotic stimulus	57.69	16.73	1.42E-03
(26 genes)	Response to endogenous stimulus	61.54	19.84	2.07E-03
	Response to other organism	53.85	16.30	6.69E-03
	Defense response	53.85	16.90	1.03E-02
	Response to hormone stimulus	57.69	19.60	1.08E-02
Pti1 suppressed	Regulation of carbohydrate biosynthetic process	45.45	0.75	2.07E-06
(11 genes)	Regulation of carbohydrate metabolic process	45.45	1.02	9.64E-06
	Regulation of glucosinolate biosynthetic process	36.36	0.43	2.27E-05
	Regulation of sulfur metabolic process	36.36	0.49	3.65E-05
	Sterol biosynthetic process	45.45	1.78	1.52E-04

flg22 and flgII-28 induced MAPK phosphorylation, there was no difference in this response between the hpPti1 and azygous control plants at the lowest concentration of each peptide that reliably activated MAPKs (10 nM for flg22 and 25 nM for flgII-28; Figure 2.7A). To measure ROS production we used leaf discs in a chemiluminescence-based assay (Chakravarthy et al., 2010; Clarke et al., 2013). We observed a reduction in ROS production to approximately 50% in hpPti1 plants compared to azygous control plants despite using relatively high concentrations of

Figure 2.6 ***(previous page).*** Genes whose expression is induced by Pti1 after *Pst* treatment are associated with PTI. **(A)** Number of genes whose expression is significantly induced or suppressed by Pti1 (P <0.05, based on a false discovery rate correction) after treatment with *Pst* DC3000 Δ*avrPto* Δ*avrPtoB* in either the single-copy hpPti1 line (F27-36) or the multi-copy hpPti1 line (F10-10). Differentially expressed genes from the 3 h and 6 h datasets were combined for each line and duplicate genes removed. The number of genes in common between the two lines is shown as patterned boxes (i.e., 26 induced and 11 suppressed). **(B)** Transcript abundance of three of the genes with reduced expression in both hpPti1 lines (i.e., genes that are normally induced by Pti1 after *Pst* treatment): *PR-1b* (Solyc00g174340) (Chen et al., 2014b), a pectin esterase gene (Solyc09g075330), and *MLO09* (Solyc11g069220) (Chen et al., 2014a). Expression levels were normalized to *CBL1* (Pombo et al., 2014) and *ATPase* is shown as an internal control. Bars show mean ± 99% confidence interval calculated from the RNA-Seq reads from the 3 h dataset of the single-copy hpPti1 line (F27-36) compared to the azygous control line. Asterisks indicate significant differences in transcript abundance between hpPti1 and azygous control plants. P values are 0.0027 for *PR-1b*, 0.0001 for the pectin esterase gene, and 0.0007 for *MLO09* (based on a false discovery rate correction). **(C)** The genes shown in (A) that are in common between the two hpPti1 lines were subjected to a GO term analysis. Shown are the top five GO terms for both the Pti1-induced genes and the Pti1-suppressed genes. The group percentage shows the frequency of a given GO term in the analyzed set of genes. The genome percentage shows the overall frequency of that GO term in the tomato genome. P values are based on a false discovery rate correction.

flg22 and flgII-28 (100 nM each; Figure 2.7B). These observations suggest that one or both of the tomato Pti1 kinases function in a signaling pathway activated by flagellin perception upstream of ROS production, but independent of the MAPKs monitored by this assay.

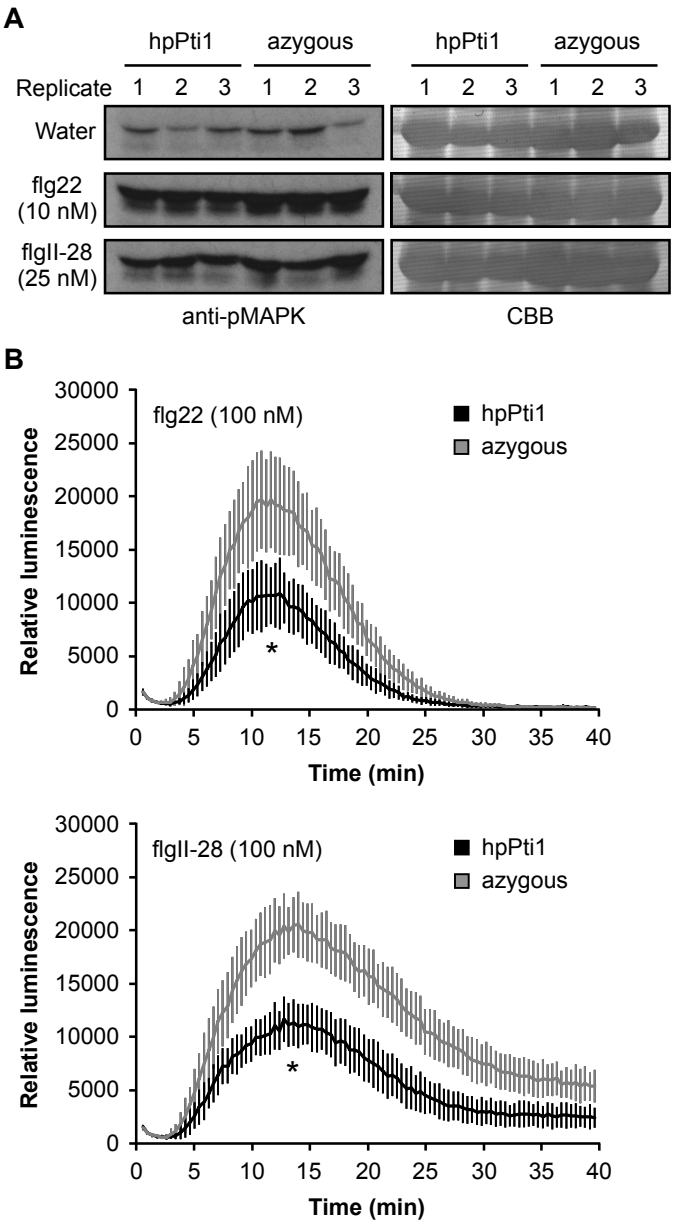
A
hpPti1
azygous
hpPti1
azygous
Replicate 1 2 3 1 2 3 1 2 3 1 2 3
Water
flg22
(10 nM)
flgII-28
(25 nM)
anti-pMAPK
CBB
B
flg22 (100 nM)
hpPti1
azygous
Relative luminescence
Time (min)
flgII-28 (100 nM)
hpPti1
azygous
Relative luminescence
Time (min)

Figure 2.7 ***(previous page).*** Silencing of the *Pti1* genes in tomato diminishes the production of ROS in response to two flagellin-derived MAMPs. **(A)** Leaf discs from hpPti1 or azygous plants were treated with water, 10 nM flg22, or 25 nM flgII-28 and examined for MAPK activation. Protein was extracted from treated leaf discs 10 min after treatment and subjected to immunoblotting using an antibody (anti-pMAPK) that detects phosphorylated (activated) MAPKs. Shown are 3 biological replicates for each treatment. CBB, coomassie brilliant blue staining to show equal loading of protein. This experiment was performed twice with similar results. **(B)** Leaf discs from hpPti1 or azygous plants were treated with 100 nM flg22 (top) or 100 nM flgII-28 (bottom) and production of ROS was measured using a chemiluminescence-based assay. Graphs show mean ± 99% confidence interval of seven plants per genotype. Asterisks indicate significant differences in the calculated areas under the curve between hpPti1 and azygous control plants based on a Student's *t*-test. *P* values are 0.0004 for flg22 and <0.0001 for flgII-28. This experiment was performed 3 times with similar results.

Transient complementation demonstrates that either Pti1a or Pti1b can restore ROS production to the hpPti1 plants

In addition to the intended gene(s), RNAi can silence other non-target genes, possibly leading to misinterpretations (Senthil-Kumar & Mysore, 2011). To determine if the reduced ROS production in response to flg22 and flgII-28 is indeed due to silencing the *Pti1* genes, we developed synthetic *Pti1a* and *Pti1b* genes that would not be silenced by the hpPti1 construct (Kumar et al., 2006; Wu et al., 2016). Specifically, the 5' portion of each gene was altered to have minimal complementarity to the hpPti1 fragment without any changes to the encoded amino acid sequence and fused to the 3' wild-type sequence of the respective gene (Figure 2.8A; Figure 2.9). To verify that these synthetic *Pti1* variants, referred to as *synPti1a* and *synPti1b*, are expressed and evade silencing, we transiently expressed *synPti1a* and *synPti1b* or wild-type *Pti1a* and *Pti1b* in *N. benthamiana*

leaves in the presence of the hpPti1 construct (Figure 2.8B). Accumulation of the synthetic variants was not significantly different from the wild-type proteins when co-expressed with the unrelated hpBti9 construct (Zeng et al., 2011). However, when co-expressed with the hpPti1 construct, accumulation of the wild-type Pti1 proteins was strongly diminished whereas the synthetic Pti1 variants accumulated to similar levels as with the hpBti9 construct, indicating the synthetic genes are not targeted by the hpPti1 fragment (Figure 2.8B). We then transiently expressed *synPti1a* and *synPti1b* in leaves of single-copy hpPti1 tomato plants, using the gene encoding yellow fluorescent protein (YFP) in hpPti1 and azygous plants as negative and positive control, respectively (Figure 2.8C). ROS production in response to flg22 increased in the presence of either *synPti1a* or *synPti1b* comparable to that in the positive control. Thus, silencing of *Pti1a* and *Pti1b* in the hpPti1 lines, and not silencing of non-target genes, leads to decreased ROS production and presumably enhanced *Pst* susceptibility.

Pti1 proteins localize to the cell periphery and S-acylation on cysteine residues 6 and 7 is implicated in this localization

Localization experiments of Pti1-like proteins in maize determined that *Zm*Pti1a localizes to the plasma membrane in onion epidermal cells, whereas an N-terminal truncation missing the first 20 amino acids was diffusely localized throughout the cell (Herrmann et al., 2006). Similarly, substitutions of glycine-2 as well as the cysteines at positions 3, 6, and 7 abolished plasma membrane localization, indicating that these residues are myristoylated and S-acylated, respectively (Herrmann et al., 2006; Boyle & Martin, 2015). More recently, the rice Pti1 ortholog *Os*Pti1a was shown to localize to the plasma membrane in rice protoplasts and this localization was dependent on the predicted S-acylation sites C6 and C7 (Matsui et al., 2014)

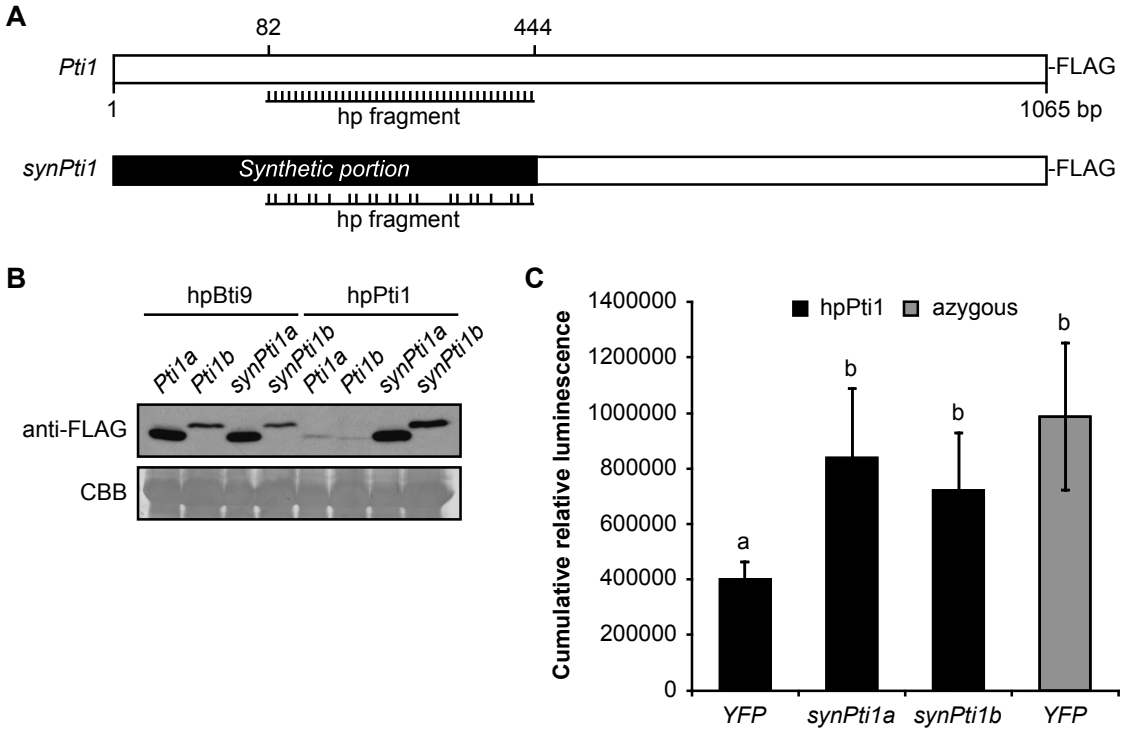

The C6 and C7 residues are conserved in the tomato Pti1 proteins and we introduced serine substitutions to test their importance in subcellular localization (Figure 2.10A). We transiently expressed wild-type *Pti1a* and *Pti1b* along with variants encoding C6S/C7S substitutions fused to *YFP* in leaves of *N. benthamiana* (Figure 2.10B). The wild-type proteins localized to the cell periphery, whereas the C6S/C7S mutants showed a more diffuse localization with obvious accumulation in the nuclei. YFP, included as a control, also accumulated in the nucleus in addition to the cytoplasm (Figure 2.10B). Because the C6 and C7 residues are predicted S-acylation sites, it is possible that the peripheral localization of wild-type Pti1 is due to S-acylation. Tomato Pti1a was previously reported to have a diffuse localization when transiently expressed in onion epidermal cells and this observed discrepancy might be due to differences in the experimental system (Herrmann et al., 2006).

Figure 2.8 ***(previous page).*** Synthetic *Pti1* genes restore ROS production in hpPti1 plants in response to flg22. **(A)** Illustration showing where the hp fragment anneals to the wild-type *Pti1* transcript. Synthetic versions of the tomato *Pti1* genes, referred to as *synPti1a* and *synPti1b*, were made by synthesizing the 5' portion of each gene with alternate codons (black) so that the hp fragment is no longer able to anneal. This synthetic portion was then fused to the 3' wild-type sequence (white) by PCR. The *synPti1* genes encode the same amino acid sequences as the wild-type *Pti1* genes and all constructs included a FLAG-tag at the C-terminus. **(B)** Wild-type and synthetic versions of *Pti1a* and *Pti1b* were transiently expressed in *N. benthamiana* leaves using agroinfiltration together with either the hpPti1 fragment or the unrelated hpBti9 fragment (Zeng et al., 2011). Tissue samples were collected 2 days after infiltration, total protein extracted, and Pti1 proteins detected by anti-FLAG immunoblotting. CBB, coomassie brilliant blue staining to show equal loading of protein. **(C)** Agroinfiltration was used to transiently express *synPti1a* and *synPti1b* in leaves of hpPti1 tomato plants along with *YFP* (negative control). Azygous plants transiently expressing *YFP* served as a positive control. Leaf discs were treated with 100 nM flg22 and production of ROS measured. Graph shows the cumulative relative luminescence (area under the curve). Bars show mean ± 99% confidence interval of 8 plants per group. Different letters indicate significant differences based on a one-way ANOVA followed by Tukey's HSD post hoc test. P values are 0.0030 for hpPti1+*synPti1a* vs hpPti1+*YFP*, 0.0375 for hpPti1+*synPti1b* vs hpPti1+YFP, and 0.0002 for hpPti1+*YFP* vs azygous+*YFP*. This experiment was performed twice with similar results.

Neither Pti1a nor Pti1b play a demonstrable role in Pto-mediated resistance to *Pst* in tomato

As explained above, Pti1a was originally discovered in a yeast two-hybrid screen as an interactor of Pto and thought to function in Pto-mediated resistance (Zhou et al., 1995). In light of our finding that one or both of the Pti1 kinases play a role in PTI, we used our hpPti1 line to examine a possible role of these kinases in the Pto resistance pathway in tomato. Recognition of AvrPto in tomato requires

Figure 2.9. Synthetic *Pti1* gene sequences have much reduced nucleotide identity compared to their wild-type sequences. Alignment of the nucleotide sequence of the synthetic portion of *Pti1a* (*synPti1a*, top) and *Pti1b* (*synPti1b*, bottom) with the respective wild-type sequence. Alignments were performed with MUSCLE and visualized using GeneDoc. Identical residues are shown in black.

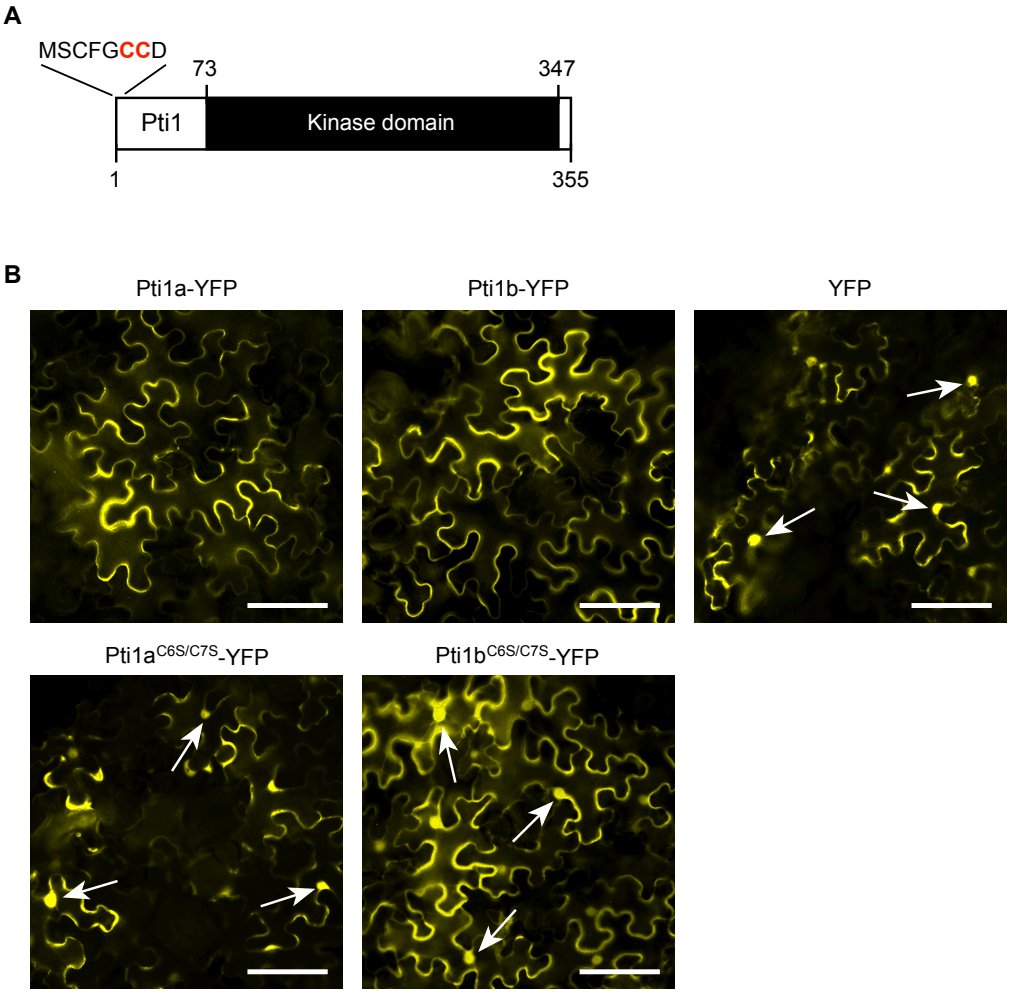

Figure 2.10. Ptil contains predicted S-acylation sites and is localized to the cell periphery. **(A)** Schematic representation of the tomato Pti1a and Pti1b proteins with the kinase domain shown in black. The amino acid sequence at the beginning of each protein is indicated with the cysteine-6 (C6) and cysteine-7 (C6) residues highlighted in red. The numbers show the amino acid position of the kinase domain as well as the N- and C-terminus of the protein. **(B)** *YFP* fusions of wild-type *Pti1a* and *Pti1b* along with mutants encoding the C6S/C7S substitutions were transiently expressed in *N. benthamiana* leaves using agroinfiltration. Free *YFP* was included as a control. Tissue samples were visualized with an epifluorescence microscope 2 days after infiltration. The white arrows indicate protein accumulation in the nuclei. Bars = 50 µM. False colors are shown.

both Pto and the nucleotide-binding leucine-rich repeat protein Prf (Martin et al., 1993; Salmeron et al., 1994; Scofield et al., 1996; Tang et al., 1996; Salmeron et al., 1996). The hpPti1 line was made in the susceptible RG-prf3 background which is homozygous for *Pto* but has a deletion in *Prf*, rendering the gene non-functional (Salmeron et al., 1996). Therefore, we crossed RG-PtoR (homozygous for both *Pto* and *Prf*) with hpPti1 plants to obtain F1 plants that contain a single functional copy of *Prf*, one copy of the hpPti1 silencing fragment, and two copies of *Pto*. As a control, we crossed RG-PtoR with RG-prf3 plants which resulted in F1 plants identical to the RG-PtoR x hpPti1 cross except that no hpPti1 construct is present.

The F1 plants were inoculated with *Pst* DC3000 (expressing *avrPto* and *avrPtoB*) at two titers (10^5 or 10^6 cfu/ml) and disease symptoms were documented and bacterial populations measured on days 3 and 2, respectively. No difference in Pto-mediated resistance was observed between the F1 plants either carrying or lacking the hpPti1 construct (Figure 2.11A and 2.11B). At the lower inoculum concentration all of the plants exhibited strong Pto/Prf-mediated resistance to *Pst* whereas, as expected, at the higher inoculum concentration the plants carrying only a single copy of *Prf* developed mild disease symptoms and showed increased bacterial growth since Pto/Prf-mediated resistance is known to be semi-dominant (Carland & Staskawicz, 1993) (Figure 2.11A and 2.11B).

It is possible that residual Pti1 protein is present due to incomplete silencing and is sufficient to fully activate the Pto/Prf pathway. Therefore, we performed a second set of inoculations using the same bacterial concentrations with resistant RG-PtoR plants and a transgenic line containing an RNAi construct that silences *Pto* in the RG-PtoR background (hpPto) (Pascuzzi, 2006). RG-PtoR has two copies of *Pto* and *Prf* and showed no signs of disease at either inoculum level (Figure 2.11A). The hpPto plants were highly susceptible, showing that silencing

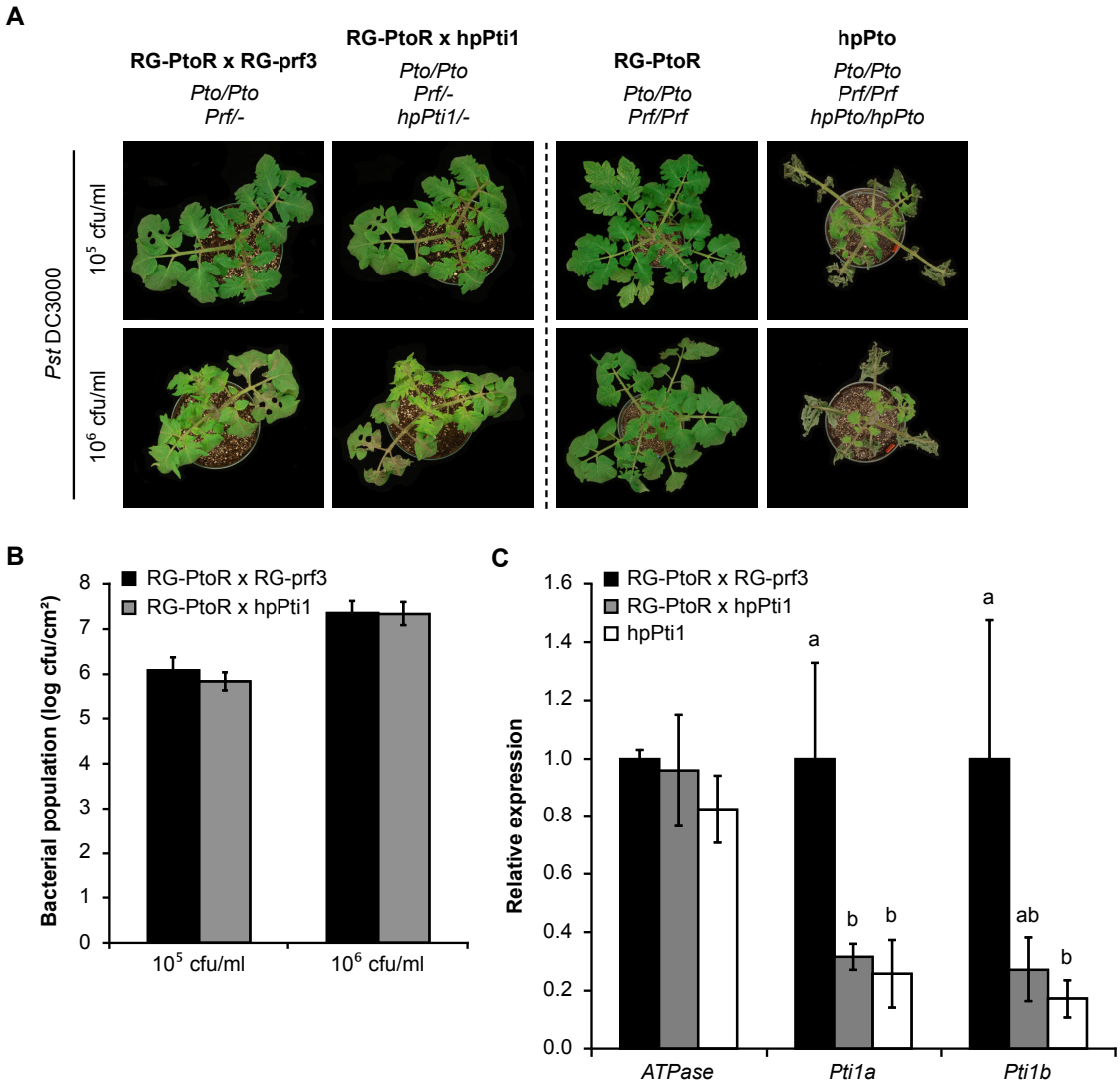

a gene directly involved in the Pto pathway leads to a complete loss of Pto/Prf-mediated resistance even when two copies of *Pto* and *Prf* are present (Figure 2.11A).

The question remained whether a single copy of the hpPti1 fragment is sufficient to effectively silence the two *Pti1* genes and whether the level of silencing is comparable to silencing of *Pto* by the hpPto construct. To address these issues, we first compared *Pti1* transcript abundance in RG-PtoR x hpPti1 F1 plants and the transgenic hpPti1 line and found that there is no significant difference in si-

Figure 2.11 ***(previous page).*** Pto-mediated resistance is not detectably impaired in hpPti1 plants. **(A)** Four week-old RG-PtoR x hpPti1 and RG-PtoR x RG-prf3 F1 plants were vacuum-infiltrated with *Pst* DC3000 at 10^5 cfu/ml or 10^6 cfu/ml and disease symptoms monitored. RG-PtoR and hpPto plants were included as resistant and susceptible controls, respectively. Photographs were taken 3 days after infiltration. Experiments involving RG-PtoR F1 plants used 4 plants per genotype and the RG-PtoR and hpPto experiments used 3 plants each. The dashed line indicates experiments performed on different days. **(B)** Bacterial populations were determined in the plants from (A). Tissue samples were taken 2 days after infiltration. Bars show mean ± 99% confidence interval. No significant difference was found in either treatment. This experiment was performed twice with similar results. **(C)** qPCR to monitor transcript levels of *Pti1a* and *Pti1b* in the F1 plants. Expression data were normalized to *CBL1* Pombo:2014fu and are shown in relation to the RG-PtoR x RG-prf3 control group. *ATPase* is shown as an internal control. Bars show mean ± 95% confidence interval of 4 plants per group. Homozygous hpPti1 plants were included for comparison. Different letters indicate significant differences based on a Brown-Forsythe test followed by a Games-Howell post hoc test. *P* values for *Pti1a* are 0.024 for RG-PtoR x RG-prf3 vs RG-PtoR x hpPti1 and 0.014 for RG-PtoR x RG-prf3 vs hpPti1 and *P* values for *Pti1b* are 0.054 for RG-PtoR x RG-prf3 vs RG-PtoR x hpPti1 and 0.040 for RG-PtoR x RG-prf3 vs hpPti1

lencing efficacy, as both lines have reduced *Pti1a* and *Pti1b* mRNA levels of about 30% compared to the RG-PtoR x RG-prf3 control F1 plants (Figure 2.11C). Second, we compared the hpPto plants to RG-PtoR plants and found that transcript abundance of *Pto* was reduced to about 10% in the presence of the silencing fragment (Figure 2.12). In conclusion, although *Pti1* transcripts are reduced to only 30% of wild-type levels in the RG-PtoR x hpPti1 F1 plants, we see no effect on Pto/Prf-mediated resistance indicating that neither Pti1a nor Pti1b demonstrably contribute to this ETI response.

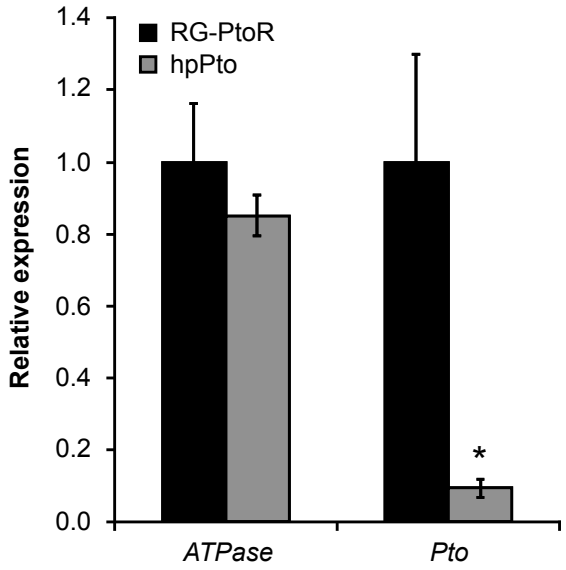

Figure 2.12. qPCR to measure transcript abundance of *Pto* in wild-type RG-PtoR and in a hpPto line. Data were normalized to *CBL1* (Pombo et al., 2014) and are shown in relation to the RG-PtoR control group. *ATPase* is shown as an internal control. Bars show mean ± 99% confidence interval of 4 plants per genotype. The asterisk indicates a significant difference (P =0.0042) compared to the control group based on a Welch's test (unequal variance t-test).

2.5 Discussion

We have found that transgenic tomato plants silenced for *Pti1* are more susceptible to infection by *Pst* DC3000 Δ*avrPto* Δ*avrPtoB*, fail to express the *PR-1b* gene normally induced during the PTI response, and have reduced ROS production in response to flagellin-derived peptides. Collectively, these observations support a role for Pti1 in PTI. Here we place our findings in the context of previous work on Pti1 and Pti1-related genes and discuss possible mechanisms by which the tomato Pti1 kinases might contribute to PTI. We also speculate on why Pti1 was originally identified as an interactor of the Pto kinase.

Previous work with transgenic tobacco plants overexpressing tomato *Pti1a* reported faster development of PCD in response to *P. syringae* pv. *tabaci* expressing

avrPto compared to control plants (Zhou et al., 1995). This phenomenon was attributed to amplification of the Pto resistance pathway due to overexpression of *Pti1a*, whose protein was thought to function downstream of Pto (Zhou et al., 1995). However, later work did not support this finding when it was determined that in tomato Pto recognizes the CD loop in the core domain of AvrPto whereas in tobacco an unknown R protein recognizes the phosphorylated C-terminal domain (CTD) of the effector (Anderson et al., 2006; Xing et al., 2007; Yeam et al., 2010). There are at least two explanations for the observation that *Pti1a* overexpression appeared to enhance the ETI response in tobacco. First, Pti1a may function downstream of the unknown R protein in tobacco that recognizes the AvrPto CTD. Second, it is possible that the overexpression of tomato *Pti1a* in tobacco had a 'dominant-negative' effect which interfered with the PTI response. Interference in PTI leads to enhanced delivery of effectors into the plant cell and faster PCD (Crabill et al., 2010; Oh et al., 2010b). We do not currently have evidence to support or refute either of these possibilities. Although it might be interesting to further study the enhanced PCD response in *Pti1a*-transgenic tobacco lines, tomato is better suited to study Pto-mediated ETI and our RG-PtoR x hpPti1 and RG-PtoR x RG-prf3 crosses clearly indicated that Pti1 is not required for the ETI response activated in tomato upon recognition of AvrPto or AvrPtoB. This is consistent with previous observations that also did not support a role for Pti1 in the Pto pathway in tomato (Xiao et al., 2003; Wu et al., 2004). Although the data from our experiments are convincing, it is possible that residual Pti1 protein present in the RG-PtoR x hpPti1 plants is sufficient to activate Pto-mediated resistance. To address this possible limitation, we are developing CRISPR/Cas9 lines with null mutations in both *Pti1* genes and expect that these plants will provide a definitive answer regarding the involvement of Pti1 in Pto-mediated ETI.

Several studies in rice have examined a role for the Pti1 ortholog *Os*Pti1a in resistance to the rice blast fungus *Magnaporthe grisea* as well as to *Xanthomonas oryzae* pv. *oryzae* (*Xoo*), the causal agent of bacterial blight (Takahashi et al., 2007; Matsui et al., 2010a,b, 2014). Rice plants with transposon-induced mutations in *OsPti1a* have a dwarf phenotype, form spontaneous lesions, show enhanced resistance to a compatible race of *M. grisea*, and have increased *PR* gene expression. These observations suggested that *Os*Pti1a negatively regulates PTI responses in rice. Overexpression of *OsPti1a* led to lesion development (disease) by an incompatible race of *M. grisea* and enhanced lesion formation after inoculation with a compatible strain of *Xoo*, indicating that *Os*Pti1a also represses ETI responses and further supported its role as a negative regulator of PTI (Takahashi et al., 2007). Silencing *RAR1*, whose protein is a component of several R protein complexes (Shirasu, 2009), negated the dwarf phenotype of rice *pti1a* mutant plants and abolished both constitutive *PR* gene expression and the enhanced lesion formation by the compatible race of *M. grisea*, thus showing that repression of immune signaling by *Os*Pti1a is dependent on RAR1 (Takahashi et al., 2007).

The results regarding *Os*Pti1a are in seeming conflict with our data showing a positive regulatory function for Pti1 in the tomato PTI response. Despite the apparent opposite function of Pti1 in rice and tomato, the two proteins function interchangeably in complementing the *pti1a* rice plants (Takahashi et al., 2007). The proposed explanation for this discrepancy is that the signaling pathways downstream of Pti1 have diverged in monocotyledonous rice and dicotyledonous tomato (Takahashi et al., 2007). Given the large evolutionary distance between the two species, this is a plausible hypothesis. However, an alternative explanation is that the lesion-mimic and dwarf phenotypes in *pti1a* rice plants are due to the effects of an R protein that normally guards *Os*Pti1a. Absence of *Os*Pti1a in null mutants

might trigger an ETI response that results in the observed autoimmune phenotypes. This would explain the enhanced resistance to the compatible race of *M. grisea* because it is an obligate biotrophic pathogen and the hypersensitive response restricts its growth (Greenberg, 1997). Such a scenario is reminiscent of RIN4 in Arabidopsis, which is guarded by two R proteins, RPM1 and RPS2 (Mackey et al., 2002; Axtell & Staskawicz, 2003; Mackey et al., 2003). RPS2 detects cleavage of RIN4 by the *Pst* effector AvrRpt2 and activates ETI (Axtell & Staskawicz, 2003; Mackey et al., 2003). Arabidopsis plants with a *rin4* null mutation are seedling-lethal because of constitutive activation of RPS2 unless they also contain a *rps2* null mutation (Mackey et al., 2003). If Pti1 does have a similar function in rice and tomato, then it is possible that the tomato variety we have used in our studies lacks an R protein that guards Pti1 or that our hpPti1 plants are not null mutants and therefore the ETI response is not autoactivated, explaining why our hpPti1 plants do not show stunted growth or autoimmune phenotypes. The *N. benthamiana* Pti1 seems to be similar to tomato Pti1 in having a positive effect on PTI and is therefore also divergent from rice in terms of downstream signaling events.

Because both *OsPti1a* and tomato *Pti1a* complement the *pti1a* mutation in rice and the two proteins are very similar (82% amino acid identity), it is possible that tomato Pti1a can substitute for *Os*Pti1a as the 'guardee' of a rice R protein. Another indication that the *pti1a* phenotype might be due to an activated R protein is its dependence on RAR1, which is required for the function of multiple R proteins in both monocot and dicot plants (Shirasu & Schulze-Lefert, 2003; Takahashi et al., 2007). Overexpression of *OsPti1a* complements the dwarf phenotype and might revert the enhanced resistance to the compatible race of *M. grisea* because the plants no longer have an autoactive immune response as indicated by normal levels of *PR-1b* expression (Takahashi et al., 2007). The increased susceptibility of plants

overexpressing *OsPti1a* to both incompatible *M. grisea* and compatible *Xoo* is reminiscent of the overexpression phenotype of tomato *Pti1a* in tobacco in response to *P. syringae* pv. *tabaci* carrying *avrPto* (Zhou et al., 1995; Takahashi et al., 2007). The development of tomato lines with null mutations in the *Pti1* genes will provide a better approach for examining the role of Pti1 in tomato and, if a tomato R protein does exist that guards Pti1, these plants might have certain autoimmune phenotypes.

Arabidopsis has 11 Pti1-like kinases (Anthony et al., 2006; Liao et al., 2016) with the gene products of At1g48210, At1g48220, At2g47060 (*PTI1-4*), At3g17410, and At3g62220 being the closest to the tomato Pti1 proteins. Of these five Pti1-like kinases only PTI1-4 has been functionally characterized and was found to interact with and be phosphorylated by the AGC kinase OXI (Forzani et al., 2011). Expression of both *OXI1* and *PTI1-4* is induced in root tissue upon wounding, cellulase treatment, and in response to H_2O_2. PTI1-4, but not OXI1, interacts with MPK6 and possibly MPK3 and both MAPKs phosphorylate OXI1 and PTI1-4. These and other observations support a model in which MPK3 and MPK6 function downstream of PTI1-4 and might regulate both OXI1 and PTI1-4 by phosphorylation, forming a feedback loop (Forzani et al., 2011). We previously observed no interaction of Pti1a with the tomato OXI1 ortholog Adi3 in yeast (data not shown) and we have no evidence that MAPKs function downstream of the Pti1 proteins as our hpPti1 tomato plants are unaffected in MAPK phosphorylation. Given these observations there does not appear to be any obvious similarities between the characterized Arabidopsis Pti1-like kinases and tomato Pti1a or Pti1b.

Our data support a role for Pti1 in the PTI signaling pathways in response to flagellin perception and indicate it acts either as part of the FLS2 and FLS3 receptor complexes or downstream of these complexes. Silencing of *Pti1a* and *Pti1b*

affected ROS production in response to flg22 and flgII-28 and had a limited effect on the transcriptome, but did not impact MAPK activation. We did not measure Ca^{2+} influx, but as this PTI response is required for MAPK activation it is likely also not affected in the *Pti1*-silenced plants (Segonzac et al., 2011). The mechanism by which Pti1 contributes to ROS production is unknown but it is possible that it regulates the NADPH oxidase RBOHD (RBOHB in tobacco) which is localized to the plasma membrane and has a well-studied role in immunity-associated ROS generation (**?**Adachi et al., 2015). The Pti1 proteins are localized to the cell periphery which places them in a position to be physically associated with the FLS2 and FLS3 receptor complexes or with an RBOH protein. In Arabidopsis, RBOHD is activated by direct Ca^{2+} binding and by phosphorylation by calcium-dependent protein kinases and BIK1 on partially overlapping residues (Boudsocq et al., 2010; Dubiella et al., 2013; Kadota et al., 2014). In *N. benthamiana*, RBOHB is required for flagellin-induced ROS production and since Pti1 is an active kinase it is possible that in tomato Pti1 phosphorylates RBOHB and this contributes to its activation and full ROS production (Zhou et al., 1995; Segonzac et al., 2011).

In rice, *Os*Pti1a exists in membrane complexes containing different 14-3-3 proteins (Matsui et al., 2014), which are highly conserved phosphopeptide binding proteins with various roles in plant immunity (Oh, 2010; Lozano-Durán & Robatzek, 2015). In tobacco, 14-3-3h/omega1 was found to interact with RBOHD and silencing of *Nt14-3-3h/omega1* significantly reduced ROS production after treatment with the elicitor cryptogein from the oomycete *Phythophthora cryptogea* (Elmayan et al., 2007). Tomato Pti1 has a putative 14-3-3 binding site (S232) predicted by 14-3-3-Pred (Madeira et al., 2015) next to the major phosphorylation site T233, both of which are phosphorylated by Pto *in vitro* (Sessa et al., 2000). A hypothesis that warrants testing is that upon flagellin perception Pti1 is phospho-

rylated directly by the FLS2-BAK1 and FLS3-BAK1 receptor complexes (or by another host kinase) and then bound by a 14-3-3 protein which might stabilize Pti1 and promote its ability to phosphorylate RBOHB. Alternatively, a 14-3-3 protein might facilitate interaction of the phosphorylated Pti1 with RBOHB, thus leading to phosphorylation and activation of the oxidase.

A large number of genes are differentially expressed during the host response to individual MAMPs or to *Pst* (Rosli et al., 2013; Pombo et al., 2014). It is striking then that, despite the role of Pti1 in enhancing PTI against *Pst*, our RNA-Seq analysis indicated the kinase plays a minor role in inducing gene expression in response to inoculation with *Pst*. Immunity-associated gene expression changes are typically regulated by MAPK cascades (Meng & Zhang, 2013). We found no evidence for an effect of Pti1 on MAPK activation although it is possible small changes do occur and are below the sensitivity of our pMAPK assay. It is perhaps more likely that another signaling pathway is affected in the hpPti1 plants, possibly one normally triggered by ROS production (Apel & Hirt, 2004). It is especially interesting that one of the genes most highly induced by Pti1 is *PR-1b*. The PR-1b protein in tomato was recently shown to encode a pro-peptide and its cleaved peptide, CAPE1, activates defense responses enhancing resistance to *Pst* DC3000 (Chen et al., 2014b). It is possible that perception of flagellin results in Pti1 activation which in turn leads to *PR-1b* expression through an unknown mechanism and the resulting CAPE1 peptide further stimulates plant defense responses.

Pti1a was identified over 20 years ago as an interactor of Pto although subsequent observations and the present work do not support a role for either Pti1a or Pti1b in the Pto pathway. A possible explanation for why Pti1 was found to interact with Pto is that the latter kinase might have evolved as a decoy of a host protein that plays a role in PTI by interacting with Pti1. A search of the

predicted tomato proteome identified two malectin-like receptor kinases, Mal1 and Mal2 (Solyc11g072910 and Solyc06g005230), whose kinase domains have the highest sequence similarity to Pto. Malectin receptor kinases (also called *Catharanthus roseus* RLK1-like kinases, *Cr*RLK1Ls) have an extracellular region containing two subdomains with similarity to the carbohydrate-binding domain of the animal malectin protein, a transmembrane domain, and an intracellular kinase domain (Lindner et al., 2012). One well-studied *Cr*RLK1L in Arabidopsis is FERONIA (FER) which plays a role in cell-cell communication during pollination, but also promotes susceptibility to certain bacterial and fungal pathogens (Kessler et al., 2010). Interestingly, FER becomes rapidly phosphorylated upon treatment of tissues with flg22 and it accumulates along with FLS2 in plasma membrane 'rafts' during PTI (Benschop et al., 2007; Keinath et al., 2010). At early time points, *fer* mutants support slightly increased bacterial growth (Keinath et al., 2010). Based on these results, it has been hypothesized that FER may act with FLS2 (Keinath et al., 2010). We are currently investigating whether Mal1 and Mal2 play a role in PTI in tomato and, if they do, whether Pti1 proteins might facilitate their function.

2.6 Acknowledgments

We thank Dr. Daniela Floss for help with the qPCR experiments; Dr. Hernan Rosli for advice on RNA-Seq data analysis; Heather McLane for developing the hpPti1 construct; Paige Reeves for plant care; and Drs. Sarah Hind and Fabian Giska for helpful comments on the manuscript. This work was supported by the National Science Foundation (grant nos. IOS-1025642 and IOS-1451754 to Dr. Gregory Martin).

2.7 Bibliography

Adachi, H., Nakano, T., Miyagawa, N., Ishihama, N., Yoshioka, M., Katou, Y., Yaeno, T., Shirasu, K., & Yoshioka, H. (2015). WRKY transcription factors phosphorylated by MAPK regulate a plant immune NADPH oxidase in *Nicotiana benthamiana*. *Plant Cell*, *27*(9), 2645–2663.

Anderson, J. C., Pascuzzi, P. E., Xiao, F., Sessa, G., & Martin, G. B. (2006). Host-mediated phosphorylation of type III effector AvrPto promotes *Pseudomonas* virulence and avirulence in tomato. *Plant Cell*, *18*(2), 502–514.

Anthony, R. G., Khan, S., Costa, J., Pais, M. S., & Bögre, L. (2006). The *Arabidopsis* protein kinase PTI1-2 is activated by convergent phosphatidic acid and oxidative stress signaling pathways downstream of PDK1 and OXI1. *J Biol Chem*, *281*(49), 37536–37546.

Apel, K., & Hirt, H. (2004). Reactive oxygen species: metabolism, oxidative stress, and signal transduction. *Annu Rev Plant Biol*, *55*, 373–399.

Axtell, M. J., & Staskawicz, B. J. (2003). Initiation of *RPS2*-specified disease resistance in *Arabidopsis* is coupled to the AvrRpt2-directed elimination of RIN4. *Cell*, *112*(3), 369–377.

Benschop, J. J., Mohammed, S., O'Flaherty, M., Heck, A. J. R., Slijper, M., & Menke, F. L. H. (2007). Quantitative phosphoproteomics of early elicitor signaling in *Arabidopsis*. *Mol Cell Proteomics*, *6*(7), 1198–1214.

Bent, A. F., & Mackey, D. (2007). Elicitors, effectors, and *R* genes: the new paradigm and a lifetime supply of questions. *Annu Rev Phytopathol*, *45*(1), 399–436.

Block, A., & Alfano, J. R. (2011). Plant targets for *Pseudomonas syringae* type III effectors: virulence targets or guarded decoys? *Curr Opin Microbiol*, *14*(1), 39–46.

Boller, T., & Felix, G. (2009). A renaissance of elicitors: perception of microbe-associated molecular patterns and danger signals by pattern-recognition receptors. *Annu Rev Plant Biol*, *60*(1), 379–406.

Bombarely, A., Rosli, H. G., Vrebalov, J., Moffett, P., Mueller, L. A., & Martin, G. B. (2012). A draft genome sequence of *Nicotiana benthamiana* to enhance molecular plant-microbe biology research. *Mol Plant Microbe Interact*, *25*(12), 1523–1530.

Boudsocq, M., Willmann, M. R., McCormack, M., Lee, H., Shan, L., He, P., Bush, J., Cheng, S.-H., & Sheen, J. (2010). Differential innate immune signalling via Ca^{2+} sensor protein kinases. *Nature*, *464*(7287), 418–422.

Boyle, P. C., & Martin, G. B. (2015). Greasy tactics in the plant-pathogen molecular arms race. *J Exp Bot*, *66*(6), 1607–1616.

Breuillin-Sessoms, F., Floss, D. S., Gomez, S. K., Pumplin, N., Ding, Y., Levesque-Tremblay, V., Noar, R. D., Daniels, D. A., Bravo, A., Eaglesham, J. B., Benedito, V. A., Udvardi, M. K., & Harrison, M. J. (2015). Suppression of arbuscule degeneration in *Medicago truncatula phosphate transporter4* mutants is dependent on the Ammonium Transporter 2 family protein AMT2;3. *Plant Cell*, *27*(4), 1352–1366.

Buell, C. R., Joardar, V., Lindeberg, M., Selengut, J., Paulsen, I. T., Gwinn, M. L., Dodson, R. J., Deboy, R. T., Durkin, A. S., Kolonay, J. F., Madupu, R., Daugherty, S., Brinkac, L., Beanan, M. J., Haft, D. H., Nelson, W. C., Davidsen, T., Zafar, N., Zhou, L., Liu, J., Yuan, Q., Khouri, H., Fedorova, N., Tran, B., Russell, D., Berry, K., Utterback, T., Van Aken, S. E., Feldblyum, T. V., D'Ascenzo, M., Deng, W.-L., Ramos, A. R., Alfano, J. R., Cartinhour, S., Chatterjee, A. K., Delaney, T. P., Lazarowitz, S. G., Martin, G. B., Schneider, D. J., Tang, X., Bender, C. L., White, O., Fraser, C. M., & Collmer, A. (2003). The complete genome sequence of the *Arabidopsis* and tomato pathogen *Pseudomonas syringae* pv. *tomato* DC3000. *Proc Natl Acad Sci*, *100*(18), 10181–10186.

Burch-Smith, T. M., Anderson, J. C., Martin, G. B., & Dinesh-Kumar, S. P. (2004). Applications and advantages of virus-induced gene silencing for gene function studies in plants. *Plant J*, *39*(5), 734–746.

Cai, R., Lewis, J., Yan, S., Liu, H., Clarke, C. R., Campanile, F., Almeida, N. F., Studholme, D. J., Lindeberg, M., Schneider, D., Zaccardelli, M., Setubal, J. C., Morales-Lizcano, N. P., Bernal, A., Coaker, G., Baker, C., Bender, C. L., Leman, S., & Vinatzer, B. A. (2011). The plant pathogen *Pseudomonas syringae* pv.

tomato is genetically monomorphic and under strong selection to evade tomato immunity. *PLoS Pathog*, *7*(8), e1002130.

Carland, F. M., & Staskawicz, B. J. (1993). Genetic characterization of the *Pto* locus of tomato: semi-dominance and cosegregation of resistance to *Pseudomonas syringae* pathovar *tomato* and sensitivity to the insecticide Fenthion. *Mol Gen Genet*, *239*(1-2), 17–27.

Chakravarthy, S., Velásquez, A. C., Ekengren, S. K., Collmer, A., & Martin, G. B. (2010). Identification of *Nicotiana benthamiana* genes involved in pathogen-associated molecular pattern-triggered immunity. *Mol Plant Microbe Interact*, *23*(6), 715–726.

Chen, Y., Wang, Y., & Zhang, H. (2014a). Genome-wide analysis of the mildew resistance locus o (*MLO*) gene family in tomato (*Solanum lycopersicum* L.). *Plant Omics*, *7*(2), 87.

Chen, Y.-L., Lee, C.-Y., Cheng, K.-T., Chang, W.-H., Huang, R.-N., Nam, H. G., & Chen, Y.-R. (2014b). Quantitative peptidomics study reveals that a wound-induced peptide from PR-1 regulates immune signaling in tomato. *Plant Cell*, *26*(10), 4135–4148.

Chinchilla, D., Bauer, Z., Regenass, M., Boller, T., & Felix, G. (2006). The *Arabidopsis* receptor kinase FLS2 binds flg22 and determines the specificity of flagellin perception. *Plant Cell*, *18*(2), 465–476.

Chinchilla, D., Zipfel, C., Robatzek, S., Kemmerling, B., Nürnberger, T., Jones, J. D. G., Felix, G., & Boller, T. (2007). A flagellin-induced complex of the receptor FLS2 and BAK1 initiates plant defence. *Nature*, *448*(7152), 497–500.

Clarke, C. R., Chinchilla, D., Hind, S. R., Taguchi, F., Miki, R., Ichinose, Y., Martin, G. B., Leman, S., Felix, G., & Vinatzer, B. A. (2013). Allelic variation in two distinct *Pseudomonas syringae* flagellin epitopes modulates the strength of plant immune responses but not bacterial motility. *New Phytol*, *200*(3), 847–860.

Cook, D. E., Mesarich, C. H., & Thomma, B. P. H. J. (2015). Understanding plant immunity as a surveillance system to detect invasion. *Annu Rev Phytopathol*, *53*, 541–563.

Crabill, E., Joe, A., Block, A., van Rooyen, J. M., & Alfano, J. R. (2010). Plant immunity directly or indirectly restricts the injection of type III effectors by the *Pseudomonas syringae* type III secretion system. *Plant Physiol*, *154*(1), 233–244.

Cunnac, S., Lindeberg, M., & Collmer, A. (2009). *Pseudomonas syringae* type III secretion system effectors: repertoires in search of functions. *Curr Opin Microbiol*, *12*(1), 53–60.

Dangl, J. L., Horvath, D. M., & Staskawicz, B. J. (2013). Pivoting the plant immune system from dissection to deployment. *Science*, *341*(6147), 746–751.

del Pozo, O., Pedley, K. F., & Martin, G. B. (2004). MAPKKKα is a positive regulator of cell death associated with both plant immunity and disease. *EMBO J*, *23*(15), 3072–3082.

Dodds, P. N., & Rathjen, J. P. (2010). Plant immunity: towards an integrated view of plant-pathogen interactions. *Nat Rev Genet*, *11*(8), 539–548.

Dong, J., Xiao, F., Fan, F., Gu, L., Cang, H., Martin, G. B., & Chai, J. (2009). Crystal structure of the complex between *Pseudomonas* effector AvrPtoB and the tomato Pto kinase reveals both a shared and a unique interface compared with AvrPto-Pto. *Plant Cell*, *21*(6), 1846–1859.

Dou, D., & Zhou, J.-M. (2012). Phytopathogen effectors subverting host immunity: different foes, similar battleground. *Cell Host Microbe*, *12*(4), 484–495.

Dubiella, U., Seybold, H., Durian, G., Komander, E., Lassig, R., Witte, C.-P., Schulze, W. X., & Romeis, T. (2013). Calcium-dependent protein kinase/NADPH oxidase activation circuit is required for rapid defense signal propagation. *Proc Natl Acad Sci*, *110*(21), 8744–8749.

Ekengren, S. K., Liu, Y., Schiff, M., Dinesh-Kumar, S. P., & Martin, G. B. (2003). Two MAPK cascades, NPR1, and TGA transcription factors play a role in Pto-mediated disease resistance in tomato. *Plant J*, *36*(6), 905–917.

Elmayan, T., Fromentin, J., Riondet, C., Alcaraz, G., Blein, J.-P., & Simon-Plas, F. (2007). Regulation of reactive oxygen species production by a 14-3-3 protein in elicited tobacco cells. *Plant Cell Environ*, *30*(6), 722–732.

Felix, G., Duran, J. D., Volko, S., & Boller, T. (1999). Plants have a sensitive perception system for the most conserved domain of bacterial flagellin. *Plant J*, *18*(3), 1–12.

Fernandez-Pozo, N., Menda, N., Edwards, J. D., Saha, S., Tecle, I. Y., Strickler, S. R., Bombarely, A., Fisher-York, T., Pujar, A., Foerster, H., Yan, A., & Mueller, L. A. (2015a). The Sol Genomics Network (SGN)–from genotype to phenotype to breeding. *Nucleic Acids Res*, *43*(D1), D1036–D1041.

Fernandez-Pozo, N., Rosli, H. G., Martin, G. B., & Mueller, L. A. (2015b). The SGN VIGS tool: user-friendly software to design virus-induced gene silencing (VIGS) constructs for functional genomics. *Mol Plant*, *8*(3), 486–488.

Forzani, C., Carreri, A., de la Fuente van Bentem, S., Lecourieux, D., Lecourieux, F., & Hirt, H. (2011). The *Arabidopsis* protein kinase Pto-interacting 1-4 is a common target of the oxidative signal-inducible 1 and mitogen-activated protein kinases. *FEBS J*, *278*(7), 1126–1136.

Gómez-Gómez, L., & Boller, T. (2000). FLS2: an LRR receptor-like kinase involved in the perception of the bacterial elicitor flagellin in *Arabidopsis*. *Mol Cell*, *5*(6), 1003–1011.

Goodin, M. M., Zaitlin, D., Naidu, R. A., & Lommel, S. A. (2008). *Nicotiana benthamiana*: its history and future as a model for plant-pathogen interactions. *Mol Plant Microbe Interact*, *21*(8), 1015–1026.

Greenberg, J. T. (1997). Programmed cell death in plant-pathogen interactions. *Annu Rev Plant Physiol Plant Mol Biol*, *48*, 525–545.

Hall, B. G. (2013). Building phylogenetic trees from molecular data with MEGA. *Mol Biol Evol*, *30*(5), 1229–1235.

He, P., Shan, L., Lin, N.-C., Martin, G. B., Kemmerling, B., Nürnberger, T., & Sheen, J. (2006). Specific bacterial suppressors of MAMP signaling upstream of MAPKKK in *Arabidopsis* innate immunity. *Cell*, *125*(3), 563–575.

Hellens, R., Mullineaux, P., & Klee, H. (2000). A guide to *Agrobacterium* binary Ti vectors. *Trends Plant Sci*, *5*(10), 446–451.

Helliwell, C. A., Wesley, S. V., Wielopolska, A. J., & Waterhouse, P. M. (2002). High-throughput vectors for efficient gene silencing in plants. *Funct Plant Biol*, *29*(10), 1217–1225.

Herrmann, M. M., Pinto, S., Kluth, J., Wienand, U., & Lorbiecke, R. (2006). The PTI1-like kinase ZmPti1a from maize (*Zea mays* L.) co-localizes with callose at the plasma membrane of pollen and facilitates a competitive advantage to the male gametophyte. *BMC Plant Biol*, *6*, 22.

Hind, S. R., Strickler, S. R., Boyle, P. C., Dunham, D. M., Bao, Z., O'Doherty, I. M., Baccile, J. A., Hoki, J. S., Viox, E. G., Clarke, C. R., Vinatzer, B. A., Schroeder, F. C., & Martin, G. B. (2016). Tomato receptor FLAGELLIN-SENSING 3 binds flgII-28 and activates the plant immune system. *Nat Plants*, *2*(9), 16128.

Jones, J. B. (1991). Bacterial speck. In J. B. Jones, J. P. Jones, R. E. Stall, & T. A. Zitter (Eds.) *Compendium of tomato diseases*, (pp. 26–27). APS Press, St. Paul, MN.

Jones, J. D. G., & Dangl, J. L. (2006). The plant immune system. *Nature*, *444*(7117), 323–329.

Kadota, Y., Sklenar, J., Derbyshire, P., Stransfeld, L., Asai, S., Ntoukakis, V., Jones, J. D., Shirasu, K., Menke, F., Jones, A., & Zipfel, C. (2014). Direct regulation of the NADPH oxidase RBOHD by the PRR-associated kinase BIK1 during plant immunity. *Mol Cell*, *54*(1), 1–13.

Keinath, N. F., Kierszniowska, S., Lorek, J., Bourdais, G., Kessler, S. A., Shimosato-Asano, H., Grossniklaus, U., Schulze, W. X., Robatzek, S., & Panstruga, R. (2010). PAMP (pathogen-associated molecular pattern)-induced changes in plasma membrane compartmentalization reveal novel components of plant immunity. *J Biol Chem*, *285*(50), 39140–39149.

Kessler, S. A., Shimosato-Asano, H., Keinath, N. F., Wuest, S. E., Ingram, G., Panstruga, R., & Grossniklaus, U. (2010). Conserved molecular components for pollen tube reception and fungal invasion. *Science*, *330*(6006), 968–971.

Kraus, C. M., Munkvold, K. R., & Martin, G. B. (2016). Natural variation in tomato reveals differences in the recognition of AvrPto and AvrPtoB effectors from *Pseudomonas syringae*. *Mol Plant*, *9*(5), 639–649.

Kumar, D., Gustafsson, C., & Klessig, D. F. (2006). Validation of RNAi silencing specificity using synthetic genes: salicylic acid-binding protein 2 is required for innate immunity in plants. *Plant J*, *45*(5), 863–868.

Kumar, S., Stecher, G., & Tamura, K. (2016). MEGA7: Molecular Evolutionary Genetics Analysis version 7.0 for bigger datasets. *Mol Biol Evol*, *33*(7), 1870–1874.

Kvitko, B. H., Park, D. H., Velásquez, A. C., Wei, C.-F., Russell, A. B., Martin, G. B., Schneider, D. J., & Collmer, A. (2009). Deletions in the repertoire of *Pseudomonas syringae* pv. *tomato* DC3000 type III secretion effector genes reveal functional overlap among effectors. *PLoS Pathog*, *5*(4), e1000388–16.

Kvitko, B. H., Ramos, A. R., Morello, J. E., Oh, H.-S., & Collmer, A. (2007). Identification of harpins in *Pseudomonas syringae* pv. *tomato* DC3000, which are functionally similar to HrpK1 in promoting translocation of type III secretion system effectors. *J Bacteriol*, *189*(22), 8059–8072.

Liao, H.-Z., Zhu, M.-M., Cui, H.-H., Du, X.-Y., Tang, Y., Chen, L.-Q., Ye, D., & Zhang, X.-Q. (2016). The *MARIS* plays important roles in *Arabidopsis* pollen tube and root hair growth. *J Integr Plant Biol*.

Lin, N.-C., & Martin, G. B. (2005). An *avrPto/avrPtoB* mutant of *Pseudomonas syringae* pv. *tomato* DC3000 does not elicit Pto-mediated resistance and is less virulent on tomato. *Mol Plant Microbe Interact*, *18*(1), 43–51.

Lindeberg, M., Cunnac, S., & Collmer, A. (2012). *Pseudomonas syringae* type III effector repertoires: last words in endless arguments. *Trends Microbiol*, *20*(4), 199–208.

Lindner, H., Müller, L. M., Boisson-Dernier, A., & Grossniklaus, U. (2012). CrRLK1L receptor-like kinases: not just another brick in the wall. *Curr Opin Plant Biol*, *15*(6), 659–669.

Liu, D., Shi, L., Han, C., Yu, J., Li, D., & Zhang, Y. (2012). Validation of reference genes for gene expression studies in virus-infected *Nicotiana benthamiana* using quantitative real-time PCR. *PLoS ONE*, *7*(9), e46451.

Liu, Y., Schiff, M., & Dinesh-Kumar, S. P. (2002). Virus-induced gene silencing in tomato. *Plant J*, *31*(6), 777–786.

Lozano-Durán, R., & Robatzek, S. (2015). 14-3-3 proteins in plant-pathogen interactions. *Mol Plant Microbe Interact*, *28*(5), 511–518.

Macho, A. P., & Zipfel, C. (2015). Targeting of plant pattern recognition receptor-triggered immunity by bacterial type-III secretion system effectors. *Curr Opin Microbiol*, *23*, 14–22.

Mackey, D., Belkhadir, Y., Alonso, J. M., Ecker, J. R., & Dangl, J. L. (2003). *Arabidopsis* RIN4 is a target of the type III virulence effector AvrRpt2 and modulates RPS2-mediated resistance. *Cell*, *112*(3), 379–389.

Mackey, D., Holt, B. F., Wiig, A., & Dangl, J. L. (2002). RIN4 interacts with *Pseudomonas syringae* type III effector molecules and is required for RPM1-mediated resistance in *Arabidopsis*. *Cell*, *108*(6), 743–754.

Madeira, F., Tinti, M., Murugesan, G., Berrett, E., Stafford, M., Toth, R., Cole, C., MacKintosh, C., & Barton, G. J. (2015). 14-3-3-Pred: improved methods to predict 14-3-3-binding phosphopeptides. *Bioinformatics*, *31*(14), 2276–2283.

Martin, G. B. (2012). Suppression and activation of the plant immune system by *Pseudomonas syringae* effectors AvrPto and AvrPtoB. In F. Martin, & S. Kamoun (Eds.) *Effectors in plant-microbe interactions*, (pp. 123–154). Wiley-Blackwell, Hoboken, NJ.

Martin, G. B., Brommonschenkel, S. H., Chunwongse, J., Frary, A., Ganal, M. W., Spivey, R., Wu, T., Earle, E. D., & Tanksley, S. D. (1993). Map-based cloning of a protein kinase gene conferring disease resistance in tomato. *Science*, *262*(5138), 1432–1436.

Mathieu, J., Schwizer, S., & Martin, G. B. (2014). Pto kinase binds two domains of AvrPtoB and its proximity to the effector E3 ligase determines if it evades degradation and activates plant immunity. *PLoS Pathog*, *10*(7), e1004227.

Mathieu, J., Warthmann, N., Küttner, F., & Schmid, M. (2007). Export of FT protein from phloem companion cells is sufficient for floral induction in *Arabidopsis*. *Curr Biol*, *17*(12), 1055–1060.

Matsui, H., Fujiwara, M., Hamada, S., Shimamoto, K., Nomura, Y., Nakagami, H., Takahashi, A., & Hirochika, H. (2014). Plasma membrane localization is es-

sential for *Oryza sativa* Pto-interacting protein 1a-mediated negative regulation of immune signaling in rice. *Plant Physiol*, *166*(1), 327–336.

Matsui, H., Miyao, A., Takahashi, A., & Hirochika, H. (2010a). Pdk1 kinase regulates basal disease resistance through the OsOxi1-OsPti1a phosphorylation cascade in rice. *Plant Cell Physiol*, *51*(12), 2082–2091.

Matsui, H., Yamazaki, M., Kishi-Kaboshi, M., Takahashi, A., & Hirochika, H. (2010b). AGC kinase OsOxi1 positively regulates basal resistance through suppression of OsPti1a-mediated negative regulation. *Plant Cell Physiol*, *51*(10), 1731–1744.

Meng, X., & Zhang, S. (2013). MAPK cascades in plant disease resistance signaling. *Annu Rev Phytopathol*, *51*, 245–266.

Monaghan, J., & Zipfel, C. (2012). Plant pattern recognition receptor complexes at the plasma membrane. *Curr Opin Plant Biol*, *15*(4), 349–357.

Mucyn, T. S., Clemente, A., Andriotis, V. M. E., Balmuth, A. L., Oldroyd, G. E. D., Staskawicz, B. J., & Rathjen, J. P. (2006). The tomato NBARC-LRR protein Prf interacts with Pto kinase in vivo to regulate specific plant immunity. *Plant Cell*, *18*(10), 2792–2806.

Nakagawa, T., Suzuki, T., Murata, S., Nakamura, S., Hino, T., Maeo, K., Tabata, R., Kawai, T., Tanaka, K., Niwa, Y., Watanabe, Y., Nakamura, K., Kimura, T., & Ishiguro, S. (2007). Improved Gateway binary vectors: high-performance vectors for creation of fusion constructs in transgenic analysis of plants. *Biosci Biotechnol Biochem*, *71*(8), 2095–2100.

Nguyen, H. P., Chakravarthy, S., Velásquez, A. C., McLane, H. L., Zeng, L., Nakayashiki, H., Park, D. H., Collmer, A., & Martin, G. B. (2010a). Methods to study PAMP-triggered immunity using tomato and *Nicotiana benthamiana*. *Mol Plant Microbe Interact*, *23*(8), 991–999.

Nguyen, H. P., Yeam, I., Angot, A., & Martin, G. B. (2010b). Two virulence determinants of type III effector AvrPto are functionally conserved in diverse *Pseudomonas syringae* pathovars. *New Phytol*, *187*(4), 969–982.

Oh, C.-S. (2010). Characteristics of 14-3-3 proteins and their role in plant immunity. *Plant Pathol J*, *26*(1), 1–7.

Oh, C.-S., & Martin, G. B. (2011a). Effector-triggered immunity mediated by the Pto kinase. *Trends Plant Sci*, *16*(3), 132–140.

Oh, C.-S., & Martin, G. B. (2011b). Tomato 14-3-3 protein TFT7 interacts with a MAP kinase kinase to regulate immunity-associated programmed cell death mediated by diverse disease resistance proteins. *J Biol Chem*, *286*(16), 14129–14136.

Oh, C.-S., Pedley, K. F., & Martin, G. B. (2010a). Tomato 14-3-3 protein 7 positively regulates immunity-associated programmed cell death by enhancing protein abundance and signaling ability of MAPKKKα. *Plant Cell*, *22*(1), 260–272.

Oh, H.-S., Park, D. H., & Collmer, A. (2010b). Components of the *Pseudomonas syringae* type III secretion system can suppress and may elicit plant innate immunity. *Mol Plant Microbe Interact*, *23*(6), 727–739.

Pascuzzi, P. E. (2006). *Structure-based functional analyses of* Pseudomonas *type III effector protein AvrPto and evaluation of putative virulence targets in tomato*. Ph.D. thesis, Cornell University.

Pedley, K. F., & Martin, G. B. (2003). Molecular basis of *Pto*-mediated resistance to bacterial speck disease in tomato. *Annu Rev Phytopathol*, *41*, 215–243.

Pombo, M. A., Zheng, Y., Fernandez-Pozo, N., Dunham, D. M., Fei, Z., & Martin, G. B. (2014). Transcriptomic analysis reveals tomato genes whose expression is induced specifically during effector-triggered immunity and identifies the Epk1 protein kinase which is required for the host response to three bacterial effector proteins. *Genome Biol*, *15*(10), 492.

Preston, G. M. (2000). *Pseudomonas syringae* pv. *tomato*: the right pathogen, of the right plant, at the right time. *Mol Plant Pathol*, *1*(5), 263–275.

Rosli, H. G., Zheng, Y., Pombo, M. A., Zhong, S., Bombarely, A., Fei, Z., Collmer, A., & Martin, G. B. (2013). Transcriptomics-based screen for genes induced by flagellin and repressed by pathogen effectors identifies a cell wall-associated kinase involved in plant immunity. *Genome Biol*, *14*(12), R139.

Salmeron, J. M., Barker, S. J., Carland, F. M., Mehta, A. Y., & Staskawicz, B. J. (1994). Tomato mutants altered in bacterial disease resistance provide evidence for a new locus controlling pathogen recognition. *Plant Cell*, *6*(4), 511–520.

Salmeron, J. M., Oldroyd, G. E., Rommens, C. M., Scofield, S. R., Kim, H. S., Lavelle, D. T., Dahlbeck, D., & Staskawicz, B. J. (1996). Tomato *Prf* is a member of the leucine-rich repeat class of plant disease resistance genes and lies embedded within the *Pto* kinase gene cluster. *Cell*, *86*(1), 123–133.

Scofield, S., Tobias, C., Rathjen, J., Chang, J., Lavelle, D., Michelmore, R., & Staskawicz, B. (1996). Molecular basis of gene-for-gene specificity in bacterial speck disease of tomato. *Science*, *274*(5295), 2063–2065.

Segonzac, C., Feike, D., Gimenez-Ibanez, S., Hann, D. R., Zipfel, C., & Rathjen, J. P. (2011). Hierarchy and roles of pathogen-associated molecular pattern-induced responses in *Nicotiana benthamiana*. *Plant Physiol*, *156*(2), 687–699.

Senthil-Kumar, M., & Mysore, K. S. (2011). Caveat of RNAi in plants: the off-target effect. *Methods Mol Biol*, *744*(Chapter 2), 13–25.

Sessa, G., D'ascenzo, M., Loh, Y. T., & Martin, G. B. (1998). Biochemical properties of two protein kinases involved in disease resistance signaling in tomato. *J Biol Chem*, *273*(25), 15860–15865.

Sessa, G., D'ascenzo, M., & Martin, G. B. (2000). The major site of the Pti1 kinase phosphorylated by the Pto kinase is located in the activation domain and is required for Pto-Pti1 physical interaction. *Eur J Biochem*, *267*(1), 171–178.

Shan, L., He, P., Li, J., Heese, A., Peck, S. C., Nürnberger, T., Martin, G. B., & Sheen, J. (2008). Bacterial effectors target the common signaling partner BAK1 to disrupt multiple MAMP receptor-signaling complexes and impede plant immunity. *Cell Host Microbe*, *4*(1), 17–27.

Shirasu, K. (2009). The HSP90-SGT1 chaperone complex for NLR immune sensors. *Annu Rev Plant Biol*, *60*, 139–164.

Shirasu, K., & Schulze-Lefert, P. (2003). Complex formation, promiscuity and multi-functionality: protein interactions in disease-resistance pathways. *Trends Plant Sci*, *8*(6), 252–258.

Takahashi, A., Agrawal, G. K., Yamazaki, M., Onosato, K., Miyao, A., Kawasaki, T., Shimamoto, K., & Hirochika, H. (2007). Rice Pti1a negatively regulates RAR1-dependent defense responses. *Plant Cell*, *19*(9), 2940–2951.

Tang, X., Frederick, R., Zhou, J., Halterman, D., Jia, Y., & Martin, G. B. (1996). Initiation of plant disease resistance by physical interaction of AvrPto and Pto kinase. *Science*, *274*(5295), 2060–2063.

Tomato Genome Consortium (2012). The tomato genome sequence provides insights into fleshy fruit evolution. *Nature*, *485*(7400), 635–641.

van der Hoorn, R. A. L., & Kamoun, S. (2008). From guard to decoy: a new model for perception of plant pathogen effectors. *Plant Cell*, *20*(8), 2009–2017.

Wei, C.-F., Kvitko, B. H., Shimizu, R., Crabill, E., Alfano, J. R., Lin, N.-C., Martin, G. B., Huang, H.-C., & Collmer, A. (2007). A *Pseudomonas syringae* pv. *tomato* DC3000 mutant lacking the type III effector HopQ1-1 is able to cause disease in the model plant *Nicotiana benthamiana*. *Plant J*, *51*(1), 32–46.

Whalen, M. C., Innes, R. W., Bent, A. F., & Staskawicz, B. J. (1991). Identification of *Pseudomonas syringae* pathogens of *Arabidopsis* and a bacterial locus determining avirulence on both *Arabidopsis* and soybean. *Plant Cell*, *3*(1), 49–59.

Wroblewski, T., Tomczak, A., & Michelmore, R. (2005). Optimization of *Agrobacterium*-mediated transient assays of gene expression in lettuce, tomato and *Arabidopsis*. *Plant Biotechnol J*, *3*(2), 259–273.

Wu, A.-J., Andriotis, V. M. E., Durrant, M. C., & Rathjen, J. P. (2004). A patch of surface-exposed residues mediates negative regulation of immune signaling by tomato Pto kinase. *Plant Cell*, *16*(10), 2809–2821.

Wu, C.-H., Belhaj, K., Bozkurt, T. O., Birk, M. S., & Kamoun, S. (2016). Helper NLR proteins NRC2a/b and NRC3 but not NRC1 are required for Pto-mediated cell death and resistance in *Nicotiana benthamiana*. *New Phytol*, *209*(4), 1344–1352.

Xiang, T., Zong, N., Zou, Y., Wu, Y., Zhang, J., Xing, W., Li, Y., Tang, X., Zhu, L., Chai, J., & Zhou, J.-M. (2008). *Pseudomonas syringae* effector AvrPto blocks innate immunity by targeting receptor kinases. *Curr Biol*, *18*(1), 74–80.

Xiao, F., Lu, M., Li, J., Zhao, T., Yi, S. Y., Thara, V. K., Tang, X., & Zhou, J.-M. (2003). Pto mutants differentially activate *Prf*-dependent, *avrPto*-independent resistance and gene-for-gene resistance. *Plant Physiol*, *131*(3), 1239–1249.

Xing, W., Zou, Y., Liu, Q., Liu, J., Luo, X., Huang, Q., Chen, S., Zhu, L., Bi, R., Hao, Q., Wu, J.-W., Zhou, J.-M., & Chai, J. (2007). The structural basis for activation of plant immunity by bacterial effector protein AvrPto. *Nature*, *449*(7159), 243–247.

Yeam, I., Nguyen, H. P., & Martin, G. B. (2010). Phosphorylation of the *Pseudomonas syringae* effector AvrPto is required for FLS2/BAK1-independent virulence activity and recognition by tobacco. *Plant J*, *61*(1), 16–24.

Young, J. M., Dye, D. W., & Wilkie, J. P. (1986). Bacterial speck. In A. F. Sherf (Ed.) *Vegetable diseases and their control*, (pp. 610–614). J. Wiley & Sons, New York, NY.

Zeng, L., Velásquez, A. C., Munkvold, K. R., Zhang, J., & Martin, G. B. (2011). A tomato LysM receptor-like kinase promotes immunity and its kinase activity is inhibited by AvrPtoB. *Plant J*, *69*(1), 92–103.

Zhou, J., Loh, Y. T., Bressan, R. A., & Martin, G. B. (1995). The tomato gene *Pti1* encodes a serine/threonine kinase that is phosphorylated by Pto and is involved in the hypersensitive response. *Cell*, *83*(6), 925–935.

Zipfel, C. (2014). Plant pattern-recognition receptors. *Trends Immunol*, *35*(7), 345–351.

Zipfel, C., Robatzek, S., Navarro, L., Oakeley, E. J., Jones, J. D. G., Felix, G., & Boller, T. (2004). Bacterial disease resistance in *Arabidopsis* through flagellin perception. *Nature*, *428*(6984), 764–767.

CHAPTER 3

MALECTIN-LIKE RECEPTOR-LIKE KINASES MIGHT PROMOTE RESISTANCE TO *PSEUDOMONAS SYRINGAE* AND ARE TARGETED BY THE AVRPTOB EFFECTOR

3.1 Summary

The plant cell wall is an important barrier that prevents pathogenic microbes from gaining access to the nutrients in the cytoplasm. Plants have evolved receptor proteins to monitor cell wall integrity and induce defense responses if a breach of the cell wall occurs. We identified several putative receptors in tomato that consist of extracellular malectin-like domains and intracellular kinase domains. The kinase domains of these putative receptors show high similarity to the tomato Pto kinase that together with the nucleotide-binding leucine-rich repeat protein Prf confers immunity to strains of the bacterial speck pathogen *Pseudomonas syringae* pv. *tomato* (*Pst*) secreting either of the type III effectors AvrPto or AvrPtoB. Interestingly, the N-terminal sequence of Pto and some of its family members is conserved in two of the identified malectin-like proteins, Mal1 and Mal2, at approximately the beginning of their kinase domains and is not found in any other predicted tomato protein. Silencing the orthologs of *Mal1* and *Mal2* in *Nicotiana benthamiana* resulted in compromised induction of immune responses and increased susceptibility to *Pst* infection. We found that AvrPtoB interacts with the kinase domains of both Mal1 and Mal2 and we speculate that these putative receptors are targeted by AvrPtoB to suppress plant immunity. Furthermore, we believe that Pto evolved from the kinase domain of either Mal1 or Mal2 (or a progenitor protein) to sense the presence of AvrPtoB inside the plant cell and induce robust defense responses.

3.2 Introduction

Plants have evolved a sophisticated immune system to detect and defend against detrimental microbial pathogens (Jones & Dangl, 2006; Dodds & Rathjen, 2010). Detection is achieved by perception of conserved macromolecules that are representative of entire classes of microbes (Nürnberger et al., 2004; Zipfel, 2014). These microbe- or pathogen-associated molecular patterns (MAMPs or PAMPs) include cell wall components such as chitin oligomers in fungi and peptidoglycans and lipopolysaccharides in bacteria (Nürnberger et al., 2004; Zipfel, 2014). Other perceived macromolecules are flagellin, a constituent of the bacterial flagellum, and elongation factor Tu (EF-Tu), a highly abundant protein in bacterial cells (Zipfel, 2008; Boller & Felix, 2009). These MAMPs are sensed by plasma membrane-spanning pattern recognition receptors (PRRs) that typically contain an extracellular receptor domain that binds the corresponding macromolecule and an intracellular kinase domain that initiates the signaling response leading to defense (Monaghan & Zipfel, 2012; Zipfel, 2014).

Two of the best-studied PRRs are FLS2 and EFR from *Arabidopsis thaliana*, which recognize a 22-amino acid peptide from flagellin (flg22) and an acetylated 18-amino acid peptide from EF-Tu (elf18), respectively (Zipfel, 2008; Boller & Felix, 2009). These PRRs form a complex with and function in concert with the co-receptor BAK1 and several intracellular receptor-like cytoplasmic kinases such as BIK1 and PBL1 to initiate signal transduction upon pathogen perception (Chinchilla et al., 2007; Lu et al., 2010; Zhang et al., 2010; Roux et al., 2011). These early signaling events include transphosphorylation of receptor complex constituents, influx of Ca^{2+} into the plant cell, activation of calcium-dependent protein kinases, and phosphorylation of mitogen-activated protein kinases (MAPKs) (Boller & Felix, 2009; Tena et al., 2011). This leads to various responses including the produc-

tion of reactive oxygen species, expression of defense-related genes, production of antimicrobial compounds, and cell wall reinforcement at the infection site designed to prevent pathogen proliferation and collectively referred to as pattern-triggered immunity (PTI) (Nürnberger et al., 2004; Nicaise et al., 2009).

In addition to MAMPs, plants can sense endogenous molecules that are produced in response to pathogen perception or wounding and are thought to reinforce PTI responses (Boller & Felix, 2009; Zipfel, 2013). In Arabidopsis, MAMP perception triggers the production of the gaseous hormone ethylene, which in turn induces the *PROPEP1* and *PROPEP2* genes (Boller & Felix, 2009; Huffaker et al., 2006; Tintor et al., 2013). The resulting propeptides are cleaved and the corresponding Pep1 and Pep2 peptides perceived by the PRRs PEPR1 and PEPR2, respectively (Huffaker et al., 2006; Yamaguchi et al., 2006; Krol et al., 2010; Yamaguchi et al., 2010). Like FLS2 and EFR, PEPR1/2 require the BAK1 co-receptor and the cytoplasmic receptor-like kinases BIK1 and PBL1 (Roux et al., 2011; Liu et al., 2013). Application of synthetic Pep peptides enhances resistance to *Pst* and triggers immune responses similar to those induced by flg22 and elf18, including ethylene production (Yamaguchi et al., 2010; Roux et al., 2011; Ma et al., 2012). Ethylene, together with jasmonate, is generally thought to be involved in defense against necrotrophic pathogens whereas salicylic acid promotes resistance to biotrophic pathogens (Glazebrook, 2005). More recent work revealed a highly interconnected signaling network between these three defense hormones that together contribute to immunity to both biotrophic and necrotrophic pathogens (Tsuda et al., 2009). It is thought that the Pep/PEPR system, including ethylene-induced *PROPEP* expression, serves as an amplification loop to maintain sustained defense responses triggered by the perception of both biotrophic and necrotrophic pathogens (Zipfel, 2013).

The plant cell wall presents a formidable barrier to microbes and organisms trying to gain access to the interior of the cell need to either take advantage of wounds or force their way through using mechanical structures or lytic enzymes to degrade the cell wall (De Lorenzo et al., 2011). The plant cell wall consists primarily of cellulose microfibrils linked with hemicellulose polymers that are embedded in a pectin matrix. Because pectin is one of the most accessible components of the cell wall and important for its structural integrity, it is among the first to be altered during an attempted microbial infection (De Lorenzo et al., 2011; Ferrari et al., 2013). Fungi secrete polygalacturonases that degrade homogalacturonan, a major component of pectin, leading to maceraction of the cell wall and release of oligogalacturonides (OGs). Plants induce endogenous polygalacturonases in response to mechanical damage and their activity also releases OGs (De Lorenzo et al., 2011; Ferrari et al., 2013). Damage to the cell wall is sensed by PRRs that perceive the presence of cell wall-derived molecules, referred to as damage-associated molecular patterns (DAMPs), such as OGs whose presence indicates that the cell wall is under attack (De Lorenzo et al., 2011). In Arabidopsis, receptor-like wall-associated kinases (WAKs) are able to bind OGs and a chimeric receptor approach revealed that WAK1 acts as a receptor of OGs (Decreux & Messiaen, 2005; Kohorn et al., 2009; Brutus et al., 2010). The responses triggered by OG perception largely overlap with those induced by MAMPs, as both types of elicitors induce ROS production, MAPK phosphorylation, and transcriptional reprogramming (Denoux et al., 2008; Galletti et al., 2008). However, OGs are weaker inducers than MAMPs such as flg22 and do not induce defense genes dependent on the plant hormones salicylic acid, jasmonate, and ethylene (Denoux et al., 2008).

The *Catharanthus roseus* RLK1-like (*Cr*RLK1L) subfamily of receptor-like kinases contain extracellular malectin-like domains with putative carbohydrate-

binding functions and might serve as sensors of cell wall integrity (Boisson-Dernier et al., 2011; Lindner et al., 2012). Malectin is a protein from *Xenopus laevis* that was shown to bind maltose and related oligosaccharides Schallus:2008by. In Arabidopsis, 17 *Cr*RLK1L proteins have been identified, some of which function in cell wall monitoring, pollen tube integrity, and fertilization (Boisson-Dernier et al., 2011; Lindner et al., 2012). One of the more interesting *Cr*RLK1Ls is FER which controls pollen tube reception in the ovule and was later found to also be required for successful powdery mildew infection (Escobar-Restrepo et al., 2007; Kessler et al., 2010). It is thought that FER is involved in the reorganization of the plasma membrane that is needed for haustoria formation upon penetration of the host cell wall (Kessler et al., 2010; Hückelhoven & Panstruga, 2011). In addition, FER seems to play a role in PTI as *fer* mutant plants display deregulated (enhanced) ROS production, MAPK phosphorylation, and stomatal closure in response to flg22 and show aberrant cell death (Keinath et al., 2010). This implies *Cr*RLK1L proteins act as potentially important sensors in plant-pathogen interactions.

3.3 Materials and methods

Plant material

Nicotiana benthamiana plants from accession Nb-1 (Bombarely et al., 2012) were grown in a controlled environment chamber with 16 h light and 65% relative humidity for 6 weeks. Temperature was 24°C during light and 22°C during dark periods. Tomato Rio Grande (RG)-prf3 (Salmeron et al., 1996) plants were grown in trays in a greenhouse without supplemental light for 3 weeks.

Phylogenetic analysis

Amino acid sequences for the tomato and *N. benthamiana* Mal proteins were obtained from the Sol Genomics Network (SGN; http://solgenomics.net) and Arabidopsis sequences were retrieved from The Arabidopsis Information Resource (http://www.arabidopsis.org). Alignment and tree construction were performed with MEGA7 (Kumar et al., 2016). Specifically, protein sequences were aligned using the MUSCLE method (align protein, default settings). The phylogenetic tree was estimated using the neighbor-joining method (p-distance, default settings otherwise). Reliability of the tree was estimated using the bootstrap method (10,000 replicates).

Cloning

The construct for virus-induced gene silencing (VIGS) was generated as previously described (Rosli et al., 2013). Suitable sequences targeting the orthologs of Mal1 and Mal2 were selected using the SGN VIGS tool (Fernandez-Pozo et al., 2015) and cloned into pCR8/GW/TOPO (Invitrogen), followed by recombination into pQ11 Liu:2002wq using the LR Clonase II enzyme mix (Invitrogen), and transformation into *Agrobacterium tumefaciens* GV2260 (Hellens et al., 2000). Full-length *Pti1* genes and the kinase domains of the eight *Mal* genes were PCR-amplified with gene specific oligonucleotides adding EcoRI sites on both ends as described previously (Mathieu et al., 2014). PCR products were EcoRI-digested and ligated into the pJG4-5 (prey) and pEG202 (bait) yeast two-hybrid vectors, respectively. Chimeric EFR-Mal genes were cloned by 'fusion' PCR as described (Mathieu et al., 2014). Briefly, the extracellular portion of EFR and the intracellular parts of Mal1 and Mal2 were amplified separately with oligonucleotides adding overlapping sequences. A second round of PCR was performed to fuse the two gene fragments and the

resulting chimeric genes were ligated into the pJLSmart Gateway entry vector (Mathieu et al., 2007) as described. The constructs were recombined into the protoplast expression vector HBT95 (He et al., 2006) using the LR Clonase II enzyme mix to obtain C-terminal HA-tag fusions.

Yeast two-hybrid assay

To investigate protein-protein interactions, pair-wise yeast two-hybrid assays using the LexA system were performed as previously described (Mathieu et al., 2014). Briefly, *Saccharomyces cerevisiae* strain EGY48 was co-transformed with bait and prey constructs and selected on dropout medium. Primary transformants were plated onto galactose/raffinose plates containing 5-bromo-4-chloro-3-indolyl-β-D-galactopyranoside (X-gal) and monitored for blue staining.

Cell death suppression assay

The cell death suppression assay in *N. benthamiana* was performed as described previously (Chakravarthy et al., 2010; Rosli et al., 2013). Briefly, seedlings were syringe-infiltrated with Agrobacterium strains carrying the VIGS constructs and the assay performed 6 weeks later. Non-pathogenic *Pseudomonas fluorescens* 55 was vacuum-infiltrated to induce the PTI response, followed 7 h later by virulent *P. syringae* pv. *tomato* DC3000 Δ*hopQ1-1* (Wei et al., 2007). Disease symptoms were monitored and plants photographed after 5 days.

Protoplast isolation and transformation

Tomato mesophyll protoplasts were prepared and transformed as previously described (Yoo et al., 2007; Nguyen et al., 2010), with modifications. RG-prf3 plants were grown in a greenhouse under natural light and shifted to low-light conditions a few days before protoplast isolation. Fully expanded leaves of four week-old plants

were selected and cut into thin strips after removal of the midvein. Leaf strips were put into a protoplast isolation medium (K3 with 0.4 M sucrose) containing 1% w/v Cellulose R-10 (Yakult Pharmaceutical) and 0.15% w/v Macerozyme R-10 (Yakult Pharmaceutical) in square petri dishes and incubated at 30°C for 12-16 h. Following digestion, petri dishes were placed on a horizontal shaker for a few minutes to release the protoplasts and the medium was poured through a Cellector tissue sieve (Bellco Glass) to remove leaf debris. The enzyme solution with the released protoplasts was transferred to round-bottom culture tubes and carefully overlaid with 2 ml W5 (0.155 M NaCl, 0.125 M $CaCl_2$, 5 mM KCl, 5 mM glucose). Protoplasts were centrifuged at 400 x *g* for 3 min in an Eppendorf 5810 with acceleration and brake set to 0. Viable protoplasts floating at the interface between the W5 and the enzyme solution were transferred to fresh round-bottom tubes and diluted with 10 ml W5. Protoplasts were centrifuged at 100 x g for 2 min (acceleration and brake set to 3), the supernatant removed, and the protoplasts resuspended in 10 ml W5. Following this wash step, the protoplasts were incubated on ice for 2 h covered with aluminum foil to allow recovery from the extraction procedure. To prevent clumping, tubes were placed horizontally and the protoplasts gently resuspended every half an hour. Protoplasts were collected after the recovery period by centrifugation at 100 x *g* for 2 min and resuspended in 1-2 ml MMG (0.4 M mannitol, 15 mM $MgCl_2$, 4 mM MES pH 5.7) in a single round-bottom tube. The number of protoplasts was counted using a hemocytometer (Hausser Scientific) and the density adjusted to 3 x 10^5 protoplasts/ml. Round-bottom microcentrifuge tubes with 10 µg plasmid DNA in a total volume of 20 µl were used for transformation. To each tube were added 200 µl of protoplasts and 220 µl PEG solution (40% w/v PEG-4000, 0.2 M mannitol, 0.1 M $Ca(NO_3)_2$), gently mixed, and incubated for 5 min. The transformation process was stopped by addition of 1 ml W5 and the

protoplasts were collected by centrifugation at 100 x g for 2 min. The remaining PEG solution was removed by washing the protoplasts once with 1 ml W5. The protoplasts were resuspended in 1 ml WI (0.5 M mannitol, 20 mM KCl, 4 mM MES pH 5.7) and incubated in the dark for 6 h. Protoplasts were treated with 100 nM elf18 (Biomatik), 100 nM flgII-28 (EZBiolab), or no peptide for 10 min. The protoplasts were collected, the supernatant removed, and the samples frozen in liquid nitrogen and stored at -80°C until processing.

Mitogen-activated protein kinase phosphorylation assay

Whole protein was extracted using a buffer containing 10% glycerol, 25 mM Tris-HCl pH 8.0, 1 mM EDTA pH 8.0, 150 mM NaCl, 10 mM DTT (American Bioanalytical), and 0.15% IGEPAL CA-630 (Nonidet P-40; Sigma-Aldrich), with cOmplete ULTRA EDTA-free protease inhibitor (Roche Diagnostics) and PhosSTOP phosphatase inhibitor (Roche Diagnostics). Samples were incubated for 15 min at 4°C, the supernatants collected, and boiled in Laemmli sample buffer. Gel electrophoresis and immunoblotting was performed following standard protocols. Mitogen-activated protein kinase (MAPK) phosphorylation was detected using the phospho-p44/42 MAPK (Erk1/2) antibody (anti-pMAPK, Cell Signaling) following the manufacturer's instructions. HA-tagged proteins were detected using anti-HA-HRP (Roche Diagnostics) to verify expression of all constructs.

3.4 Results

The tomato genome contains several predicted malectin-like receptor-like proteins with kinase domains similar to Pto

In tomato, the Pto protein kinase together with the nucleotide-binding leucine-rich repeat protein Prf mediates recognition of two effectors from *Pseudomonas syringae* pv. *tomato* (*Pst*) DC3000, AvrPto and AvrPtoB, that serve to suppress PTI responses (Martin, 2012). It has been proposed that Pto is not the operative target of these effectors because in the absence of AvrPto and AvrPtoB the Pto kinase does not promote resistance to *Pst* DC3000 (Lin & Martin, 2005; van der Hoorn & Kamoun, 2008; Mathieu et al., 2014). Instead, it is thought that Pto acts as a guarded decoy for the intracellular kinase domains (KDs) of plasma membrane-localized PRRs such as FLS2, EFR, and BAK1 to sense the presence of AvrPto and AvrPtoB inside the plant cell and activate effector-triggered immunity (ETI), a strong defense response capable of halting pathogen proliferation (Jones & Dangl, 2006; van der Hoorn & Kamoun, 2008; Martin, 2012; Zipfel, 2014). However, the amino acid sequence of Pto is very different from those KDs (their identities range between 30-40%) and it seems unlikely that Pto has evolved from any PRR that has been shown to interact with either AvrPto or AvrPtoB to date (Göhre et al., 2008; Shan et al., 2008; Xiang et al., 2008; Gimenez-Ibanez et al., 2009; **?**; Xiang et al., 2011; Zeng et al., 2011; Zhou et al., 2014).

In an attempt to find the progenitor from which Pto might have evolved we searched the tomato genome for predicted proteins with high similarity to Pto and in addition to other Pto family members we found a number of receptor-like kinases. We utilized our previously published RNA sequencing (RNA-Seq) data to identify the genes that are well-expressed in tomato leaves and chose to focus on only those genes (Rosli et al., 2013). Analysis of the eight predicted proteins revealed

that they consist of a secretion signal peptide, an extracellular malectin-like domain containing two malectin domains, a single-pass transmembrane domain, and an intracellular KD (Figure 3.1A). We refer to these uncharacterized proteins as Mal1 through Mal8 because of their malectin-like domains. We then performed a phylogenetic analysis with the KDs of the eight Mals as well as Pto and the closely related Fen, another Pto family member (Rosebrock et al., 2007) (Figure 3.1B). The resulting phylogenetic tree confirmed the BLAST search ranking indicating that Mal1 and Mal2 are the closest homologs of Pto outside the Pto family of kinases and the most likely candidates from which Pto might have evolved (Figure 3.1B).

Mal1 and Mal2 contain a unique amino acid motif only found in Pto family members

To appreciate the similarities and differences at the amino acid level, we performed an alignment of the eight Mals and the five Pto family members. We noticed that Pto, Fen, and PtoG begin with an MGSKYS sequence and this motif is conserved in both Mal1 and Mal2 at approximately the beginning of their predicted kinase domains but is not found in any of the other six Mals (nor in PtoA and PtoD). We then searched the tomato genome for predicted proteins containing the MGSKYS motif but found no additional instances of this sequence anywhere in those proteins. The presence of this conserved motif together with the overall similarity of their KDs (Mal1 is 70% identical to Pto; Mal2 is 69% identical) supports our hypothesis that Pto family members might have evolved from the KDs of Mal1 and Mal2. It should be noted that the two Mals have a C-terminal region of ~60 amino acids after their predicted KDs that is not present in any Pto family member. The function of these additional amino acids is presently unknown. To understand how the tomato Mal proteins relate to members of the

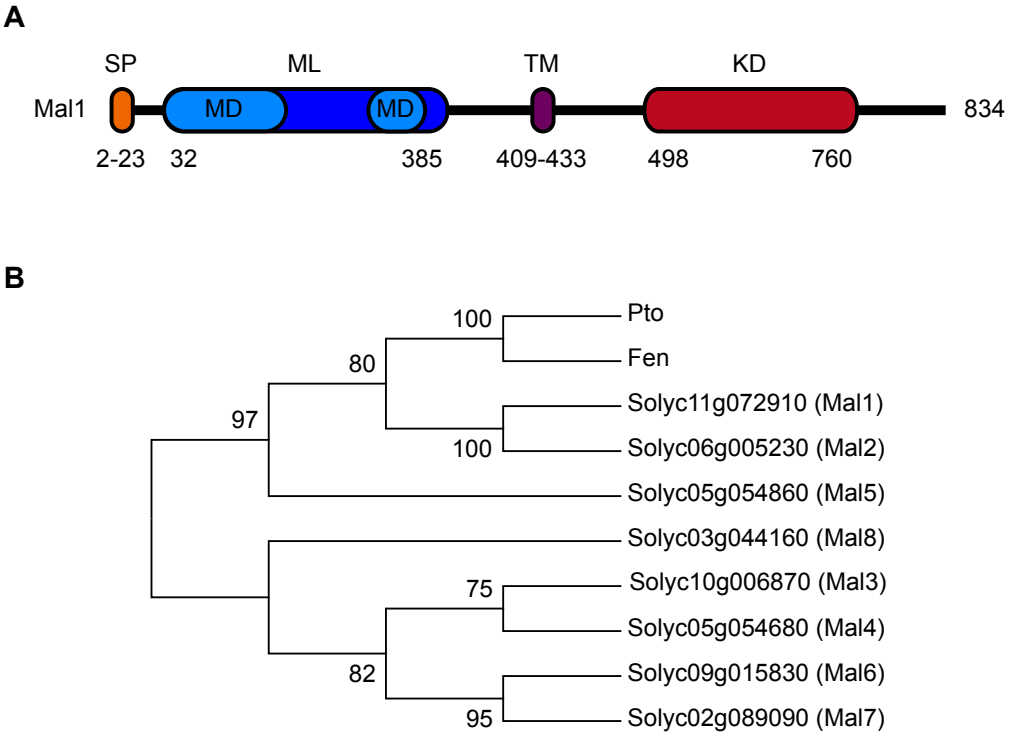

Figure 3.1. Malectin-like receptor-like kinases in the tomato genome resemble the Pto protein kinase. **(A)** Composition of malectin-like receptor-like kinases in plants illustrated using Mal1 as an example. SP, secretion signal peptide; ML, malectin-like domain; MD, malectin subdomain; TM, single-pass transmembrane domain; KD, kinase domain. The numbers indicate the amino acid position where the various domains begin and end as well as the length of the protein. **(B)** Phylogenetic tree showing the eight Mal proteins along with Pto and Fen. Only the kinase domains (KDs) including the C-terminal 'tails' have been used for the tree construction. Numbers at the branch points indicate bootstrap percentages.

Arabidopsis *Cr*RLK1L family, we searched the Arabidopsis genome for predicted proteins with similarity to the eight Mals and used the resulting sequences to build a phylogenetic tree (Figure 3.2B). This revealed that 13 Arabidopsis proteins cluster with the eight tomato Mals, six of which have known functions (Boisson-Dernier et al., 2011; Lindner et al., 2012) (Figure 3.2B). The closest Arabidopsis orthologs to Mal1 and Mal2 seem to be HERK1 and At5g59700, a protein with as of yet unknown function. HERK1 functions in cell elongation during vegetative

growth together with THE1 and FER (Guo et al., 2009). Interestingly, HERK1 contains the MGSKYS motif at approximately the same position as Mal1 and Mal2 and a search of the Arabidopsis predicted proteins revealed no other instances of this motif. Given that HERK1 functions in monitoring cell wall integrity and the malectin-like domains are thought to bind carbohydrates (Boisson-Dernier et al., 2011; Lindner et al., 2012), it is possible that Mal1 and Mal2 function as DAMP receptors.

Mal1 and Mal2 interact in a yeast two-hybrid system with the Pti1 protein kinases involved in PTI

The Pti1a protein kinase was first discovered as an interactor of Pto in a yeast two-hybrid screen and we recently showed that Pti1a and/or Pti1b contribute to the oxidative burst in response to flagellin perception and promote resistance to *Pst* infection (Zhou et al., 1995) (Chapter 2). Given the similarities between Pto and the KDs of Mal1 and Mal2, we speculated that the Pti1 proteins might interact with and function downstream of these putative receptors and interact with Pto because the latter evolved as a decoy from Mal1 and Mal2. Therefore, we performed a pair-wise yeast two-hybrid experiment to test for interaction of the KDs of all eight Mals with Pti1a and Pti1b and their respective kinase inactive forms (K96N substitutions) (Zhou et al., 1995) (Figure 3.3). We chose to use only the KDs because full-length plasma membrane receptors can be problematic in the yeast system. Pto and Fen were included as positive and negative control, respectively. We observed what appeared to be clear interaction of the Mal1 KD with all four Pti1 proteins and weaker interaction of the Mal2 KD. The KDs of Mal3 and Mal4 showed very faint interaction but did not seem promising enough to pursue further. More importantly, the KD of Mal5, the protein most closely related to Mal1 and Mal2, did not interact with any of the Pti1 proteins. It is not surprising that the

A

```
  Pto    1       MGSKYSKATN..
  Fen    1       MGSKYSKATN..
 Mal1  461 ..TSHTMGSKYSNGTT..
 Mal2  458 ..LSHTMGSKYSNGTT..
HERK1  452 ..NGTSMGSKYSNGTT..
```

B

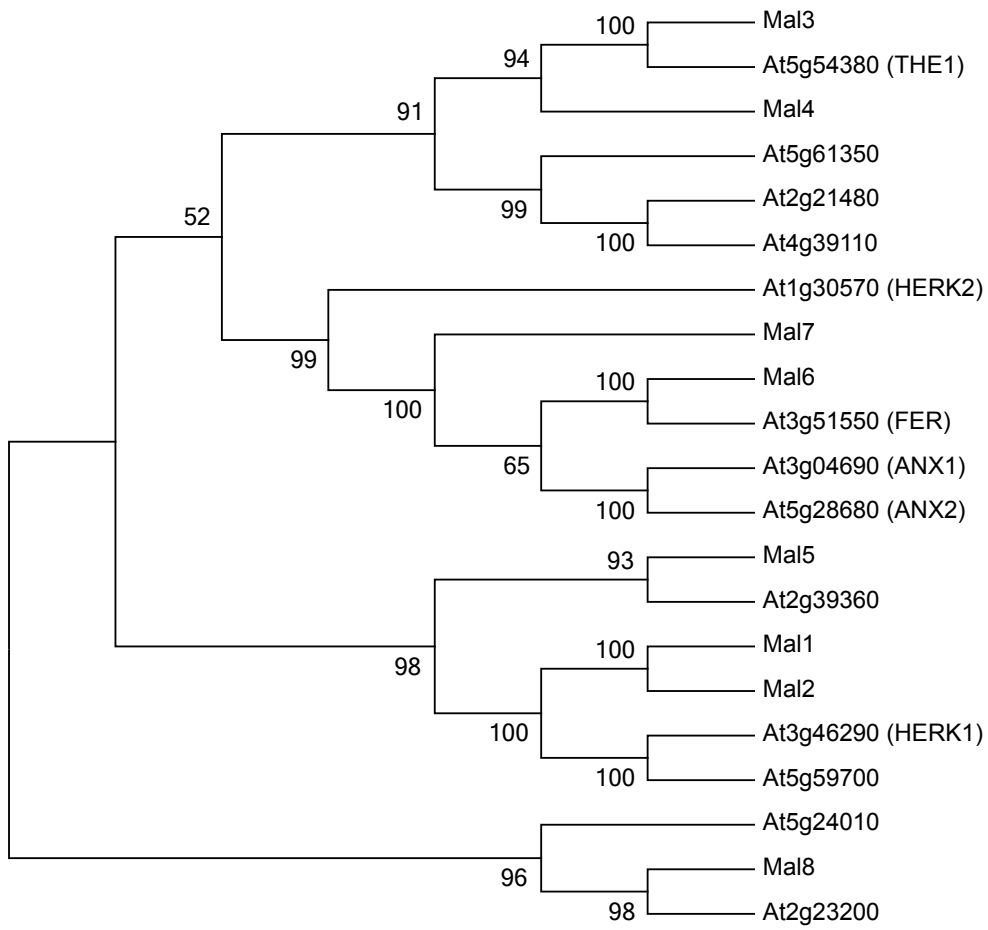

Figure 3.2. Arabidopsis contains several proteins closely related to the tomato Mals but only one contains the MGSKYS motif. **(A)** Illustration showing the position of the MGSKYS motif present in some Pto family members, Mal1, Mal2, and the only Arabidopsis protein, HERK1. Note that whereas Pto and Fen begin with this motif, Mal1, Mal2, and HERK1 have MGSKYS embedded within as denoted by the numbers indicating the residue positions of the methionine within the protein. **(B)** Phylogenetic tree showing the eight tomato Mals along with similar proteins in Arabidopsis. Full-length protein sequences have been used for the tree construction. Bootstrap percentages are indicated at the branching nodes.

kinase inactive Pti1 proteins still interact with the KDs of Mal1 and Mal2 since it is known that kinase activity of Pti1a is not required for the interaction with Pto, whereas kinase activity of Pto is necessary (Zhou et al., 1995). It remains to be seen if kinase inactive versions of Mal1 and Mal2 can still interact with Pti1a and Pti1b or if these mutant forms loose their capacity for interaction. Furthermore, the ability of Pti1a to be phosphorylated on T233 is crucial for its interaction with Pto and it remains to be seen if this phosphorylation site is equally important for interaction with Mal1 and Mal2 and if these two receptor-like kinases are able to phosphorylate the Pti1 proteins on that residue (Sessa et al., 2000).

The *Nicotiana benthamiana* orthologs of Mal1 and Mal2 promote resistance to *Pst*

To test whether Mal1 and Mal2 are involved in plant immune responses, we decided to identify the orthologs in *N. benthamiana* and silence the corresponding genes. For this we searched the *N. benthamiana* genome for predicted proteins similar to Mal1 and Mal2 and found two proteins that appear to be the orthologs of Mal1 and one protein that seems to be the ortholog of Mal2 (Figure 3.4A). We designed two silencing constructs, designated NbM1 and NbM2, intended to silence the genes corresponding to the orthologs of Mal1 and Mal2, respectively. In order to effectively silence all three genes, we constructed a concatenated virus-induced gene silencing (VIGS) construct containing both the NbM1 and NbM2 silencing fragments (Figure 3.4B). We then infected *N. benthamiana* plants with this tobacco rattle virus-based silencing construct along with EC1 (negative control) and NbFLS2 (positive control) using agroinfiltration (Chakravarthy et al., 2010; Rosli et al., 2013) (Figure 3.4C). Five week-old silenced plants were vacuum-infiltrated with *P. fluorescens* 55 to induce PTI, followed seven hours later with pathogenic *Pst* DC3000 Δ*hopQ1-1* (Wei et al., 2007; Chakravarthy et al., 2010; Rosli et al.,

Figure 3.3. The kinase domains of Mal1 and Mal2 interact with Pti1 in yeast. Pairwise yeast two-hybrid experiment to test the interaction of the kinase domains of the eight tomato Mal proteins against tomato Pti1a and Pti1b and their kinase inactive mutants (K96N). Blue staining indicates interaction of the protein pairs. EV, empty vector; KD, kinase domain.

2013). While the NbFLS2 plants displayed severe disease symptoms seven days after infiltration, the NbM1/2 plants showed fewer symptoms but markedly more than the EC1 controls (Figure 3.4C). This suggests that the three genes targeted by the concatenated VIGS construct play a role in the defense response against *Pst*. In our hands, VIGS works less reliably in tomato and we decided to forego repeating this experiment in tomato and instead develop CRISPR/Cas9 lines with null mutations in Mal1 and Mal2 for evaluation of disease resistance (Jinek et al., 2012). These lines are currently being advanced and analyzed.

Chimeric EFR-Mal receptors are not active or unable to signal PTI responses

Because the ligands for the putative Mal1 and Mal2 receptors are not known, we decided to construct chimeric receptors comprising a receptor domain with a known ligand. The Arabidopsis EFR receptor recognizing EF-Tu was a good candidate for this endeavor because it has been successfully used to construct chimeric receptors with FLS2 and WAK1 (Zipfel et al., 2006; Albert et al., 2010; Brutus et al., 2010). Furthermore, the elf18 peptide that is recognized by EFR is not sensed in tomato because it does not have any receptors capable of recognizing this peptide (Zipfel et al., 2006; Boller & Felix, 2009), allowing the chimeric receptors to be easily tested for gain-of-function phenotypes. We constructed our chimeric receptors using the extracellular receptor domain (including the outer juxtamembrane domain) of EFR and the transmembrane domain and entire intracellular portion of Mal1 or Mal2 (Figure 3.5A). Previous work evaluating various EFR-WAK1 chimeras revealed that chimeric receptors containing the entire extracellular domain of EFR up to but not including the transmembrane domain resulted in the most active receptor and we constructed our EFR-Mal chimeras identically (Brutus et al., 2010) (Figure 3.5A). To test the two EFR-Mal chimeras in tomato, we isolated mesophyll

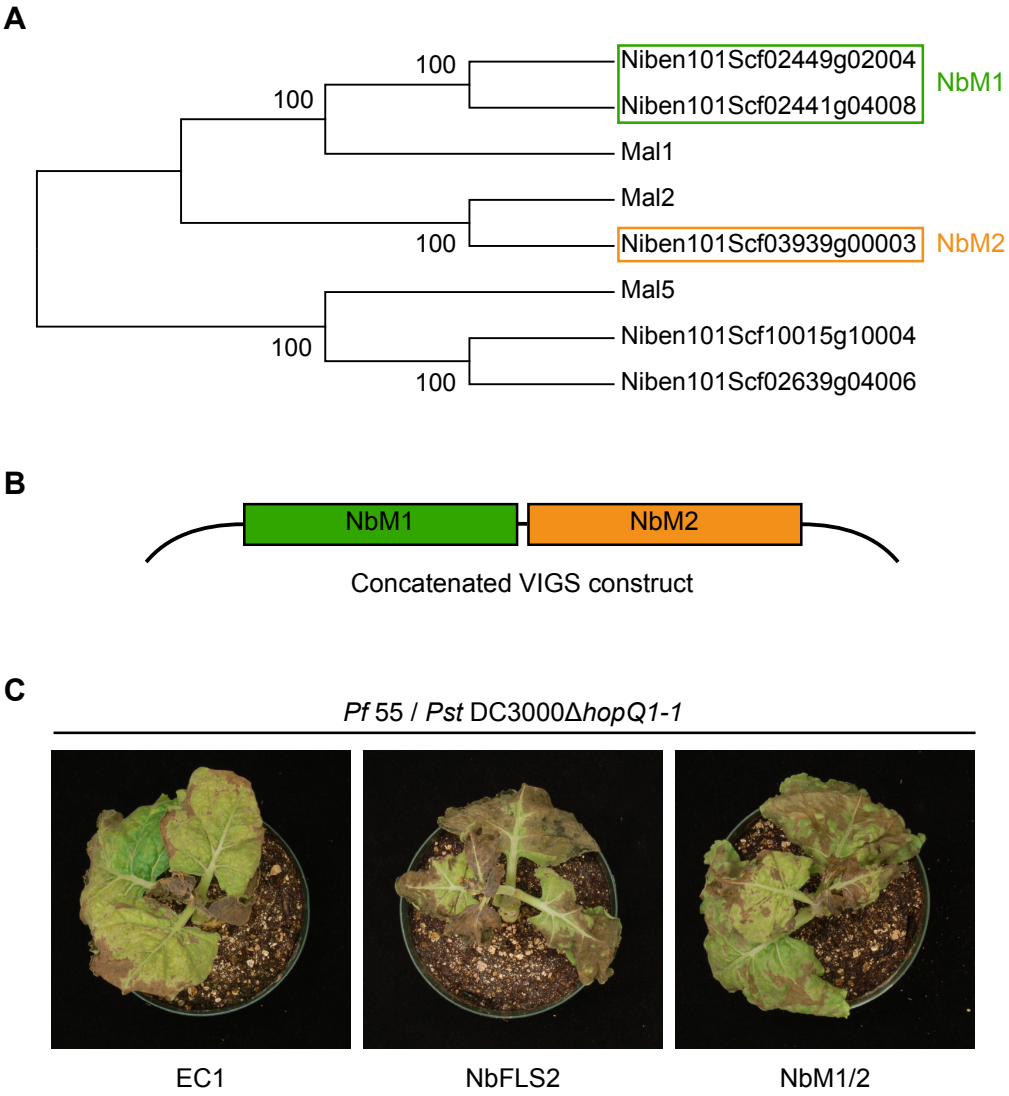

protoplasts from Rio Grande-prf3 leaves and transfected them with *EFR-Mal1*, *EFR-Mal2*, wild-type *EFR* (positive control), or the gene encoding yellow fluorescent protein (*YFP*; negative control) (Salmeron et al., 1996; Yoo et al., 2007; Nguyen et al., 2010) (Figure 3.5B). Each transfection was done in triplicate and we further split each transfection into three tubes to treat the protoplasts with either water (negative control), flgII-28 (positive control; does not require EFR for recognition), or elf18 (Cai et al., 2011). Treated protoplasts were assayed for MAPK

Figure 3.4 ***(previous page).*** Silencing the orthologs of Mal1 and Mal2 in *N. benthamiana* promotes susceptibility to *Pst*. **(A)** Phylogenetic tree showing tomato Mal1, Mal2, and Mal5 along with their orthologs in *N. benthamiana*. The tree was constructed using full-length protein sequences. Bootstrap percentages are indicated at the branching nodes. NbM1, silencing fragment targeting the two orthologs of Mal1 indicated in green; NbM2, silencing fragment targeting the single ortholog of Mal2 indicated in orange. **(B)** Illustration showing the concatenated virus-induced gene silencing (VIGS) construct used in this experiment. The NbM1 and NbM2 silencing fragments were fused by PCR and inserted into a tobacco rattle virus-based vector to obtain a single VIGS construct targeting all three orthologs in *N. benthamiana*. **(C)** *N. benthamiana* seedlings were inoculated with tobacco rattle virus-based VIGS constructs for EC1 (negative control), NbFLS2 (positive control), and NbM1/2 (designed to silence all three *Mal1/2* orthologs). Six weeks later, the whole plants were vacuum-infiltrated with non-pathogenic *Pf* 55 to induce PTI, followed 7 h later with disease-causing *Pst* DC3000 Δ*hopQ1-1*. Compromised induction of PTI by *Pf* 55 as a result of gene silencing leads to faster disease development. Photographs were taken 5 days after infiltration.

activation using an antibody to detect phosphorylated (activated) MAPKs. While wild-type EFR showed clear activation of MAPKs upon elf18 treatment, demonstrating that the transiently expressed receptor enables perception of this peptide, neither of the EFR-Mal chimeras resulted in MAPK activation. Treatment with flgII-28, whose perception is independent of EFR, activated MAPK phosphorylation in all protoplasts samples, indicating that the protoplasts were not damaged, stressed, or otherwise unable to activate MAPK signaling. To verify expression of the chimeric receptors, the same protoplast samples were probed with anti-HA (all transfected constructs encoded an HA-tag) and we observed accumulation of all proteins to respectable levels (Figure 3.5B). These experiments indicate that the EFR-Mal chimeras are stable even though they may not be signaling competent.

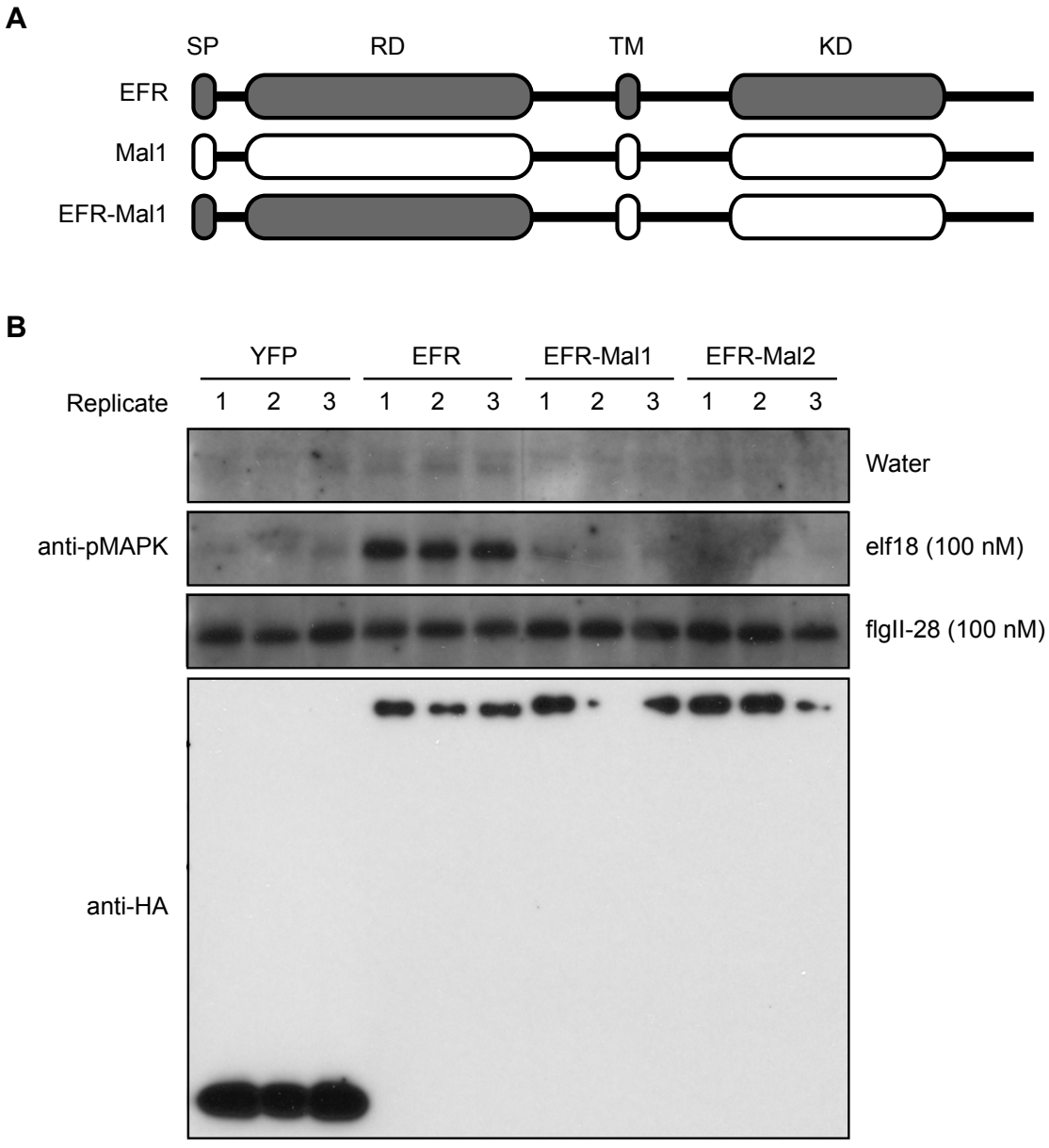
A
SP
RD
TM
KD
EFR
Mal1
EFR-Mal1
B
YFP
EFR
EFR-Mal1
EFR-Mal2
Replicate
1 2 3 1 2 3 1 2 3 1 2 3
Water
anti-pMAPK
elf18 (100 nM)
flgII-28 (100 nM)
anti-HA

Figure 3.5 ***(previous page).*** Chimeric EFR-Mal receptors do not activate MAPKs in response to elf18. **(A)** Illustration showing the constituent parts of the EFR-Mal chimeras using Mal1 as an example. Grey, domains originating from EFR; White, domains originating from Mal1; SP, secretion signal peptide; RD, extracellular receptor domain; TM, single-pass transmembrane domain; KD, kinase domain. **(B)** Tomato mesophyll protoplasts were isolated and transformed with either *YFP* (negative control), *EFR* (positive control), or either of the two *EFR-Mal* chimeras, each encoding an HA-tag. Each transformation was treated with either water (negative control), flgII-28 (positive control), or elf18. Each treatment was performed in triplicates. Anti-pMAPK shows phosphorylation (activation) of MAPKs upon peptide perception. Anti-HA shows accumulation of the expressed proteins.

The *Pst* effector AvrPtoB, but not AvrPto, interacts with Mal1 and Mal2 in yeast

If Pto is indeed derived from and has evolved as a decoy for the KDs of Mal1 and Mal2, we would expect that the *Pst* effectors AvrPto and AvrPtoB target these putative receptors and interact with their KDs. Therefore we tested for interaction of AvrPto and AvrPtoB with the KDs of Mal1 and Mal2 in the yeast system (Figure 3.6). We included Pto and Fen as controls because their interaction patterns with the two effectors are known (Rosebrock et al., 2007; Mathieu et al., 2014; Kraus et al., 2016). We observed no apparent interaction of either AvrPto or wild-type AvrPtoB with the KDs of Mal1 and Mal2, but a version of AvrPtoB lacking a functional E3 ligase domain (E3-LOF) clearly interacted with both KDs (Figure 3.6). This is identical to Fen which is known to interact with AvrPtoB, but not AvrPto, and to be targeted for degradation by the 26S proteasome by way of polyubiquitination by the AvrPtoB E3 ligase domain, thus masking the interaction in yeast unless the E3 ligase activity is abolished (Rosebrock et al., 2007; Mathieu et al., 2014; Kraus et al., 2016). It is possible that full-length Mal1 and Mal2 are

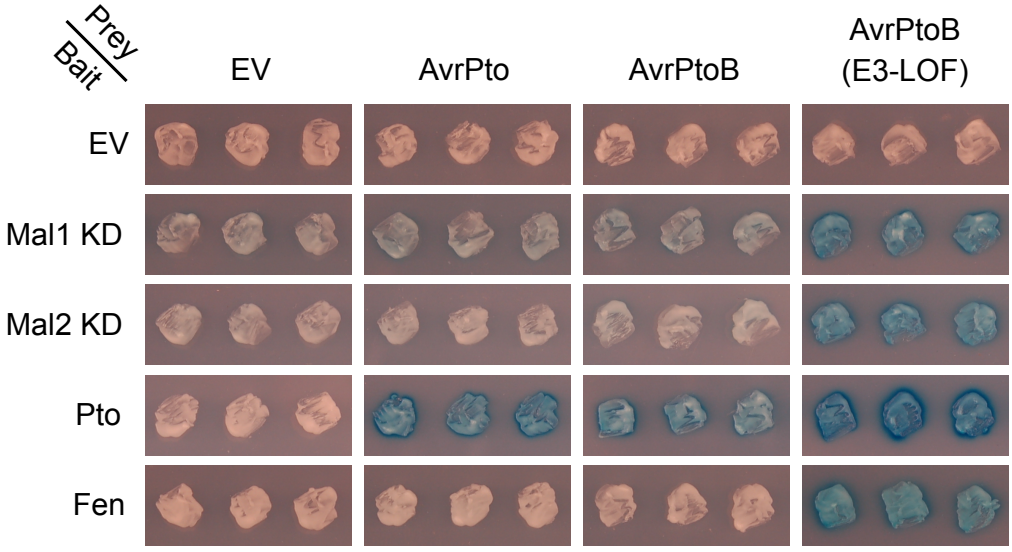

Figure 3.6. AvrPtoB without a functional E3 ligase domain interacts with the kinase domains of Mal1 and Mal2 in yeast. Pairwise yeast two-hybrid experiment to test the interaction of the kinase domains of Mal1 and Mal2 against the *Pst* effectors AvrPto and AvrPtoB. AvrPtoB(E3-LOF) contains three point mutations in the E3 ligase domain rendering it inactive (Mathieu et al., 2014). Pto and Fen were included as controls. Blue staining indicates interaction of the protein pairs. EV, empty vector; KD, kinase domain.

likewise targeted for degradation by the E3 ligase activity of AvrPtoB, although we have not tested this experimentally. Precedence for this hypothesis exists in the form of the Arabidopsis chitin receptor CERK1 which is polyubiquitinated by AvrPtoB and targeted for degradation in a vacuole-dependent manner (Gimenez-Ibanez et al., 2009).

The interaction of AvrPtoB with Mal1 and Mal2 resembles its interaction with Pto

To further analyze the interaction of AvrPtoB with Mal1 and Mal2, we tested a series of AvrPtoB point mutants with known interaction patterns regarding Pto and, in some cases, Fen (Xiao et al., 2007; Dong et al., 2009; Mathieu et al.,

2014). AvrPtoB has two well-documented virulence domains, referred to as the Pto-interacting domain (PID) and the Fen-interacting domain (FID), which can interfere with PTI and the E3 ligase domain which promotes pathogenicity by interfering with ETI responses in tomato (Rosebrock et al., 2007; Xiao et al., 2007; **?**; Zeng et al., 2011; Mathieu et al., 2014) (Figure 3.7A). Recently, it was found that a version of AvrPtoB with mutations in all three domains retains the ability to suppress ETI by inhibiting MAPK signaling (Wei et al., 2015). We already established that AvrPtoB without a functional E3 ligase domain can interact with the KDs of both Mal1 and Mal2. As a next step we wanted to test whether the Mal KDs bind the PID, the FID, or some other part of AvrPtoB. Therefore, we performed a yeast two-hybrid experiment using AvrPtoB point mutants that interrupt either the PID (F173A), the FID (G325A), or both domains (F173A/G325A) in the background of the E3-LOF mutant version (Figure 3.7A and 3.7B). We found that the F173A mutation significantly reduced interaction with the KDs of both Mal1 and Mal2, but did not abolish the interactions. The G325A mutation had a much smaller effect and the F173A/G325A double mutation abolished both interactions (Figure 3.7B). This is very similar to the interaction of AvrPtoB with Pto and would suggest that the KDs of Mal1 and Mal2 are able to bind both the PID and the FID but predominantly interact with the PID. Furthermore, the E3 ligase activity of AvrPtoB appears to be able to target both Mal KDs for degradation irrespective of which domain they are bound to. This is in contrast to Pto which is only degraded when it binds the FID located next to the E3 ligase domain and not the more distal PID (Mathieu et al., 2014).

We next evaluated a series of point mutants that were shown to abolish interaction with Pto in the context of a truncated AvrPtoB protein comprising the first 307 amino acids ($AvrPtoB_{1\text{-}307}$) that encompasses the PID and is sufficient

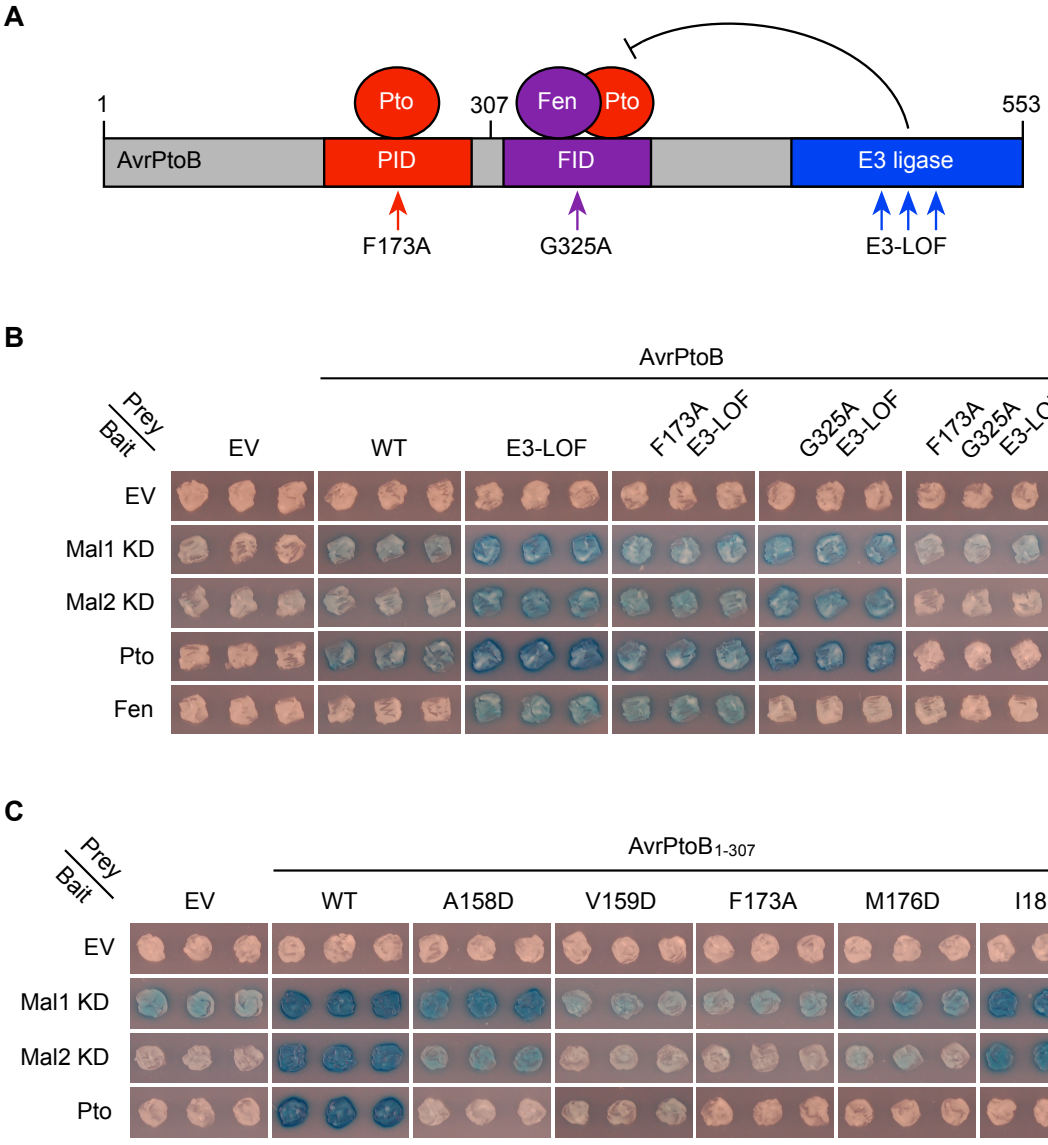

for interaction with Pto (Xiao et al., 2007; Dong et al., 2009) (Figure 3.7C). We found that in addition to F173A, V159D and M176D abolished interaction with the KDs of both Mal1 and Mal2, whereas A158D reduced but did not abolish the interactions and I181D did not have a significant effect (Figure 3.7C). While some residues of AvrPtoB are clearly important for interaction with both Pto and the Mal KDs, some residues are required only for interaction with Pto and others, presumably, are important only for interaction with the KDs of Mal1 and Mal2.

Figure 3.7 ***(previous page).*** The interaction of AvrPtoB with Mal1 and Mal2 is similar to its interaction with Pto. **(A)** Illustration showing the three well-defined domains of AvrPtoB and where it binds Pto and Fen. Red, Pto-interacting domain (PID); Purple, Fen-interacting domain (FID); Blue, E3 ligase domain. The T-shaped arrow indicates the ability of the E3 ligase domain to degrade Pto and Fen bound to the FID. Arrows below each domain indicate point mutations that abolish interaction of Pto and Fen with the PID (F173A) and FID (G325A) or render the E3 ligase domain inactive (E3-LOF). The numbers above the AvrPtoB protein show amino acid positions. Adapted from Mathieu et al. (2014); Wei et al. (2015). **(B)** Pairwise yeast two-hybrid experiment to test the interaction of the kinase domains of Mal1 and Mal2 against different variants of AvrPtoB, including wild-type (WT), E3 loss-of-function (E3-LOF), and point mutations in the PID (F173A), the FID (G325A), or both domains (F173A/G325A) in the background of the E3-LOF mutant. Pto and Fen were included as controls. Blue staining indicates interaction of the protein pairs. EV, empty vector; KD, kinase domain. **(C)** Pairwise yeast two-hybrid experiment to test the interaction of the kinase domains of Mal1 and Mal2 against a truncated version of AvrPtoB containing only the PID ($AvrPtoB_{1\text{-}307}$) and various point mutations in that truncated effector protein. Pto was included as a control. Blue staining indicates interaction of the protein pairs. EV, empty vector; KD, kinase domain.

3.5 Discussion

Our experiments indicate that Pto interacts more strongly with AvrPtoB than Mal1 and Mal2. If Pto indeed evolved as a decoy for the KDs of Mal1 and/or Mal2 and does not have a function other than binding AvrPtoB (and AvrPto) and thus inducing Prf-mediated ETI, then there are no evolutionary constraints preventing it from optimizing its binding capacity to these effectors (van der Hoorn & Kamoun, 2008). Indeed, increased affinity is advantageous because it presumably allows more efficient or sensitive detection of these two effector proteins and is thus favored by evolution (van der Hoorn & Kamoun, 2008). The Mal1/2 KDs on the other hand are restrained by their function and their need to interact with downstream

signaling components. Furthermore, Pto seems to have evolved the ability to partially resist degradation mediated by the AvrPtoB E3 ligase domain as Pto bound to the distal PID, but not the proximal FID, is able to evade degradation (Mathieu et al., 2014). The KDs of both Mal1 and Mal2 on the other hand are degraded regardless of which domain of AvrPtoB they are bound to, even though they seem to preferentially bind the distal PID, like Pto (Mathieu et al., 2014). The observation that Pto is able to bind both AvrPto and AvrPtoB, but only AvrPtoB is able to interact with the Mal1/2 KDs in yeast suggests that AvrPtoB evolved to target these putative PRRs. We hypothesize that after the Pto family of kinases evolved from the Mal1/2 KDs, presumably through gene duplication, to detect and guard against AvrPtoB did Pto acquire the ability to also detect AvrPto. The closely related Fen can only interact with AvrPtoB without an active E3 ligase and it has been proposed that Fen is the more ancient protein and that Pto evolved from Fen to evade degradation and restore immunity (Rosebrock et al., 2007). In addition, Fen can only interact with AvrPtoB but not AvrPto (Scofield et al., 1996; Tang et al., 1996), further supporting the hypothesis that Fen is the more ancient protein. Recent work with the wild tomato accession *Solanum chmielewskii* LA2677 revealed that the ortholog of Pto, Pto-2677, confers resistance only to AvrPtoB but not AvrPto (Kraus et al., 2016). The two Pto proteins differ by 14 amino acids and it was found that mutating three of them to the residues found in Pto enables Pto-2677 to detect AvrPto (Kraus et al., 2016), suggesting that the progenitor of *S. pimpinellifolium* and LA2677 was able to detect only AvrPtoB and that the ability to sense AvrPto evolved after the two accessions diverged.

In Arabidopsis, the PBS1 kinase is a candidate for a guarded decoy. The *P. syringae* effector AvrPphB is a cysteine protease that cleaves PBS1 and that cleavage is recognized by the nucleotide-binding leucine-rich repeat protein RPS5,

leading to ETI activation (Shao et al., 2003; Ade et al., 2007). It was speculated that PBS1 is a decoy because *pbs1* mutant plants show no enhanced susceptibility to virulent *P. syringae* and virulence targets should contribute to plant immunity otherwise is does not benefit the pathogen to target the host protein (Warren et al., 1999; van der Hoorn & Kamoun, 2008). Like our hypothesis that kinases similar to Pto might be the true targets of AvrPto and/or AvrPtoB, it was hypothesized that other kinases similar to PBS1 might be targeted by AvrPphB for PTI inhibition (Zhang et al., 2010). Indeed, several PBS1-like kinases, including BIK1, were found to be cleaved by AvrPphB (Zhang et al., 2010). BIK1 is a constituent of PRR complexes and associates with FLS2 and becomes rapidly phosphorylated after flg22 treatment in a BAK1-dependent manner (Lu et al., 2010; Zhang et al., 2010). *bik1* mutant plants show reduced ROS production upon FLS2 activation and it was recently shown that BIK1 phosphorylates the NADPH oxidase RBOHD and contributes to its activation (Zhang et al., 2010; Kadota et al., 2014; **?**) More importantly, *bik1* plants are more susceptible to *P. syringae* infection (Zhang et al., 2010), suggesting that it is the true virulence target. It should be noted that AvrPphB is an effector from *P. syringae* pv. *phaseolicola* which is not virulent on Arabidopsis. It is likely that BIK1 orthologs exist in bean that are targeted by AvrPphB to promote *P. syringae* pv. *phaseolicola* infection.

Damage perception is important for defense against necrotrophic pathogens. Arabidopsis plants that have been wounded or pretreated with OGs are more resistant to subsequent *Botrytis cinerea* infection (Aziz et al., 2004; Ferrari et al., 2007; Chassot et al., 2008). Similarly, Arabidopsis plants overexpressing *WAK1* are more resistant to both *B. cinerea* and *Pectobacterium carotovorum* (Brutus et al., 2010; De Lorenzo et al., 2011). The domain swap experiments between WAK1 and EFR revealed that the KD of EFR can mediate resistance against

B. cinerea when it is fused to the extracellular domain of WAK1 and thus able to perceive cell wall damage (Brutus et al., 2010). Likewise, the WAK1 KD is able to promote PTI against Agrobacterium when paired with the extracellular domain of EFR, comparable to wild-type EFR (Zipfel et al., 2006; Brutus et al., 2010). This shows that DAMP receptors serve an important function in plant immunity and that they can promote defense responses to a range of pathogens. To date, no DAMP receptor functioning in resistance to *P. syringae* has been established. Given that *P. syringae* is a hemibiotrophic pathogen that transitions from a biotrophic to a necrotrophic stage before dispersal (Melotto et al., 2008), it is conceivable that DAMP receptors function late during disease development to limit pathogen spread.

Little is known about the function of *Cr*RLK1L proteins in plant defense and while they serve diverse functions in monitoring cell wall integrity (Boisson-Dernier et al., 2011; Lindner et al., 2012), no evidence exists that they serve as bona fide DAMP receptors. FER is involved in the interaction between Arabidopsis and powdery mildew, but it seems to promote haustoria formation and disease establishment similar to MLO, not enhance resistance (Consonni et al., 2006; Kessler et al., 2010). More recently, a rapid alkalization factor secreted peptide has been shown to bind FER and thus suppress primary root elongation (Haruta et al., 2014). Furthermore, the Pti1-like kinase MRI was found to function downstream of FER to mediate signaling to coordinate cell wall integrity and root tip growth (Boisson-Dernier et al., 2015).

Our data indicate that in *N. benthamiana*, the orthologs of tomato Mal1 and Mal2 promote resistance to *P. syringae* infection. We propose that the Mal proteins function as DAMP receptors to perceive unknown ligands via their extracellular malectin-like domains (Figure 8). Ligand binding activates the intracellular KD to

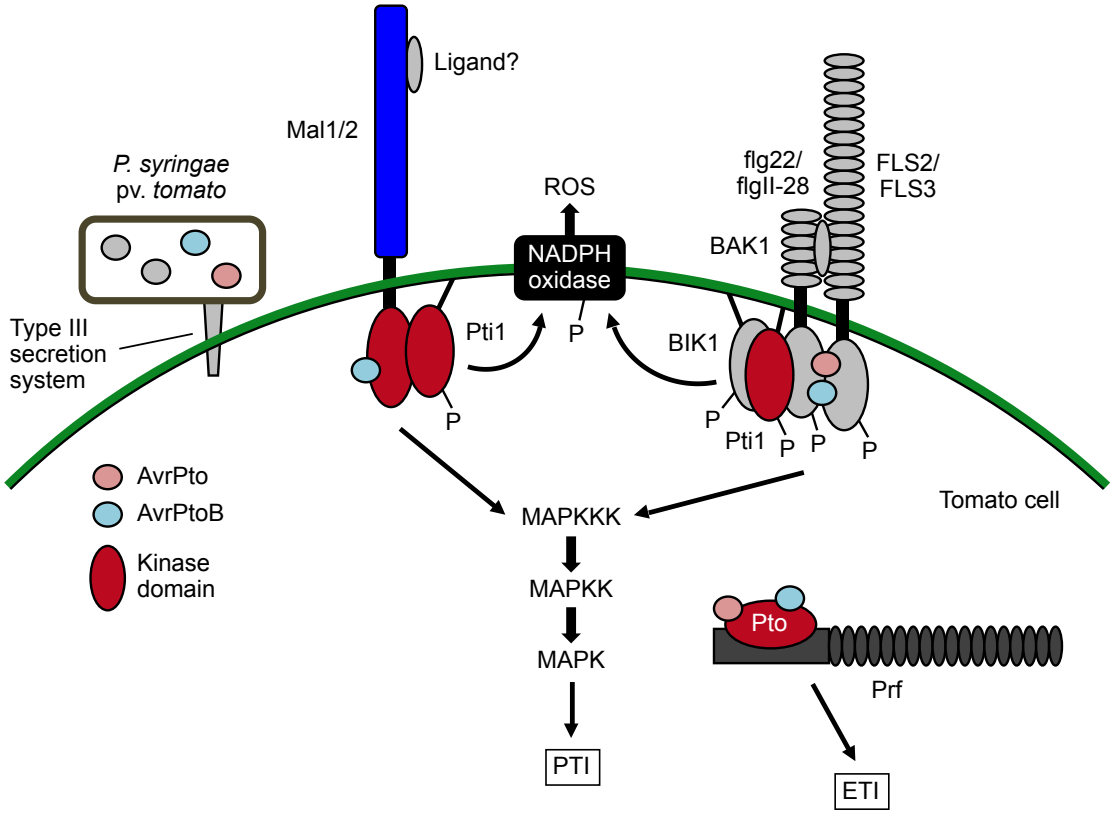

Figure 3.8. Model showing how Mal1 and Mal2 might function in pathogen perception. Upon binding of an unknown ligand (grey) to the extracellular receptor domain (blue) of Mal1 and/or Mal2 the intracellular kinase domain (KD; red) might initiate downstream MAPK signaling cascades, leading to PTI induction. Pti1 (red), which is anchored to the plasma membrane (green) by means of putative S-acylation, might interact with Mal1/2 and become phosphorylated (P) upon ligand binding. Phosphorylated (activated) Pti1 might in turn contribute to NADPH oxidase activation through phosphorylation, leading to the production of reactive oxygen species (ROS). Additionally, Pti1 might be part of the FLS2 and FLS3 receptor complexes (grey) and along with BIK1 contribute to NADPH oxidase activation. AvrPtoB (light blue), a type III-secreted effector from *P. syringae* pv. *tomato*, binds to the KD of Mal1/2, possibly inhibiting its activity or leading to removal of the receptor through polyubiquitination and subsequent degradation. Pto (red), which mimics the KD of Mal1/2, binds to both AvrPtoB as well as the unrelated AvrPto effector (light purple) and together with the nucleotide-binding leucine-rich repeat protein Prf leads to activation of effector-triggered immunity (ETI).

initiate downstream signaling cascades, leading to PTI induction. The receptor-like cytoplasmic kinase Pti1 might become phosphorylated by the Mal1/2 KD and contribute to ROS production by phosphorylation of NADPH oxidases. The *P. syringae* effector AvrPtoB is able to interact with and possibly mediate the degradation of the Mal1/2 receptors, thus promoting bacterial proliferation. Pto seems to have evolved from the Mal1/2 KD to detect the presence of AvrPtoB and, together with Prf, confer resistance to *P. syringae* strains employing this effector, thus safeguarding the Mal1/2 receptors against pathogen manipulation (Figure 8). Future work will elucidate the function of these putative PRRs and establish the molecular mechanism by which they contribute to disease resistance.

3.6 Acknowledgments

We thank Dr. Zhangjun Fei for searching the tomato and Arabidopsis predicted proteins for the MGSKYS motif; Dr. Hernan Rosli for providing the EC1 and NbFLS2 VIGS constructs; Brandon Maziuk for recombining the NbM1/2 entry clone into pQ11 and transforming the expression clone into Agrobacterium; and Diane Dunham and Paige Reeves for plant care. This work was supported by the National Science Foundation (grant no. IOS-1451754 to Dr. Gregory Martin).

3.7 Bibliography

Ade, J., DeYoung, B. J., Golstein, C., & Innes, R. W. (2007). Indirect activation of a plant nucleotide binding site-leucine-rich repeat protein by a bacterial protease. *Proc Natl Acad Sci*, *104*(7), 2531–2536.

Albert, M., Jehle, A. K., Mueller, K., Eisele, C., Lipschis, M., & Felix, G. (2010). *Arabidopsis thaliana* pattern recognition receptors for bacterial elongation factor Tu and flagellin can be combined to form functional chimeric receptors. *J Biol Chem*, *285*(25), 19035–19042.

Aziz, A., Heyraud, A., & Lambert, B. (2004). Oligogalacturonide signal transduction, induction of defense-related responses and protection of grapevine against *Botrytis cinerea*. *Planta*, *218*(5), 767–774.

Boisson-Dernier, A., Franck, C. M., Lituiev, D. S., & Grossniklaus, U. (2015). Receptor-like cytoplasmic kinase MARIS functions downstream of CrRLK1L-dependent signaling during tip growth. *Proc Natl Acad Sci*, *112*(39), 12211–12216.

Boisson-Dernier, A., Kessler, S. A., & Grossniklaus, U. (2011). The walls have ears: the role of plant CrRLK1Ls in sensing and transducing extracellular signals. *J Exp Bot*, *62*(5), 1581–1591.

Boller, T., & Felix, G. (2009). A renaissance of elicitors: perception of microbe-associated molecular patterns and danger signals by pattern-recognition receptors. *Annu Rev Plant Biol*, *60*(1), 379–406.

Bombarely, A., Rosli, H. G., Vrebalov, J., Moffett, P., Mueller, L. A., & Martin, G. B. (2012). A draft genome sequence of *Nicotiana benthamiana* to enhance molecular plant-microbe biology research. *Mol Plant Microbe Interact*, *25*(12), 1523–1530.

Brutus, A., Sicilia, F., Macone, A., Cervone, F., & De Lorenzo, G. (2010). A domain swap approach reveals a role of the plant wall-associated kinase 1 (WAK1) as a receptor of oligogalacturonides. *Proc Natl Acad Sci*, *107*(20), 9452–9457.

Cai, R., Lewis, J., Yan, S., Liu, H., Clarke, C. R., Campanile, F., Almeida, N. F., Studholme, D. J., Lindeberg, M., Schneider, D., Zaccardelli, M., Setubal, J. C., Morales-Lizcano, N. P., Bernal, A., Coaker, G., Baker, C., Bender, C. L., Leman, S., & Vinatzer, B. A. (2011). The plant pathogen *Pseudomonas syringae* pv. *tomato* is genetically monomorphic and under strong selection to evade tomato immunity. *PLoS Pathog*, *7*(8), e1002130.

Chakravarthy, S., Velásquez, A. C., Ekengren, S. K., Collmer, A., & Martin, G. B. (2010). Identification of *Nicotiana benthamiana* genes involved in pathogen-associated molecular pattern-triggered immunity. *Mol Plant Microbe Interact*, *23*(6), 715–726.

Chassot, C., Buchala, A., Schoonbeek, H.-J., Métraux, J.-P., & Lamotte, O. (2008). Wounding of Arabidopsis leaves causes a powerful but transient protection against *Botrytis* infection. *Plant J*, *55*(4), 555–567.

Chinchilla, D., Zipfel, C., Robatzek, S., Kemmerling, B., Nürnberger, T., Jones, J. D. G., Felix, G., & Boller, T. (2007). A flagellin-induced complex of the receptor FLS2 and BAK1 initiates plant defence. *Nature*, *448*(7152), 497–500.

Consonni, C., Humphry, M. E., Hartmann, H. A., Livaja, M., Durner, J., Westphal, L., Vogel, J., Lipka, V., Kemmerling, B., Schulze-Lefert, P., Somerville, S. C., & Panstruga, R. (2006). Conserved requirement for a plant host cell protein in powdery mildew pathogenesis. *Nat Genet*, *38*(6), 716–720.

De Lorenzo, G., Brutus, A., Savatin, D. V., Sicilia, F., & Cervone, F. (2011). Engineering plant resistance by constructing chimeric receptors that recognize damage-associated molecular patterns (DAMPs). *FEBS Lett*, *585*(11), 1521–1528.

Decreux, A., & Messiaen, J. (2005). Wall-associated kinase WAK1 interacts with cell wall pectins in a calcium-induced conformation. *Plant Cell Physiol*, *46*(2), 268–278.

Denoux, C., Galletti, R., Mammarella, N., Gopalan, S., Werck, D., De Lorenzo, G., Ferrari, S., Ausubel, F. M., & Dewdney, J. (2008). Activation of defense response pathways by OGs and Flg22 elicitors in *Arabidopsis* seedlings. *Mol Plant*, *1*(3), 423–445.

Dodds, P. N., & Rathjen, J. P. (2010). Plant immunity: towards an integrated view of plant-pathogen interactions. *Nat Rev Genet*, *11*(8), 539–548.

Dong, J., Xiao, F., Fan, F., Gu, L., Cang, H., Martin, G. B., & Chai, J. (2009). Crystal structure of the complex between *Pseudomonas* effector AvrPtoB and the tomato Pto kinase reveals both a shared and a unique interface compared with AvrPto-Pto. *Plant Cell*, *21*(6), 1846–1859.

Escobar-Restrepo, J.-M., Huck, N., Kessler, S., Gagliardini, V., Gheyselinck, J., Yang, W.-C., & Grossniklaus, U. (2007). The FERONIA receptor-like kinase mediates male-female interactions during pollen tube reception. *Science*, *317*(5838), 656–660.

Fernandez-Pozo, N., Rosli, H. G., Martin, G. B., & Mueller, L. A. (2015). The SGN VIGS tool: user-friendly software to design virus-induced gene silencing (VIGS) constructs for functional genomics. *Mol Plant*, *8*(3), 486–488.

Ferrari, S., Galletti, R., Denoux, C., De Lorenzo, G., Ausubel, F. M., & Dewdney, J. (2007). Resistance to *Botrytis cinerea* induced in Arabidopsis by elicitors is independent of salicylic acid, ethylene, or jasmonate signaling but requires PHYTOALEXIN DEFICIENT3. *Plant Physiol*, *144*(1), 367–379.

Ferrari, S., Savatin, D. V., Sicilia, F., Gramegna, G., Cervone, F., & Lorenzo, G. D. (2013). Oligogalacturonides: plant damage-associated molecular patterns and regulators of growth and development. *Front Plant Sci*, *4*, 49.

Galletti, R., Denoux, C., Gambetta, S., Dewdney, J., Ausubel, F. M., De Lorenzo, G., & Ferrari, S. (2008). The AtrbohD-mediated oxidative burst elicited by oligogalacturonides in Arabidopsis is dispensable for the activation of defense responses effective against *Botrytis cinerea*. *Plant Physiol*, *148*(3), 1695–1706.

Gimenez-Ibanez, S., Hann, D. R., Ntoukakis, V., Petutschnig, E., Lipka, V., & Rathjen, J. P. (2009). AvrPtoB targets the LysM receptor kinase CERK1 to promote bacterial virulence on plants. *Curr Biol*, *19*(5), 423–429.

Glazebrook, J. (2005). Contrasting mechanisms of defense against biotrophic and necrotrophic pathogens. *Annu Rev Phytopathol*, *43*, 205–227.

Göhre, V., Spallek, T., Häweker, H., Mersmann, S., Mentzel, T., Boller, T., de Torres, M., Mansfield, J. W., & Robatzek, S. (2008). Plant pattern-recognition receptor FLS2 is directed for degradation by the bacterial ubiquitin ligase AvrPtoB. *Curr Biol*, *18*(23), 1824–1832.

Guo, H., Li, L., Ye, H., Yu, X., Algreen, A., & Yin, Y. (2009). Three related receptor-like kinases are required for optimal cell elongation in *Arabidopsis thaliana*. *Proc Natl Acad Sci*, *106*(18), 7648–7653.

Haruta, M., Sabat, G., Stecker, K., Minkoff, B. B., & Sussman, M. R. (2014). A peptide hormone and its receptor protein kinase regulate plant cell expansion. *Science*, *343*(6169), 408–411.

He, P., Shan, L., Lin, N.-C., Martin, G. B., Kemmerling, B., Nürnberger, T., & Sheen, J. (2006). Specific bacterial suppressors of MAMP signaling upstream of MAPKKK in *Arabidopsis* innate immunity. *Cell*, *125*(3), 563–575.

Hellens, R., Mullineaux, P., & Klee, H. (2000). A guide to *Agrobacterium* binary Ti vectors. *Trends Plant Sci*, *5*(10), 446–451.

Hückelhoven, R., & Panstruga, R. (2011). Cell biology of the plant-powdery mildew interaction. *Curr Opin Plant Biol*, *14*(6), 738–746.

Huffaker, A., Pearce, G., & Ryan, C. A. (2006). An endogenous peptide signal in *Arabidopsis* activates components of the innate immune response. *Proc Natl Acad Sci*, *103*(26), 10098–10103.

Jinek, M., Chylinski, K., Fonfara, I., Hauer, M., Doudna, J. A., & Charpentier, E. (2012). A programmable dual-RNA-guided DNA endonuclease in adaptive bacterial immunity. *Science*, *337*(6096), 816–821.

Jones, J. D. G., & Dangl, J. L. (2006). The plant immune system. *Nature*, *444*(7117), 323–329.

Kadota, Y., Sklenar, J., Derbyshire, P., Stransfeld, L., Asai, S., Ntoukakis, V., Jones, J. D., Shirasu, K., Menke, F., Jones, A., & Zipfel, C. (2014). Direct regulation of the NADPH oxidase RBOHD by the PRR-associated kinase BIK1 during plant immunity. *Mol Cell*, *54*(1), 1–13.

Keinath, N. F., Kierszniowska, S., Lorek, J., Bourdais, G., Kessler, S. A., Shimosato-Asano, H., Grossniklaus, U., Schulze, W. X., Robatzek, S., & Panstruga, R. (2010). PAMP (pathogen-associated molecular pattern)-induced changes in plasma membrane compartmentalization reveal novel components of plant immunity. *J Biol Chem*, *285*(50), 39140–39149.

Kessler, S. A., Shimosato-Asano, H., Keinath, N. F., Wuest, S. E., Ingram, G., Panstruga, R., & Grossniklaus, U. (2010). Conserved molecular components for pollen tube reception and fungal invasion. *Science*, *330*(6006), 968–971.

Kohorn, B. D., Johansen, S., Shishido, A., Todorova, T., Martinez, R., Defeo, E., & Obregon, P. (2009). Pectin activation of MAP kinase and gene expression is WAK2 dependent. *Plant J*, *60*(6), 974–982.

Kraus, C. M., Munkvold, K. R., & Martin, G. B. (2016). Natural variation in tomato reveals differences in the recognition of AvrPto and AvrPtoB effectors from *Pseudomonas syringae*. *Mol Plant*, *9*(5), 639–649.

Krol, E., Mentzel, T., Chinchilla, D., Boller, T., Felix, G., Kemmerling, B., Postel, S., Arents, M., Jeworutzki, E., Al-Rasheid, K. A. S., Becker, D., & Hedrich, R. (2010). Perception of the *Arabidopsis* danger signal peptide 1 involves the pattern recognition receptor *At*PEPR1 and its close homologue *At*PEPR2. *J Biol Chem*, *285*(18), 13471–13479.

Kumar, S., Stecher, G., & Tamura, K. (2016). MEGA7: Molecular Evolutionary Genetics Analysis version 7.0 for bigger datasets. *Mol Biol Evol*, *33*(7), 1870–1874.

Lin, N.-C., & Martin, G. B. (2005). An *avrPto/avrPtoB* mutant of *Pseudomonas syringae* pv. *tomato* DC3000 does not elicit Pto-mediated resistance and is less virulent on tomato. *Mol Plant Microbe Interact*, *18*(1), 43–51.

Lindner, H., Müller, L. M., Boisson-Dernier, A., & Grossniklaus, U. (2012). CrRLK1L receptor-like kinases: not just another brick in the wall. *Curr Opin Plant Biol*, *15*(6), 659–669.

Liu, Z., Wu, Y., Yang, F., Zhang, Y., Chen, S., Xie, Q., Tian, X., & Zhou, J.-M. (2013). BIK1 interacts with PEPRs to mediate ethylene-induced immunity. *Proc Natl Acad Sci*, *110*(15), 6205–6210.

Lu, D., Wu, S., Gao, X., Zhang, Y., Shan, L., & He, P. (2010). A receptor-like cytoplasmic kinase, BIK1, associates with a flagellin receptor complex to initiate plant innate immunity. *Proc Natl Acad Sci*, *107*(1), 496–501.

Ma, Y., Walker, R. K., Zhao, Y., & Berkowitz, G. A. (2012). Linking ligand perception by PEPR pattern recognition receptors to cytosolic Ca^{2+} elevation and downstream immune signaling in plants. *Proc Natl Acad Sci*, *109*(48), 19852–19857.

Martin, G. B. (2012). Suppression and activation of the plant immune system by *Pseudomonas syringae* effectors AvrPto and AvrPtoB. In F. Martin, & S. Kamoun (Eds.) *Effectors in plant-microbe interactions*, (pp. 123–154). Wiley-Blackwell, Hoboken, NJ.

Mathieu, J., Schwizer, S., & Martin, G. B. (2014). Pto kinase binds two domains of AvrPtoB and its proximity to the effector E3 ligase determines if it evades degradation and activates plant immunity. *PLoS Pathog*, *10*(7), e1004227.

Mathieu, J., Warthmann, N., Küttner, F., & Schmid, M. (2007). Export of FT protein from phloem companion cells is sufficient for floral induction in *Arabidopsis*. *Curr Biol*, *17*(12), 1055–1060.

Melotto, M., Underwood, W., & He, S. Y. (2008). Role of stomata in plant innate immunity and foliar bacterial diseases. *Annu Rev Phytopathol*, *46*, 101–122.

Monaghan, J., & Zipfel, C. (2012). Plant pattern recognition receptor complexes at the plasma membrane. *Curr Opin Plant Biol*, *15*(4), 349–357.

Nguyen, H. P., Chakravarthy, S., Velásquez, A. C., McLane, H. L., Zeng, L., Nakayashiki, H., Park, D. H., Collmer, A., & Martin, G. B. (2010). Methods to study PAMP-triggered immunity using tomato and *Nicotiana benthamiana*. *Mol Plant Microbe Interact*, *23*(8), 991–999.

Nicaise, V., Roux, M., & Zipfel, C. (2009). Recent advances in PAMP-triggered immunity against bacteria: pattern recognition receptors watch over and raise the alarm. *Plant Physiol*, *150*(4), 1638–1647.

Nürnberger, T., Brunner, F., Kemmerling, B., & Piater, L. (2004). Innate immunity in plants and animals: striking similarities and obvious differences. *Immunol. Rev.*, *198*, 249–266.

Rosebrock, T. R., Zeng, L., Brady, J. J., Abramovitch, R. B., Xiao, F., & Martin, G. B. (2007). A bacterial E3 ubiquitin ligase targets a host protein kinase to disrupt plant immunity. *Nature*, *448*(7151), 370–374.

Rosli, H. G., Zheng, Y., Pombo, M. A., Zhong, S., Bombarely, A., Fei, Z., Collmer, A., & Martin, G. B. (2013). Transcriptomics-based screen for genes induced by flagellin and repressed by pathogen effectors identifies a cell wall-associated kinase involved in plant immunity. *Genome Biol*, *14*(12), R139.

Roux, M., Schwessinger, B., Albrecht, C., Chinchilla, D., Jones, A., Holton, N., Malinovsky, F. G., Tör, M., de Vries, S., & Zipfel, C. (2011). The *Arabidopsis* leucine-rich repeat receptor-like kinases BAK1/SERK3 and BKK1/SERK4 are

required for innate immunity to hemibiotrophic and biotrophic pathogens. *Plant Cell*, *23*(6), 2440–2455.

Salmeron, J. M., Oldroyd, G. E., Rommens, C. M., Scofield, S. R., Kim, H. S., Lavelle, D. T., Dahlbeck, D., & Staskawicz, B. J. (1996). Tomato *Prf* is a member of the leucine-rich repeat class of plant disease resistance genes and lies embedded within the *Pto* kinase gene cluster. *Cell*, *86*(1), 123–133.

Scofield, S., Tobias, C., Rathjen, J., Chang, J., Lavelle, D., Michelmore, R., & Staskawicz, B. (1996). Molecular basis of gene-for-gene specificity in bacterial speck disease of tomato. *Science*, *274*(5295), 2063–2065.

Sessa, G., D'ascenzo, M., & Martin, G. B. (2000). The major site of the Pti1 kinase phosphorylated by the Pto kinase is located in the activation domain and is required for Pto-Pti1 physical interaction. *Eur J Biochem*, *267*(1), 171–178.

Shan, L., He, P., Li, J., Heese, A., Peck, S. C., Nürnberger, T., Martin, G. B., & Sheen, J. (2008). Bacterial effectors target the common signaling partner BAK1 to disrupt multiple MAMP receptor-signaling complexes and impede plant immunity. *Cell Host Microbe*, *4*(1), 17–27.

Shao, F., Golstein, C., Ade, J., Stoutemyer, M., Dixon, J. E., & Innes, R. W. (2003). Cleavage of *Arabidopsis* PBS1 by a bacterial type III effector. *Science*, *301*(5637), 1230–1233.

Tang, X., Frederick, R., Zhou, J., Halterman, D., Jia, Y., & Martin, G. B. (1996). Initiation of plant disease resistance by physical interaction of AvrPto and Pto kinase. *Science*, *274*(5295), 2060–2063.

Tena, G., Boudsocq, M., & Sheen, J. (2011). Protein kinase signaling networks in plant innate immunity. *Curr Opin Plant Biol*, *14*(5), 519–529.

Tintor, N., Ross, A., Kanehara, K., Yamada, K., Fan, L., Kemmerling, B., Nürnberger, T., Tsuda, K., & Saijo, Y. (2013). Layered pattern receptor signaling via ethylene and endogenous elicitor peptides during *Arabidopsis* immunity to bacterial infection. *Proc Natl Acad Sci*, *110*(15), 6211–6216.

Tsuda, K., Sato, M., Stoddard, T., Glazebrook, J., & Katagiri, F. (2009). Network properties of robust immunity in plants. *PLoS Genet*, *5*(12), e1000772.

van der Hoorn, R. A. L., & Kamoun, S. (2008). From guard to decoy: a new model for perception of plant pathogen effectors. *Plant Cell*, *20*(8), 2009–2017.

Warren, R. F., Merritt, P. M., Holub, E., & Innes, R. W. (1999). Identification of three putative signal transduction genes involved in *R* gene-specified disease resistance in Arabidopsis. *Genetics*, *152*(1), 401–412.

Wei, C.-F., Kvitko, B. H., Shimizu, R., Crabill, E., Alfano, J. R., Lin, N.-C., Martin, G. B., Huang, H.-C., & Collmer, A. (2007). A *Pseudomonas syringae* pv. *tomato* DC3000 mutant lacking the type III effector HopQ1-1 is able to cause disease in the model plant *Nicotiana benthamiana*. *Plant J*, *51*(1), 32–46.

Wei, H.-L., Chakravarthy, S., Mathieu, J., Helmann, T. C., Stodghill, P., Swingle, B., Martin, G. B., & Collmer, A. (2015). *Pseudomonas syringae* pv. *tomato* DC3000 type III secretion effector polymutants reveal an interplay between HopAD1 and AvrPtoB. *Cell Host Microbe*, *17*(6), 752–762.

Xiang, T., Zong, N., Zhang, J., Chen, J., Chen, M., & Zhou, J.-M. (2011). BAK1 is not a target of the *Pseudomonas syringae* effector AvrPto. *Mol Plant Microbe Interact*, *24*(1), 100–107.

Xiang, T., Zong, N., Zou, Y., Wu, Y., Zhang, J., Xing, W., Li, Y., Tang, X., Zhu, L., Chai, J., & Zhou, J.-M. (2008). *Pseudomonas syringae* effector AvrPto blocks innate immunity by targeting receptor kinases. *Curr Biol*, *18*(1), 74–80.

Xiao, F., He, P., Abramovitch, R. B., Dawson, J. E., Nicholson, L. K., Sheen, J., & Martin, G. B. (2007). The N-terminal region of *Pseudomonas* type III effector AvrPtoB elicits Pto-dependent immunity and has two distinct virulence determinants. *Plant J*, *52*(4), 595–614.

Yamaguchi, Y., Huffaker, A., Bryan, A. C., Tax, F. E., & Ryan, C. A. (2010). PEPR2 Is a second receptor for the Pep1 and Pep2 peptides and contributes to defense responses in *Arabidopsis*. *Plant Cell*, *22*(2), 508–522.

Yamaguchi, Y., Pearce, G., & Ryan, C. A. (2006). The cell surface leucine-rich repeat receptor for *At*Pep1, an endogenous peptide elicitor in *Arabidopsis*, is functional in transgenic tobacco cells. *Proc Natl Acad Sci*, *103*(26), 10104–10109.

Yoo, S.-D., Cho, Y.-H., & Sheen, J. (2007). *Arabidopsis* mesophyll protoplasts: a versatile cell system for transient gene expression analysis. *Nat Protoc*, *2*(7), 1565–1572.

Zeng, L., Velásquez, A. C., Munkvold, K. R., Zhang, J., & Martin, G. B. (2011). A tomato LysM receptor-like kinase promotes immunity and its kinase activity is inhibited by AvrPtoB. *Plant J*, *69*(1), 92–103.

Zhang, J., Li, W., Xiang, T., Liu, Z., Laluk, K., Ding, X., Zou, Y., Gao, M., Zhang, X., Chen, S., Mengiste, T., Zhang, Y., & Zhou, J.-M. (2010). Receptor-like cytoplasmic kinases integrate signaling from multiple plant immune receptors and are targeted by a *Pseudomonas syringae* effector. *Cell Host Microbe*, *7*(4), 290–301.

Zhou, J., Loh, Y. T., Bressan, R. A., & Martin, G. B. (1995). The tomato gene *Pti1* encodes a serine/threonine kinase that is phosphorylated by Pto and is involved in the hypersensitive response. *Cell*, *83*(6), 925–935.

Zhou, J., Wu, S., Chen, X., Liu, C., Sheen, J., Shan, L., & He, P. (2014). The *Pseudomonas syringae* effector HopF2 suppresses *Arabidopsis* immunity by targeting BAK1. *Plant J*, *77*(2), 235–245.

Zipfel, C. (2008). Pattern-recognition receptors in plant innate immunity. *Curr Opin Immunol*, *20*(1), 10–16.

Zipfel, C. (2013). Combined roles of ethylene and endogenous peptides in regulating plant immunity and growth. *Proc Natl Acad Sci*, *110*(15), 5748–5749.

Zipfel, C. (2014). Plant pattern-recognition receptors. *Trends Immunol*, *35*(7), 345–351.

Zipfel, C., Kunze, G., Chinchilla, D., Caniard, A., Jones, J. D. G., Boller, T., & Felix, G. (2006). Perception of the bacterial PAMP EF-Tu by the receptor EFR restricts *Agrobacterium*-mediated transformation. *Cell*, *125*(4), 749–760.

CHAPTER 4

DETECTING N-MYRISTOYLATION AND S-ACYLATION OF HOST AND PATHOGEN PROTEINS IN PLANTS USING CLICK CHEMISTRY

4.1 Summary

The plant plasma membrane is a key battleground in the war between plants and their pathogens. Plants detect the presence of pathogens at the plasma membrane using sensor proteins, many of which are targeted to this lipophilic locale by way of fatty acid modifications. Pathogens secrete effector proteins into the plant cell to suppress the plant's defense mechanisms. These effectors are able to access and interfere with the surveillance machinery at the plant plasma membrane by hijacking the host's fatty acylation apparatus. Despite the important involvement of protein fatty acylation in both plant immunity and pathogen virulence mechanisms, relatively little is known about the role of this modification during plant-pathogen interactions. This dearth in our understanding is due largely to the lack of methods to monitor protein fatty acid modifications in the plant cell. We describe a rapid method to detect two major forms of fatty acylation, N-myristoylation and S-acylation, of candidate proteins using alkyne fatty acid analogs coupled with click chemistry. We applied our approach to confirm and decisively demonstrate that the archetypal pattern recognition receptor FLS2, the well-characterized pathogen effector AvrPto, and one of the best-studied intracellular resistance proteins, Pto, all undergo plant-mediated fatty acylation. In addition to providing a means to readily determine fatty acylation, particularly myristoylation, of candidate pro-

This chapter was published in modified form in *Plant Methods* (2016, 12:38) and was written by Patrick Boyle*, Simon Schwizer*, Sarah Hind, Christine Kraus, Susana De la Torre Diaz, Bin He, and Gregory Martin. *These authors contributed equally to this work.

teins, this method is amenable to a variety of expression systems. We demonstrate this using both Arabidopsis protoplasts and stable transgenic Arabidopsis plants and we leverage Agrobacterium-mediated transient expression in *Nicotiana benthamiana* leaves as a means for high-throughput evaluation of candidate proteins. The metabolic labeling approach leveraging alkyne fatty acid analogs and click chemistry described here has the potential to provide mechanistic details of the molecular tactics used at the host plasma membrane in the battle between plants and pathogens.

4.2 Introduction

The covalent attachment of fatty acids to specific protein residues, a process referred to as fatty acylation, increases the hydrophobicity of the substrate protein and affects various properties, most notably subcellular localization (Resh, 1999; Hemsley, 2015). These lipid moieties often serve as hydrophobic anchors that promote protein-membrane associations (Resh, 1999). There are a number of different types of protein fatty acylations, the two best characterized forms in plants being N-myristoylation and S-acylation (Hemsley, 2015).

N-myristoylation describes the irreversible amide bond formation between myristate, a saturated 14-carbon fatty acid, and the N-terminal amine of a glycine residue exposed as a result of co-translational N-terminal methionine excision, or more rarely, post-translational proteolytic processing (Resh, 1999; Wright et al., 2010; Martin et al., 2011). This modification is mediated by N-myristoyltransferases, cytosolic entities often associated with ribosomes since protein myristoylation is typically a co-translational modification (Qi et al., 2000; Boisson et al., 2003; Pierre et al., 2007; Renna et al., 2013). In many cases, myristoylation is necessary for targeting a protein to the plasma membrane (PM), but this modification alone

is not sufficient to provide permanent anchoring to the membrane and as a result myristoylation is often found in combination with other membrane interaction motifs, including polybasic domains and those involving S-acylation (Resh, 1999; Wright et al., 2010; Martin et al., 2011).

S-acylation refers to the reversible thioester bond formation between a fatty acid and a cysteine residue side chain (Hurst & Hemsley, 2015). The saturated 16-carbon palmitate is the fatty acid most frequently featured in S-acylation and therefore this modification is often termed palmitoylation (Resh, 1999; Aicart-Ramos et al., 2011). However, other fatty acids can be covalently attached to cysteine side chains, most notably the saturated 18-carbon stearate, and a small number of studies suggest that in plants, protein stearylation is as prevalent as palmitoylation (Sorek et al., 2007; Batistic et al., 2008, 2012; Hemsley, 2015). The enzymes responsible for S-acylation are known as S-acyltransferases, or more commonly, palmitoyl acyltransferases (Batistic, 2012). These enzymes are integral membrane proteins found at the PM and at the membranes of various cellular compartments, including endosomes, the Golgi apparatus, and the endoplasmic reticulum (Batistic, 2012). Unlike myristoylation, protein S-acylation with palmitate or stearate is sufficient for stable interaction with the membrane (Shahinian & Silvius, 1995; Hemsley, 2015). This modification is suggested to serve roles in retaining proteins at various membranes and trafficking previously myristoylated proteins to the PM, in addition to dynamically regulating protein activity, stability, and complex assembly (Resh, 1999; Batistic, 2012; Hurst & Hemsley, 2015). Proteins bearing both myristoylation and proximal S-acylation are said to be N-terminally dual fatty acylated and this combination of lipid modifications appears to drive stable association with the PM (Resh, 1999).

Fatty acylation is a form of protein modification that is conserved among eu-

karyotes and most of the information available about this modification is based on studies from yeast and animal systems. However, what little is known about myristoylation and S-acylation in plants suggests that this kingdom is sufficiently unique in its use of these modifications to merit independent investigation (Maurer-Stroh et al., 2002; Boisson et al., 2003; Podell & Gribskov, 2004; Martinez et al., 2008; Traverso et al., 2008; Hemsley et al., 2013). Prediction based studies indicate that the plant proteome is proportionally more myristoylated than those of metazoans and fungi (Maurer-Stroh et al., 2002; Boisson et al., 2003; Podell & Gribskov, 2004; Traverso et al., 2008). Interestingly, many of the protein families predicted to be myristoylated exclusively in plants are implicated in stress and defense responses (Boisson et al., 2003; Traverso et al., 2008).

In contrast to the absolute requirement of an N-terminal glycine for myristoylation, S-acylation does not have a clear consensus sequence beyond a requisite cysteine residue, which can occur at essentially any position in a protein (Hemsley et al., 2013). The lack of an S-acylation consensus sequence has largely prevented the use of predictive bioinformatics approaches to study this modification (Smotrys & Linder, 2004; Sorek et al., 2009; Aicart-Ramos et al., 2011). However, the labile nature of thioester bonds has permitted the use of an acyl-biotin exchange (ABE) approach to identify S-acylated proteins present in the plant proteome. A recent study based on the ABE method indicated that more than 500 proteins are subject to S-acylation in Arabidopsis root suspension cells, which far exceeds the number of Arabidopsis proteins predicted to be myristoylated (Hemsley et al., 2013). Similar to what has been reported with plant proteins subject to myristoylation, many of the proteins identified as being S-acylated appear to be involved in pathogen perception (Hemsley et al., 2013). The prevalence for fatty acylation of proteins functioning in defense is not unexpected because these modifications are known

to target proteins to the PM and this lipophilic locale constitutes the initial point of pathogen perception in plants (Hemsley, 2015). The organization of the plant palmitoyl acyltransferases, which are present at the PM in greater proportions than in mammalian and yeast systems, suggests that the plant S-acylation apparatus is uniquely arranged for the stable recruitment of proteins to this particular membrane locale (Batistic, 2012).

The use of host-mediated myristoylation by plant pathogen effectors supports suggestions that the plant PM is a critical interface during plant-pathogen interactions and that the fatty acylation mechanisms are distinctively organized and/or accessible in the plant cell environment (Boyle & Martin, 2015). The exploitation of host-mediated protein lipidation mechanisms for the spatial regulation of pathogen effectors seems to be a general virulence strategy, yet only the effectors of plant pathogenic bacteria appear to hijack the host myristoylation machinery (Nimchuk et al., 2000; Dean, 2011; Hicks et al., 2011; Méresse, 2011; Feng & Zhou, 2012; Geissler, 2012; Hicks & Galán, 2013; Ivanov & Roy, 2013). To date, the reason for this observation remains unclear, but the modification is essential for the virulence activity of several bacterial effectors and is required for the recognition of many effectors in host plants armed with the appropriate intracellular sensor proteins, more commonly referred to as resistance proteins (Nimchuk et al., 2000; Shan et al., 2000; Robert-Seilaniantz et al., 2006; Dowen et al., 2009).

Despite the distinct features of protein fatty acylation in plants and its importance in plant-pathogen interactions, methods to readily and decisively detect specific fatty acid modifications of host and pathogen proteins in the plant cell are currently lacking. The ability to monitor plant-mediated myristoylation has proven particularly problematic because of the irreversible nature of this modification. Traditional approaches to directly demonstrate protein fatty acylation *in*

vivo have relied on metabolic labeling with radiolabeled fatty acids, such as [^{3}H]- or [^{125}I]-myristic and palmitic acids, followed by purification of the protein of interest and visualization using autoradiography (Hannoush & Sun, 2010). This method, although effective, typically requires lengthy film exposure times to visualize fatty acylated proteins and requires the use of radioactive materials (Dowen et al., 2009; Hannoush & Sun, 2010; Wright et al., 2010; Martin et al., 2011). Furthermore, radiolabeling techniques do not present any straightforward means to capture labeled proteins, preventing proteome-wide identification of fatty acylated targets (Hannoush & Sun, 2010). Lipid modification analysis by gas chromatography coupled with mass spectrometry (GC-MS) is another approach that has advanced our understanding of candidate protein S-acylation, particularly in plants (Sorek & Yalovsky, 2010). The advantages of this approach are its ability to unambiguously identify S-acylation modifications, such as palmitoylation and stearylation, and to do so without the requirement of feeding radiolabeled materials to the cells or tissues being interrogated (Farnsworth et al., 1990). However this technique cannot be applied to the analysis of protein myristoylation and, like radiolabeling approaches, is not amenable to whole proteome analysis. The ABE approach was developed as a relatively rapid nonradioactive alternative to study protein fatty acylation and enables proteome-wide identification of S-acylated proteins (Drisdel & Green, 2004; Roth et al., 2006). ABE leverages the labile nature of thioester linkages to replace S-acylation modifications present on cysteine residues with a chosen label, most often biotin. The labeled proteins are then enriched on affinity resin and subsequently identified using mass spectrometry. Alternatively, the labeled proteins can be visualized by in-gel fluorescence or western blotting. However, the ABE method has some limitations, most notably that this approach, like the GC-MS strategy, can only be applied to study S-acylation and not myristoy-

lation Hannoush:2010jo. Also, due to its indirect nature the technique does not allow for the discernment of different thioester linkages, many of which are not involved in S-acylation, and therefore results in false positives (Roth et al., 2006; Hannoush & Sun, 2010; Hemsley et al., 2013; Martin, 2013; Zhou et al., 2014a).

Metabolic labeling approaches using fatty acid analogs containing bio-orthogonal chemical handles, which allow for the attachment of reporter or detection tags, have recently emerged as means to circumvent many of the difficulties that have impeded the study of fatty acid modifications (Charron et al., 2009; Martin & Cravatt, 2009; Hannoush & Sun, 2010; Yap et al., 2010; Hannoush, 2012). The strategy involves feeding cells a fatty acid analog bearing a bio-orthogonal azide or alkyne handle, resulting in metabolic incorporation of the analog into target proteins. Click chemistry is then used to react the bio-orthogonal functionality present in the fatty acid analog with a reporter tag. These fatty acids are termed bio-orthogonal analogs because the sleek nature of the azide or alkyne handles present in terminal positions of these modified lipids interfere neither with the hydrophobic character of these molecules nor the acid moiety, preserving the ability to insert into membranes and interact with the native fatty acylation apparatus which allows their metabolic incorporation into target proteins (Hannoush, 2012). These chemical tools enable the rapid detection of protein myristoylation and S-acylation without the need for radioactivity (Hannoush & Sun, 2010). Click chemistry, based primarily on the Huisgen [3+2] Cu(I)-catalyzed azide-alkyne cycloaddition, has an ever growing number of applications and has been employed in plant systems to determine the targets of reactive small molecules, visualize cell lignification, track Golgi protein dynamics, and detect protein prenylation, but it has not yet been leveraged to study fatty acid modifications of plant proteins (Kaschani et al., 2009; Tobimatsu et al., 2014; Bourge et al., 2015; Dutilleul et al., 2016).

Protein fatty acylation in plants has many interesting features compared to other eukaryotes. However, many questions still remain about the role of these protein modifications in this kingdom due to the lack of techniques currently available to study fatty acylation, particularly post-translational myristoylation, in plants. Here we describe the development of a click chemistry-based method using ω-alkynyl fatty acid analogs to facilitate the study of fatty acylation of both host and pathogen effector proteins in the plant cell environment.

4.3 Materials and methods

Plant material

Seeds of *Arabidopsis thaliana* accession Columbia (Col-0) or the derived transgenic line conditionally expressing *avrPto* (Hauck et al., 2003) were suspended in 0.1% agarose and cold-stratified for 3 days at 4°C. The plants were grown in a controlled environment chamber with 8 h light and 16 h dark periods at 22°C and 20°C, respectively, with 60% relative humidity for 6 weeks. *Nicotiana benthamiana* accession Nb-1 (Bombarely et al., 2012) was grown in a controlled environment chamber with a light/dark cycle of 16 h and 8 h, respectively, with 65% relative humidity and temperatures of 24°C during light and 22°C during dark periods for 4-5 weeks.

Cloning

To generate the Gateway entry clones, complete open reading frames (ORFs) without the stop codons were amplified with Phusion DNA polymerase (Thermo Scientific) from existing plasmids. The ORFs were blunt-end ligated into the SmaI (New England Biolabs) site of pJLSmart (Mathieu et al., 2007) or pJM51 (**?**)

with T4 DNA ligase (New England Biolabs). Point mutations were introduced using complementary custom DNA oligonucleotides (Integrated DNA Technologies) following standard protocols (e.g. Stratagene QuikChange site-directed mutagenesis kit). Entry clones were recombined into destination vectors using the LR Clonase II enzyme mix (Invitrogen) following the manufacturer's protocol. Destination vectors used were HBT95 (He et al., 2006) for protoplast expression and the pGWB series (Nakagawa et al., 2007) for Agrobacterium-mediated transformation. All constructs were control digested with BsrGI (cNew England Biolabs) and sequence-verified prior to use. Sequencing services were provided by the Biotechnology Resource Center at Cornell University. The pBTEX constructs have been described previously (Frederick et al., 1998; Abramovitch et al., 2003).

Protoplast isolation and transformation

Arabidopsis protoplasts were prepared and transformed as previously described (Yoo et al., 2007; Wu et al., 2009). Briefly, the epidermis on the abaxial side of fully expanded leaves was peeled off and the leaves floated in protoplast isolation medium. The protoplasts were collected, washed, and the cell density adjusted. Plasmid DNA was added and the protoplasts were transformed by PEG-calcium transfection. Protoplasts were washed again and resuspended in the presence of the palmitic acid analog Alk14 (Cayman Chemical) at a final concentration of 10 µM. Cells were incubated for 6 h, collected, and stored at -80°C until further processing. For the comparison between azide and alkyne fatty acid analogs, transformed protoplasts were resuspended in the presence of the myristic acid analog Az12 (Invitrogen) or Alk12 (Cayman Chemical) at the indicated final concentrations. All fatty acid analogs were prepared following their manufacturers' protocols. Cells were incubated overnight, collected, and protein levels analyzed by western blotting.

Conditional expression of *avrPto* in transgenic Arabidopsis

Transgenic Arabidopsis conditionally expressing *avrPto* under the control of a dexamethasone-inducible promoter (Hauck et al., 2003) were sprayed with 20 µM dexamethasone (Sigma-Aldrich) in 0.1% ethanol with 0.01% Silwet L-77 (Lehle Seeds) to induce gene expression. Leaves were infiltrated twice with 10 µM myristic acid analog Alk12, 6 h after induction and 6 h before sampling. Tissue was collected 30 h after induction and stored at -80°C until further processing.

Agrobacterium-mediated transient expression

Agrobacterium tumefaciens strain GV3101 with helper plasmid pMP90 (Hellens et al., 2000) was transformed with the pGWB constructs; the pBTEX constructs had previously been moved into *A. tumefaciens* strain GV2260 (Abramovitch et al., 2003). Confirmed strains were grown on lysogeny broth (LB) plates with appropriate antibiotics at 30°C for 36-48 h. Bacteria were then scraped from plates and resuspended in infiltration buffer containing 10 mM $MgCl_2$, 10 mM MES pH 5.7, and 200 µM acetosyringone (Sigma-Aldrich). The OD_{600} was adjusted to a final density of 0.3 for each strain and the bacteria incubated for at least 1 h at room temperature. Leaves of *N. benthamiana* were infiltrated with needleless syringes and the plants placed on a shaded growth chamber shelf. Leaves were infiltrated twice with 10 µM Alk12, 24 h after Agrobacterium infiltration and 6 h before sampling. Tissue samples were collected 48 h after transformation. For the cell death assay, leave tissue was infiltrated once with 50 µM Alk12, Alk14, Alk16 (Cayman Chemical), or buffer 24 h after Agrobacterium infiltration.

Click reaction

Leaf tissue was ground with a TissueLyser II (Qiagen) and proteins extracted in 'RIPA' buffer containing 1x PBS pH 7.4, 1% v/v Triton X-100 (Sigma-Aldrich), 0.5% w/v sodium deoxycholate, and 0.1% w/v SDS, with EDTA-free protease inhibitor (Roche Diagnostics). Protoplasts were lysed by brief vortexing in RIPA buffer with EDTA-free protease inhibitor. Affinity resin was added to the cleared supernatant and immunoprecipitation performed. FLS2-HA was purified with anti-HA (Sigma-Aldrich); YFP fusions were purified with anti-GFP (ChromoTek); and untagged AvrPto was purified with custom anti-AvrPto antibody (Shan et al., 2000) coupled to protein A resin (Sigma-Aldrich). Agarose beads were resuspended in RIPA buffer and the following components added for the click reaction: 500 µM BTTP ligand, 250 µM $CuSO_4$, 2 mM sodium ascorbate, and 100 µM azide tag. The reaction was incubated for 1 h at room temperature or overnight at 4°C and the beads were washed and resuspended in Laemmli sample buffer for protein detection. For the myristoylome pilot experiment, total protein was extracted in 1x PBS pH 7.4 with 4% w/v SDS and EDTA-free protease inhibitor. Standard methanol/chloroform precipitation was used to purify and concentrate the proteins (Wessel & Flügge, 1984). Click chemistry with the crude protein extract was performed in 1x PBS pH 7.4 with 4% w/v SDS in the presence of 1 mM $CuSO_4$ to attach a biotin tag to AvrPto. We found that higher concentrations of the copper catalyst are required for efficient click reactions in crude protein extracts. A second methanol/chloroform precipitation was used to clean the sample, proteins were resuspended in 1x PBS pH 7.4 with 4% w/v SDS and EDTA-free protease inhibitor, diluted with 1x PBS pH 7.4 to reduce SDS concentration to around 0.7%, and the myristoylated proteins enriched using streptavidin resin (Thermo Scientific). The BTTP ligand 3-[4-(bis[(1-tert-butyl-1H-1,2,3-triazol-4-

yl)methyl]aminomethyl)-1H-1,2,3-triazol-1-yl]propanol was a gift from Dr. Frank Schroeder (Boyce Thompson Institute and Department of Chemistry and Chemical Biology, Cornell University). BTTP is not commercially available at the time of writing, but it can be obtained from the Chemical Biology Core Facility of the Albert Einstein College of Medicine (http://www.einstein.yu.edu/research/shared-facilities/chemical-biology/Ligands-for-CuAAC). The N_3-biotin reagent biotin-PEG3-azide, used as both a reporter and affinity purification handle, was purchased from Click Chemistry Tools. The infrared fluorescent reporter IRDye 800CW azide was obtained from LI-COR Biosciences.

Protein detection

All samples were boiled in Laemmli sample buffer, with Orange G (Sigma-Aldrich) substituted for bromophenol blue for the fluorescence imaging experiments to minimize signal interference. Gel electrophoresis and western blotting was performed following standard protocols (e.g. Bio-Rad bulletin 6040 and 2895, respectively). Detection of attached infrared fluorescent dye was performed using an Odyssey infrared imager (LI-COR Biosciences) after fixing the gel by incubation in 40% methanol and 10% acetic acid protected from light with gentle shaking overnight at room temperature. Attached biotin was detected using streptavidin-HRP (Invitrogen); untagged AvrPto was detected using custom anti-AvrPto antibody followed by anti-rabbit-HRP (Promega); FLS2-HA and AvrPto-HA were detected using anti-HA-HRP (Roche Diagnostics); YFP fusion proteins were detected using anti-GFP (Roche Diagnostics) followed by anti-mouse-HRP (Santa Cruz Biotechnology); and YFP-FLAG was detected with anti-FLAG-HRP (Sigma-Aldrich).

4.4 Results

General scheme for assessing fatty acylation of candidate proteins using clickable fatty acid analogs

We developed and optimized an approach to determine the fatty acylation status, especially myristoylation, of candidate proteins in plant cells using ω-alkynyl fatty acid analogs and click chemistry based largely on methods previously described (Yount et al., 2011; Hannoush, 2012) (Figure 4.1). Plant cells are transformed with a candidate gene construct, preferably encoding a commercial epitope tag, following standard protocols. The alkyne fatty acid analog for the metabolite of interest is applied to the plant cells and subsequently incorporated during protein synthesis. Total protein is extracted and the candidate protein purified using immunoprecipitation. A reporter, such as a biotin tag or a fluorescent dye, is added to the alkyne group of the fatty acid analog using click chemistry and detected by western blotting or fluorescence imaging (Figure 4.1). The experimental steps outlined here can be completed within a few days and we describe below the successful application of this approach to detect fatty acid modifications in a variety of candidate proteins using different expression methods and plant systems.

Alkyne fatty acid analogs are better tolerated by plant cells than preparations of azide fatty acid analogs

To assess the potential phytotoxicity of different forms of fatty acid analogs, we transformed Arabidopsis protoplasts with an expression vector encoding yellow fluorescent protein (YFP) and treated the protoplasts with either Az12 or Alk12, which are the azide- and alkyne-functionalized myristic acid analogs, respectively (Figure 4.2). We found that even very low concentrations of Az12 strongly diminished YFP accumulation, whereas Alk12 showed inhibitory effects only at relatively

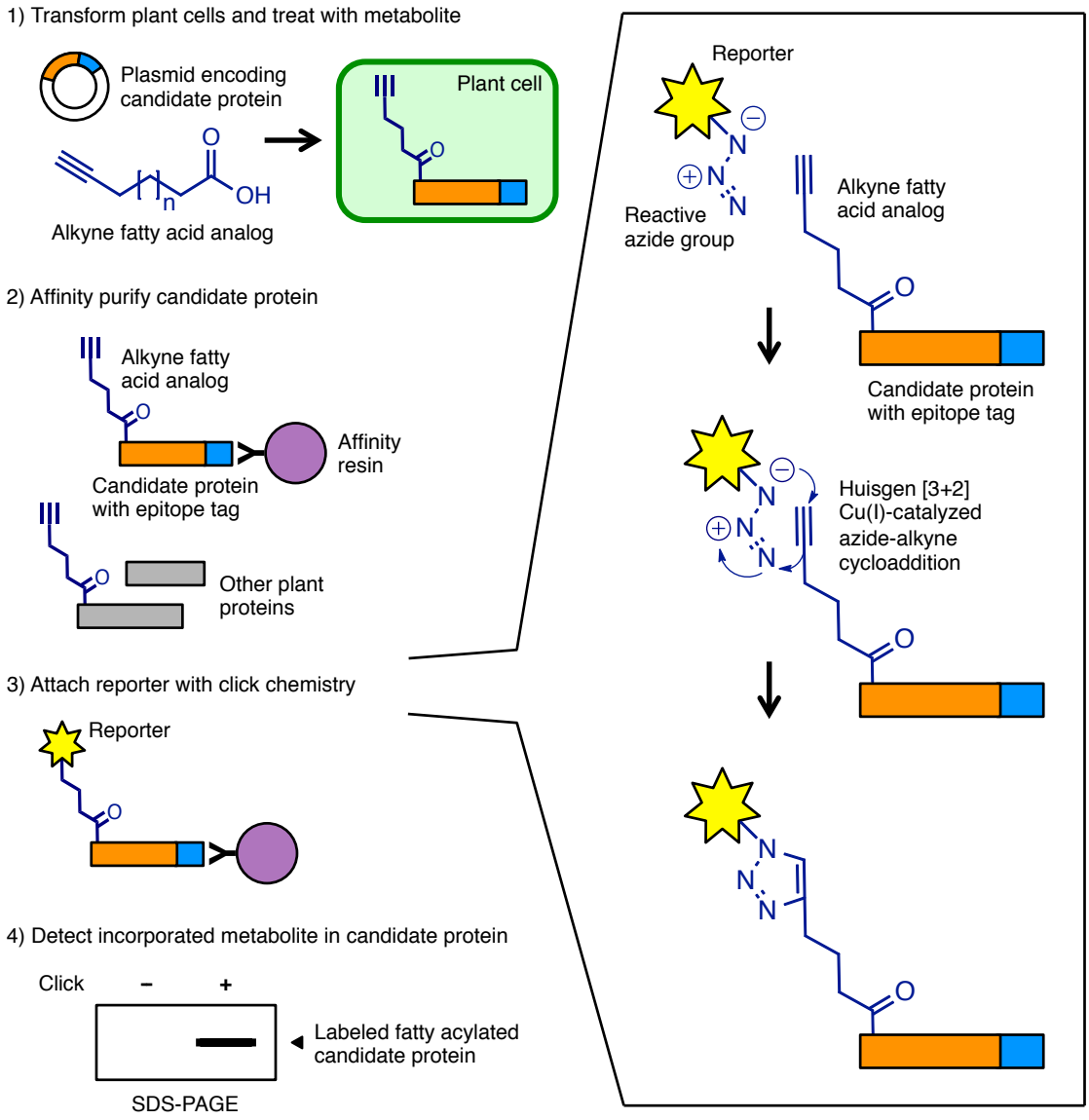

Figure 4.1. Experimental scheme for assessing fatty acylation of proteins in plant cells using clickable fatty acid analogs. Adapted from Kaschani et al. (2009).

high concentrations (Figure 4.2). Therefore, we decided to perform all subsequent experiments using preparations of alkyne fatty acid analogs.

The pattern recognition receptor FLS2 is S-acylated

The plant PM is armed with a series of sensors that function as a surveillance system to detect the presence of invading microbes and much of the machinery

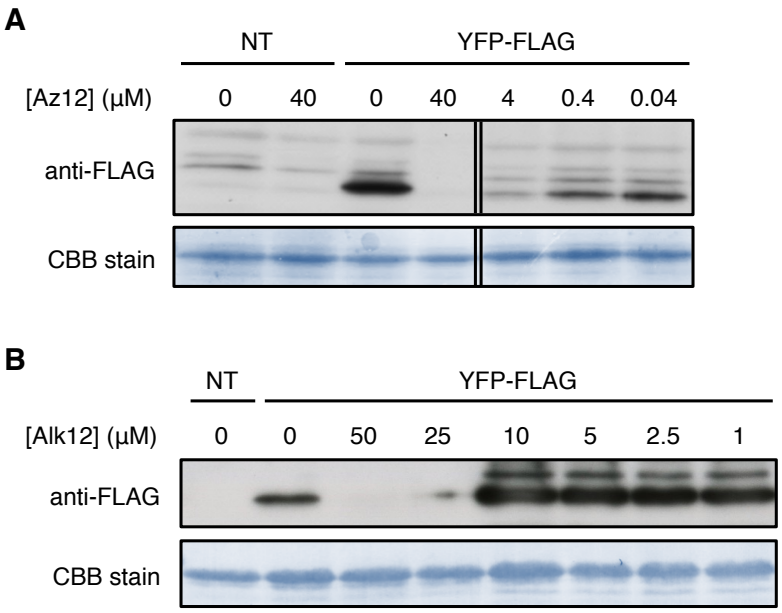

Figure 4.2. Azide fatty acid analogs, but not alkyne fatty acid analogs, interfere with cellular functions. **(A)** Arabidopsis protoplasts were transformed with FLAG epitope-tagged *YFP* and treated with different concentrations of the azide fatty acid analog Az12. Cells were incubated overnight and total protein extracted. Anti-FLAG western blotting was used to detect YFP accumulation. Coomassie brilliant blue (CBB) stain was used to visualize total protein and demonstrate equal loading. NT, not transformed. Black dividing lines indicate removal of irrelevant lanes from the blot and gel images. **(B)** Arabidopsis protoplasts were transformed with FLAG epitope-tagged *YFP* and treated with different concentrations of the alkyne fatty acid analog Alk12. Cells were incubated overnight and total protein extracted. Anti-FLAG western blotting was used to detect YFP accumulation. CBB stain was used to visualize total protein and demonstrate equal loading.

involved in monitoring this crucial lipophilic locale features some form of fatty acylation (Zipfel, 2014; Boyle & Martin, 2015). These PM-localized pattern recognition receptors (PRRs) are able to perceive the presence of pathogens through the recognition of conserved microbe-associated molecular patterns (Zipfel, 2014). Activation of PRRs stimulates signaling through intracellular protein kinases, resulting in the deployment of a broad-spectrum defense response referred to as pattern-triggered immunity (PTI) Jones:2006ih.

One of the best-characterized PRRs is Arabidopsis flagellin-sensitive 2 (FLS2), which recognizes a highly conserved 22-amino acid sequence from the N-terminal portion of bacterial flagellin (Felix et al., 1999; Gómez-Gómez & Boller, 2000). A recent survey of protein S-acylation in Arabidopsis using an ABE approach strongly suggested that FLS2 is S-acylated at cysteine residues 830 and 831 (Hemsley et al., 2008, 2012). To validate our click chemistry-based approach and to directly show incorporation of palmitic acid at these sites, we expressed wild-type *FLS2* and a mutant encoding serine substitutions at residues 830 and 831 (C830S,C831S) in Arabidopsis protoplasts in the presence of the palmitic acid analog Alk14 (Figure 4.3A). Following protein extraction and immunoprecipitation, we introduced a fluorescent reporter tag using click chemistry to visualize Alk14 incorporation. We were able to detect a strong fluorescent signal only with wild-type FLS2, and not the C830S,C831S mutant. Anti-HA western blotting showed comparable accumulation of the two proteins (Figure 4.3A). Importantly, given that the C830S,C831S mutant is targeted to the PM like wild-type FLS2 (Hemsley et al., 2013), the lack of labeling observed with the mutant indicates that fatty acid analogs are not attached to these proteins simply due to their proximity to the lipid-rich PM. Taken together, this result demonstrates that our approach is well suited to study the fatty acylation status of candidate proteins in plant cells.

Alkyne fatty acid analogs do not appear to interfere with programmed cell death and permeate intact cells in leaf tissue

The alkyne-functionalized fatty acid analogs do not appear to interfere with protein synthesis when used at moderate concentrations and are readily incorporated into proteins in a protoplast system. However, it remained possible that in the context of whole leaf tissue these analogs could cause spurious cell death symptoms, interfere with certain immune responses, or are unable to permeate intact cells. To

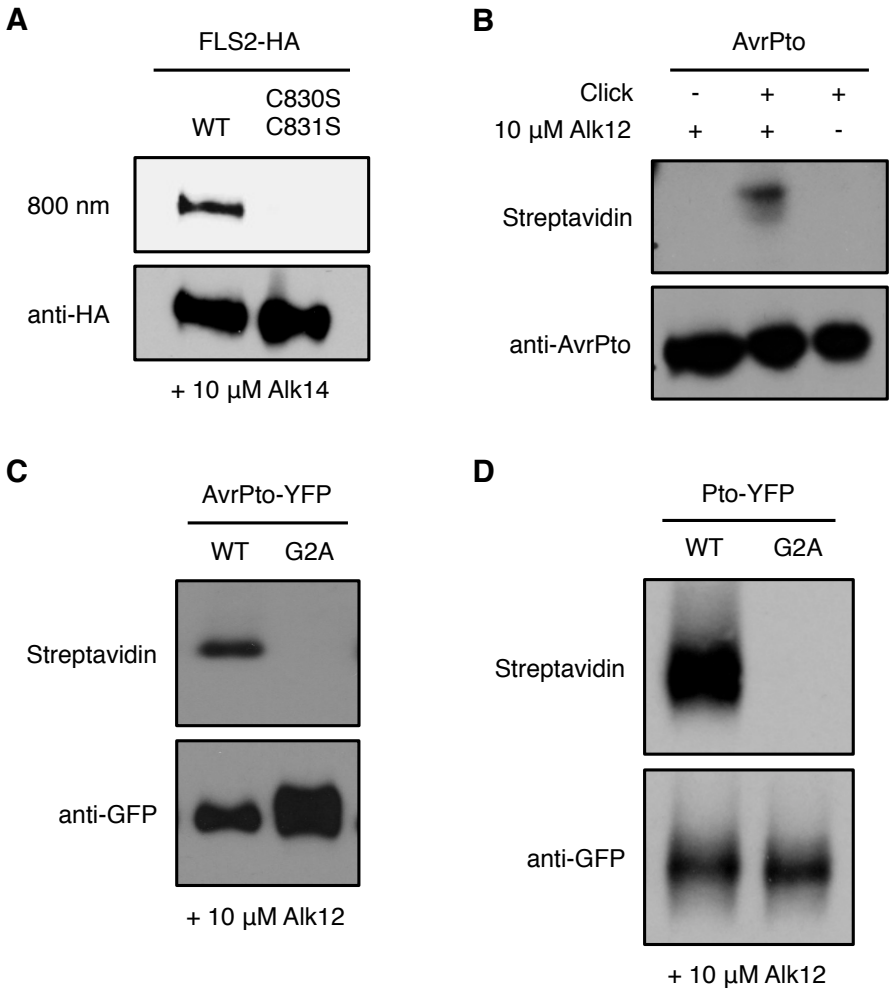

address these concerns, we tested if the tomato resistance protein Pto, which mediates recognition of the *Pseudomonas syringae* pv. *tomato* effector AvrPto, retains the ability to trigger programmed cell death (PCD) in the presence of the different alkyne fatty acid analogs (Scofield et al., 1996; Tang et al., 1996; Martin et al., 2003). We transiently expressed *Pto* together with *avrPto* or an empty vector in *Nicotiana benthamiana* leaf tissue using Agrobacterium-mediated transformation, followed by infiltration of the alkyne fatty acid analogs (Figure 4.4A). We found that neither the myristic acid analog Alk12, the palmitic acid analog Alk14, nor the stearic acid analog Alk16 produced any spurious symptoms nor did they affect

Figure 4.3 ***(previous page).*** Fatty acid modifications of proteins involved in plant immunity. **(A)** Arabidopsis protoplasts were transformed with HA epitope-tagged *FLS2* wild-type (WT) or a mutant encoding C830S,C831S. Protoplasts were treated with 10 µM Alk14, incubated for 6 h, and cells collected. Total protein was extracted, FLS2 proteins immunoprecipitated using anti-HA resin, and click chemistry performed. Incorporated Alk14 was visualized by fluorescence imaging and total protein was detected by anti-HA western blotting. **(B)** Transgenic Arabidopsis plants conditionally expressing *avrPto* were treated with 20 µM dexamethasone to induce transgene expression. Leaves were infiltrated twice with 10 µM Alk12, 6 h after induction and 6 h before sampling. Tissue was collected 30 h after induction and total protein extracted. AvrPto was immunoprecipitated using anti-AvrPto resin and a biotin tag added using click chemistry. Streptavidin-HRP western blotting was used to detect incorporation of Alk12. Anti-AvrPto western blotting was used to verify equal amounts of protein in all samples. **(C)** *N. benthamiana* leaves were infiltrated with Agrobacterium strains carrying *avrPto-YFP* fusion constructs encoding the WT protein or a G2A mutant. 10 µM Alk12 was infiltrated twice, 24 h after Agrobacterium infiltration and 6 h before sampling. Tissue was collected 48 h after transformation and total protein extracted. AvrPto proteins were immunoprecipitated using anti-GFP resin and a biotin tag attached using click chemistry. Incorporated Alk12 was detected by streptavidin-HRP western blotting. The anti-GFP western blot shows relative protein levels. **(D)** *N. benthamiana* was used to transiently express *Pto-YFP* fusions encoding the WT protein or a G2A mutant. 10 µM Alk12 was infiltrated twice, 24 h after Agrobacterium infiltration and 6 h before sampling. Tissue was collected 48 h after transformation, total protein extracted, and Pto proteins immunoprecipitated using anti-GFP resin. A biotin tag was attached using click chemistry and incorporation of Alk12 was detected by streptavidin-HRP western blotting. Protein levels were visualized by anti-GFP western blotting.

PCD in response to AvrPto, even though all of the alkyne-bearing metabolites were used at high concentrations (Figure 4.4A), suggesting that they are suitable to study the role of protein fatty acylation in plant-pathogen interactions.

To ensure that the metabolites are able to permeate intact plant cells and label fatty acylated proteins in the context of whole leaf tissue, we transiently expressed the *avrPto* effector in *N. benthamiana* leaves and syringe-infiltrated preparations of the alkyne fatty acid analogs into the transformed leaf tissue (Nimchuk et al., 2000; de Vries et al., 2006) (Figure 4.4B). We chose this particular protein to test the ability of the three fatty acid analogs for cell permeation and protein incorporation because AvrPto contains a predicted dual fatty acylation motif suggesting that it is subject to both plant-mediated myristoylation and S-acylation (Shan et al., 2000; Maurer-Stroh & Eisenhaber, 2004). We performed whole protein extraction, affinity purified the epitope-tagged AvrPto, and attached a fluorescent dye using click chemistry as described for FLS2. We visualized incorporation of the different alkyne fatty acid analogs using fluorescence imaging and detected incorporation of all three probes, although with varying signal strength (Figure 4.4B). This demonstrates that the alkyne fatty acid analogs are able to permeate intact leaf cells and are likely incorporated by way of innate metabolic processes, making this approach suitable for the study of protein fatty acylation in leaf tissue.

A transgenic Arabidopsis line shows incorporation of a myristic acid analog into AvrPto

Bacterial plant pathogens employ the type III secretion system to inject effector proteins directly into the plant cell to subvert PTI signaling, ultimately rendering the host susceptible to infection (Jones & Dangl, 2006; Dou & Zhou, 2012). Spatial regulation of effectors is required for their virulence function because it ensures that they engage their intended targets and enhances the local concentration of these

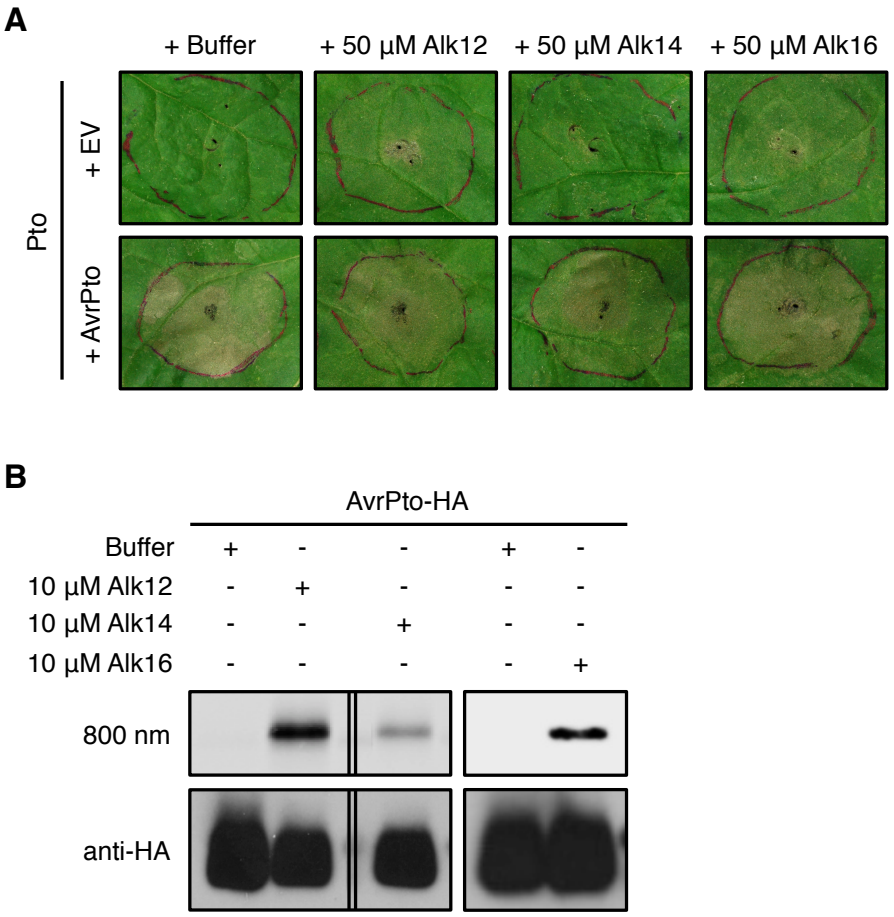

Figure 4.4. Alkyne fatty acid analogs do not interfere with immunity mechanisms and are incorporated in fatty acylated proteins in the context of intact plant leaf tissue. **(A)** *N. benthamiana* leaves were infiltrated with Agrobacterium strains carrying *Pto* and empty vector (EV) or *avrPto*. 50 µM Alk12, Alk14, Alk16, or buffer were infiltrated 24 h after Agrobacterium infiltration. Plants were monitored for programmed cell death and pictures taken 2 days after transformation. **(B)** *N. benthamiana* was used to transiently express HA epitope-tagged avrPto. 10 µM Alk12, Alk14, Alk16, or buffer was infiltrated twice, 24 h after Agrobacterium infiltration and 6 h before sampling. Tissue was collected 48 h after transformation, total protein extracted, AvrPto immunoprecipitated using anti-HA resin, and a fluorescent tag added using click chemistry. Incorporated alkyne fatty acid analogs were visualized by fluorescence imaging and total protein was detected by anti-HA western blotting. Black dividing lines indicate removal of irrelevant lanes from the blot and gel images.

pathogen-derived proteins, which are likely delivered into the host cell in very small amounts (Hicks & Galán, 2013). Several effectors have been shown to target the PTI machinery present at the intracellular face of the plant PM and a number of these bacterial proteins appear to hijack the host fatty acylation apparatus to access this lipophilic locale (Dowen et al., 2009; Nimchuk et al., 2000; Shan et al., 2000; Zhou et al., 2014b). Notably, plant-mediated fatty acylation has not been decisively demonstrated for most effectors, but rather inferred from studies showing that N-terminal glycine and/or cysteine substitutions prevent PM localization and render the effectors unable to exert their virulence function or elicit an immune response, depending on the host plant (Shan et al., 2000; Robert-Seilaniantz et al., 2006; Dowen et al., 2009). A recent review elaborates on the exploitation of host-mediated fatty acylation by plant pathogenic effectors (Boyle & Martin, 2015).

The AvrPto effector promotes bacterial pathogenesis by targeting the FLS2 receptor complex in order to suppress flagellin perception (Shan et al., 2008; Xiang et al., 2008). Like the PM-associated FLS2, AvrPto was shown to localize to the cell periphery (Shan et al., 2000; He et al., 2006; Göhre et al., 2008). It is strongly suggested that targeting of this pathogen protein to the plant PM requires post-translational host-mediated myristoylation of the glycine-2 (G2) residue in AvrPto, since the G2A mutation abolishes both PM localization and virulence function of the effector (Shan et al., 2000; He et al., 2006). To test if AvrPto is indeed myristoylated in plant cells, we took advantage of a transgenic Arabidopsis line conditionally expressing *avrPto* under control of a dexamethasone-inducible system (Hauck et al., 2003) (Figure 4.3B). We syringe-infiltrated leaves with the myristic acid analog Alk12 following dexamethasone treatment, extracted total protein, and immunoprecipitated AvrPto using anti-AvrPto resin. The incorporated fatty acid was then biotinylated using click chemistry and visualized by western blotting. We

were able to detect a specific band of the expected size in samples treated with Alk12 and subsequently subjected to click chemistry. To control for unspecific detection in the absence of an AvrPto G2A mutant, we included samples without performing click chemistry and without infiltrating the metabolite. Anti-AvrPto western blotting was used to verify equal amounts of the effector protein in all samples (Figure 4.3B). This result shows that AvrPto is myristoylated in plant cells and demonstrates that our approach can be applied to assess fatty acylation of candidate proteins stably expressed in transgenic Arabidopsis leaf tissue. However, the lack of a stable Arabidopsis line expressing a G2 point mutant of AvrPto prevented us from determining whether this modification is mediated by way of canonical G2 myristoylation or not; we address this limitation in the next section.

Transient expression in *N. benthamiana* demonstrates that AvrPto is myristoylated at its N-terminus

To establish a higher-throughput system for validation of multiple candidate proteins, we took advantage of Agrobacterium-mediated transient gene expression in *N. benthamiana*. This approach also enables the use of point mutants to validate predicted fatty acylation sites and to control for nonspecific incorporation of alkyne fatty acid analogs. We transiently expressed *avrPto* variants and infiltrated the leaf tissue with the myristic acid analog Alk12 (Figure 4.3C). To counter previously observed instability of the AvrPto G2A mutant, we fused the effector to YFP in an attempt to stabilize the protein. We were able to detect click-mediated biotinylation using streptavidin with wild-type AvrPto, but no band was detected with the predicted myristoylation mutant G2A despite high protein accumulation (Figure 4.3C). Thus, using the *N. benthamiana* system, we were able to extend our data obtained in Arabidopsis to conclusively show typical G2-mediated myristoylation of AvrPto through the use of a specific point mutant.

As previously mentioned, the AvrPto N-terminus contains a predicted dual fatty acylation motif, MGNICVGGSR, due to the G2 and proximal cysteine-5 (C5) residues (Shan et al., 2000; Maurer-Stroh & Eisenhaber, 2004). While we showed labeling of this pathogen effector with Alk12, Alk14, and Alk16 (Figure 4.4B), we were unable to map S-acylation to the C5 position due to instability and inconsistent labeling of the AvrPto mutant forms (data not shown). However, it is likely that AvrPto is S-acylated at the C5 position because this residue is the only cysteine present in the effector protein.

Detection of Pto myristoylation in plant cells is greatly enhanced using metabolic labeling coupled with click chemistry

Plants have evolved intracellular surveillance mechanisms to perceive the presence and activity of pathogen effectors (Dodds & Rathjen, 2010). Detection of effectors within the host cell indicates infection by an adapted pathogen and as a result the plant activates an amplified defense response referred to as effector-trigger immunity (ETI) which is often associated with PCD (Dodds & Rathjen, 2010; Oh & Martin, 2011). ETI signaling is typically mediated by nucleotide-binding leucine-rich repeat (NB-LRR) proteins that are often physically partnered with either a decoy which resembles a host protein targeted by effectors, or an actual host target (van der Hoorn & Kamoun, 2008; Qi & Innes, 2013). In either case, interactions between effectors and host proteins are sensed by the associated NB-LRRs which subsequently activate ETI Qi:2013cf. Regardless of the specific mode of detection, the precise localization of these surveillance mechanisms is critical to their function and because the intracellular face of the plant PM is an area intensely attacked by effectors, many of these sensors are positioned at this crucial locale by way of lipid modifications (Kim et al., 2005; Takemoto & Jones, 2005; Gao et al., 2011; Qi et al., 2012; Takemoto et al., 2012; Qi & Innes, 2013).

Some tomato accessions rely upon the Pto kinase, acting in concert with the NB-LRR protein Prf, to recognize the fatty acylated pathogen effector AvrPto (Martin et al., 1993; Pedley & Martin, 2003; Mucyn et al., 2006; Gutierrez et al., 2010; Mathieu et al., 2014). Pto appears to function as a decoy that mimics the structure of the kinase domains present in PRR signaling complexes, such as that of FLS2, but in contrast to the PM-spanning receptors it is proposed to mimic, Pto lacks a transmembrane domain (Martin et al., 1993). Previous work using a radiolabeled myristic acid feeding approach showed that Pto is myristoylated in plant cells and that the G2 residue associated with myristoylation is required for full recognition of AvrPto (de Vries et al., 2006; Balmuth & Rathjen, 2007). To confirm incorporation of myristic acid with our click chemistry-based approach, we transiently expressed wild-type *Pto* and a mutant encoding the G2A substitution in *N. benthamiana* (Figure 4.3D). Following the strategy used for AvrPto, we fused Pto to YFP to stabilize the G2A mutant as demonstrated by the anti-GFP western blot. We were able to detect incorporation of the myristic acid analog Alk12 into wild-type Pto using streptavidin after adding a biotin tag via click chemistry. No band was detected for the G2A mutant (Figure 4.3D). This experiment confirms Pto myristoylation and extends our click chemistry-based method to assess fatty acylation to include a PM receptor, a pathogen effector, and an intracellular host resistance protein.

Myristoylome labeling using alkyne fatty acid analogs

The strict requirement of an N-terminal glycine residue coupled with the availability of plant genome sequences has enabled the prediction of myristoylated proteins across the proteome, a collection of proteins also referred to as the myristoylome (Boisson et al., 2003; Maurer-Stroh et al., 2002; Podell & Gribskov, 2004; Traverso et al., 2008). However, methods to directly validate the predicted myristoylome in

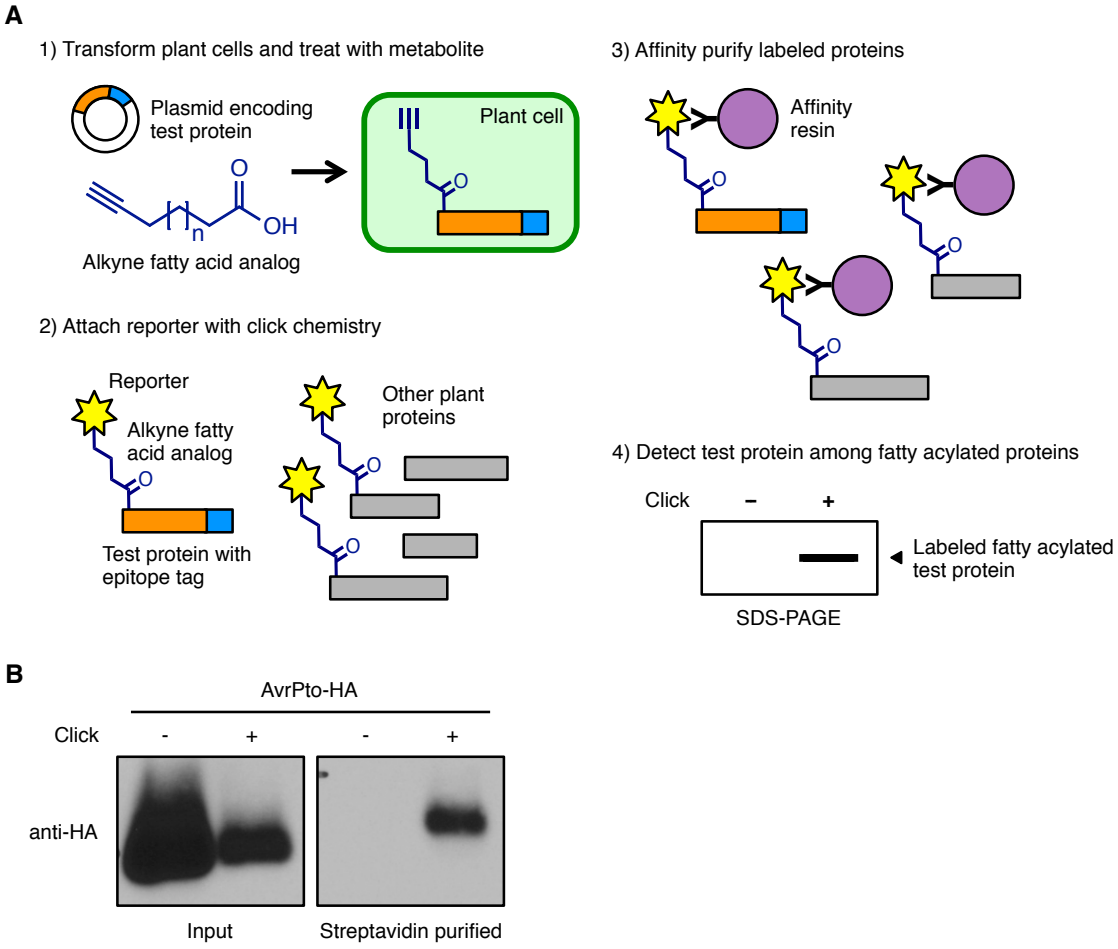

Figure 4.5. Protein capture by means of myristoylation provides a potential method for the enrichment and investigation of the plant myristoylome. **(A)** Modified experimental scheme to capture and enrich myristoylated proteins using AvrPto as a test protein. **(B)** *N. benthamiana* was used to transiently express HA epitope-tagged *avrPto*. 50 µM Alk12 was infiltrated twice, 24 h after Agrobacterium infiltration and 6 h before sampling. Tissue was collected 48 h after transformation, total protein extracted, and a biotin tag added using click chemistry. Streptavidin affinity purification was used to enrich biotinylated proteins and AvrPto was detected using anti-HA western blotting. Input shows AvrPto levels before affinity purification.

plant cells are lacking. Furthermore, bioinformatic approaches are unable to predict non-canonical myristoylation, such as the post-translational protein myristic acid modification required for the virulence function and recognition of the bacterial effector AvrPphB in plant cells (Dowen et al., 2009). To begin to address these limitations, our click chemistry-based approach could be modified and applied to enrich and investigate the myristoylome and potentially enable proteome-wide analysis of other fatty acid modifications in plants (Maurer-Stroh et al., 2002; Boisson et al., 2003; Podell & Gribskov, 2004) (Figure 4.5A). We performed a pilot experiment using AvrPto and transiently expressed the effector in *N. benthamiana* leaf tissue and subsequently introduced the myristic acid analog Alk12 by infiltration (Figure 4.5B). Total protein was extracted, a standard methanol/chloroform precipitation performed, and click chemistry used to biotinylate the incorporated Alk12. A second methanol/chloroform precipitation was used to remove unreacted azido-biotin prior to affinity purification using streptavidin resin. We interrogated this biotinylated material for the presence of AvrPto by anti-HA western blotting and were able to detect the effector from among the multitude of biotinylated proteins (Figure 4.5B). This result demonstrates that using the described protocol it is possible to capture a myristoylated protein from among a complex plant lysate by way of its fatty acid modification. Admittedly, the AvrPto protein used in this pilot experiment was overexpressed and future work is required to determine if this method is sufficient for the labeling and enrichment of natively expressed plant proteins and if it is amenable to subsequent mass spectrometry analysis.

4.5 Discussion

We describe the development of a click chemistry-based method using metabolic labeling with ω-alkynyl fatty acid analogs to study the fatty acylation, especially

myristoylation, of both host and pathogen proteins in the plant cell. Our data directly demonstrate that the FLS2 receptor is S-acylated and the AvrPto effector that targets this sensor protein is subject to myristoylation and possibly S-acylation, supporting previous findings that strongly suggested these proteins were subject to such modifications in plants (Shan et al., 2000; Hemsley et al., 2013). Using our approach we also recapitulated an experiment demonstrating the myristoylation of Pto, the resistance protein responsible for recognition of AvrPto, that was initially performed with radiolabeled myristic acid and we were able to reduce the exposure time required to detect this fatty acid modification from a month to less than a minute (de Vries et al., 2006). Notably, these results were obtained using a combination of biotin and fluorescent reporters from an array of plant-based expression systems, including transiently transformed Arabidopsis protoplasts, stably transformed Arabidopsis plants, and transiently transformed *N. benthamiana* leaf tissue.

There are several examples demonstrating that feeding cultured cells fatty acid analogs results in their incorporation into cellular proteins through native metabolic mechanisms, without any obvious disruption to cellular processes (Charron et al., 2009; Yap et al., 2010). Metabolic labeling of proteins with 'clickable' fatty acid analogs has several advantages over the use of radiolabeled fatty acids, GC-MS approaches, and the ABE method for investigating protein fatty acylation. Proteins metabolically labeled with these bio-orthogonal analogs can be selectively and covalently modified with a variety of secondary tags via click chemistry. These secondary tags can include various affinity purification groups, such as biotin, or fluorescent reporter dyes. The click-mediated addition of affinity purification tags enables the capture and analysis of proteins modified by a given fatty acid and unlike the ABE and GC-MS approaches this technique can be applied to the study

of myristoylated proteins. A further advantage over the ABE method is the decisive nature of the labeling offered with the fatty acid analogs. The direct tagging of proteins metabolically labeled with a given fatty acid analog, rather than the removal and replacement of all protein thioesters, can avoid much of the ambiguity and false positives associated with the ABE approach (Roth et al., 2006; Hannoush & Sun, 2010; Martin, 2013; Zhou et al., 2014a).

It should be noted that the ABE method does not require feeding fatty acids to the cells or organism of interest, which is a disadvantage of metabolic labeling approaches using either radiolabeled or ω-alkynyl/-azido fatty acid analogs. However, these feeding approaches make it possible to perform pulse-chase experiments, enabling the study of S-acylation turnover dynamics which have been shown to regulate plant protein function (Sorek et al., 2007; Zhou et al., 2014a). Therefore, the methods described here have the potential to enable dynamic protein S-acylation analysis in plants without the need for radioactive materials (Martin, 2013). The incubation period is critical to the success of all labeling experiments and may have to be adjusted depending on the fatty acid analog, protein of interest, and metabolism of the system under investigation (Martin, 2013). The major advantages of the clickable fatty acid analogs over radiolabeled fatty acids, beyond enabling proteome-wide enrichment of proteins modified by a particular form of fatty acylation, are the nonradioactive nature of these reagents and the signal strength of the click-compatible biotin and fluorescent reporters. A study comparing the detection of protein myristoylation using [^{3}H]-myristic acid versus that produced by ω-azido myristic acid, with subsequent biotinylation, showed that the latter produced signal intensities up to one million times stronger than that of the tritiated fatty acid (Martin et al., 2008). Similarly, using our technique we were able to detect myristoylation of Pto transiently expressed in *N. benthamiana* with

exposure times of less than one minute, in contrast to the month-long exposure time required to see the signal for the fatty acylation of a similarly expressed and immunoprecipitated Pto with tritiated myristic acid (de Vries et al., 2006).

Unlike myristoylation, S-acylation is a reversible modification mainly due to the thioester bond between the cysteine side chain and the fatty acid, which is less stable than the amide linkage responsible for coupling myristate to an N-terminal glycine (Bizzozero, 1995; Martin, 2013). The strong amide attachment of the Alk12 myristic acid analog as a result of myristoylation-type modifications provides a stable handle for protein purification and detection, which has worked very reliably in our hands. In contrast, the labile nature of S-acylation requires more delicate handling, particularly during elution steps following enrichment via immunoprecipitation procedures (Bizzozero, 1995; Martin, 2013). Whereas myristoylation labeling was resistant to 10% 2-mercaptoethanol in the Laemmli sample buffer, in instances analyzing S-acylation the 2-mercaptoethanol concentrations were lowered to 0.1% to preserve the thioester bonds (Bizzozero, 1995; Hicks et al., 2011; Martin, 2013). We found that the use of fluorescent dyes is preferable for the study of S-acylation because it allows rapid in-gel detection and does not require blotting of the labeled proteins, a process that can lead to thioester hydrolysis and loss of the reporter molecule (Charron et al., 2009; Martin, 2013). Even so, biotin-based reporters remain an attractive option because western blotting is highly sensitive and the materials are more readily accessible compared to fluorescent dye reagents that are expensive and require somewhat specialized scanners for detection.

Metabolic labeling methods, such as the one we present here, are generally acknowledged to avoid the false positive problems inherent to ABE-type approaches; however, labeling also has the potential for false positives. The fatty acid analogs can be metabolized into the cellular lipid pools if the labeling period is too long,

resulting in non-target fatty acids possessing the alkyne moiety which can yield false positives (Yap et al., 2010; Martin, 2013). For this reason it is imperative to determine the fatty acid analog incubation period for a given protein and/or plant system and note that this period might differ considerably from the times compatible with the proteins in our particular study (Yount et al., 2011; Hannoush, 2012). It has also been reported that Alk12 and Alk14 can participate in both myristoylation and S-acylation, which was attributed to a lack of specificity in the fatty acylation machinery rather than metabolism of the fatty acid analogs (Charron et al., 2009). Alk16 on the other hand seems to more specifically label S-acylated proteins and might be a better choice for detecting this specific form of fatty acid modification (Charron et al., 2009; Thinon & Hang, 2015). Another potential source for false positives when using labeling approaches is the addition of fatty acids to non-target amino acids. The most notable example of this phenomenon is the labeling of the G2A mutant of the mammalian membrane-associated non-tyrosine protein kinase Fyn, the native form of which is known to be subject to N-terminal dual fatty acylation, with both radioactive and alkyne bearing myristic acid analogs (Charron et al., 2009). We also observed some instances of non-target labeling, primarily when working with the palmitic acid analog Alk14 and the stearic acid analog Alk16, which could be attributable to any of the phenomena described above (data not shown). It should be noted that the unique sensitivity of S-acyl adducts to treatments with strong reducing agents and nucleophiles such as 2-mercaptoethanol, dithiothreitol, and hydroxylamine can be leveraged to address some issues with ambiguous labeling (Charron et al., 2009). In our experience, detection of myristoylation with the Alk12 reagent has been very specific because the G2A mutants reliably abolished labeling by the fatty acid analog. Another potential problem with labeling approaches is that the presumed overabundance

of the fatty acid analogs in these feeding assays leads to unspecific incorporation at non-target residues. However, our results with FLS2 would suggest that this may not be an issue because the C830S,C831S mutant appeared to abolish incorporation of the palmitic acid analog Alk14 despite being properly localized at the PM (Hemsley et al., 2013). Toxicity of these fatty acid analogs can be a concern and should be evaluated for the plant system under investigation. For example, it was found that analogs of lauric acid bearing a terminal alkyne similar to the alkyne fatty acid analogs used in our study inhibited a lauric acid ω-hydroxylase in microsome preparations from *Vicia sativa* (Helvig et al., 1997). In our experiments with Arabidopsis protoplasts we observed strong phytotoxicity with the azide fatty acid analog Az12, however, the alkyne fatty acid analog Alk12 showed no adverse effects and for this reason we decided to use the alkyne-functionalized analogs for our work. It should be noted that the reagents were prepared in accordance with their manufacturers' instructions, which called for the use of different solvents. The Az12 was prepared as a 40 mM stock in dimethyl sulfoxide (DMSO) and the Alk12 as a 50 mM stock in ethanol. The DMSO used for the Az12 stock solution could contribute to the observed toxicity, but in all treatments the stock solution was diluted at least 1,000-fold, meaning that the plant cells were maximally exposed to 0.1% DMSO. While we believe that the Az12 is most likely responsible for the observed toxicity to the protoplasts, we cannot rule out negative contributions from the DMSO.

Finally, our experiments were performed with overexpressed proteins and it will likely be more difficult to detect fatty acylation of natively expressed proteins. To test candidate proteins, transient overexpression with a commercial epitope tag is ideal because this enables the use of point mutants and allows for easy purification and concentration of the proteins prior to performing click chemistry.

In our experience, amino acid substitutions that prevent protein fatty acylation and enable mapping of the modification to specific residues can result in protein instability and it can be helpful to employ fusions with green fluorescent protein variants to stabilize problematic substitution mutant proteins. In instances where the study of natively expressed proteins is desirable specific antibodies can be used to purify and concentrate the protein of interest, providing optimal buffer conditions for an efficient click reaction.

We described the development and application of a metabolic labeling approach coupled with click chemistry to quickly and easily determine fatty acylation, especially myristoylation, of candidate proteins in plant cells. Our method can reduce the time required to assess protein fatty acid modifications from months to less than a week and relies on neither radioactivity nor mass spectrometry. We demonstrated the ability of our approach to determine the fatty acylation status of three representative proteins involved in plant-pathogen interactions using a variety of expression systems. Although presently most effective for determining protein myristoylation, this technique promises to provide mechanistic details of the molecular tactics used at the host plasma membrane in the battle between plants and pathogens. In addition, we expect that with some modifications this approach will be broadly applicable for the study of protein fatty acylation in plants and will shed light on new mechanisms not only involving plant-pathogen interactions but the wider field of plant biology.

4.6 Acknowledgments

We thank Dr. Frank Schroeder, Dr. Inish O'Doherty, Joshua Baccile, and Jason Hoki for help with the click chemistry; Dr. Johannes Mathieu for providing the *FLS2* entry clone and helpful discussions; Dr. Brendan Riely for contribut-

ing the *Pto-YFP* strains; and Diane Dunham, Christopher D'Angelo, and Paige Reeves for their help with sample preparation and plant care. We are also grateful to the reviewers for their helpful suggestions. This work was supported by the U.S. Department of Agriculture?National Institute of Food and Agriculture (grant no. USDA-NIFA 2010-65108-20503 to Dr. Gregory Martin), the National Science Foundation (grant no. IOS-1451754 to Dr. Gregory Martin), the Human Frontier Science Program (grant no. HFSP-LT000608/2011-L to Dr. Patrick Boyle), and the Triad Foundation (to Drs. Patrick Boyle, Sarah Hind, and Gregory Martin).

4.7 Bibliography

Abramovitch, R. B., Kim, Y.-J., Chen, S., Dickman, M. B., & Martin, G. B. (2003). *Pseudomonas type* III effector AvrPtoB induces plant disease susceptibility by inhibition of host programmed cell death. *EMBO J*, *22*(1), 60–69.

Aicart-Ramos, C., Valero, R. A., & Rodriguez-Crespo, I. (2011). Protein palmitoylation and subcellular trafficking. *Biochim Biophys Acta*, *1808*(12), 2981–2994.

Balmuth, A., & Rathjen, J. P. (2007). Genetic and molecular requirements for function of the Pto/Prf effector recognition complex in tomato and *Nicotiana benthamiana*. *Plant J*, *51*(6), 978–990.

Batistic, O. (2012). Genomics and localization of the Arabidopsis DHHC-cysteine-rich domain S-acyltransferase protein family. *Plant Physiol*, *160*(3), 1597–1612.

Batistic, O., Rehers, M., Akerman, A., Schlücking, K., Steinhorst, L., Yalovsky, S., & Kudla, J. (2012). S-acylation-dependent association of the calcium sensor CBL2 with the vacuolar membrane is essential for proper abscisic acid responses. *Cell Res*, *22*(7), 1155–1168.

Batistic, O., Sorek, N., Schültke, S., Yalovsky, S., & Kudla, J. (2008). Dual fatty acyl modification determines the localization and plasma membrane targeting of CBL/CIPK Ca^{2+} signaling complexes in *Arabidopsis*. *Plant Cell*, *20*(5), 1346–1362.

Bizzozero, O. A. (1995). Chemical analysis of acylation sites and species. *Meth Enzymol*, *250*, 361–379.

Boisson, B., Giglione, C., & Meinnel, T. (2003). Unexpected protein families including cell defense components feature in the N-myristoylome of a higher eukaryote. *J Biol Chem*, *278*(44), 43418–43429.

Bombarely, A., Rosli, H. G., Vrebalov, J., Moffett, P., Mueller, L. A., & Martin, G. B. (2012). A draft genome sequence of *Nicotiana benthamiana* to enhance molecular plant-microbe biology research. *Mol Plant Microbe Interact*, *25*(12), 1523–1530.

Bourge, M., Fort, C., Soler, M.-N., Satiat-Jeunemaître, B., & Brown, S. C. (2015). A pulse-chase strategy combining click-EdU and photoconvertible fluorescent reporter: tracking Golgi protein dynamics during the cell cycle. *New Phytol*, *205*(2), 938–950.

Boyle, P. C., & Martin, G. B. (2015). Greasy tactics in the plant-pathogen molecular arms race. *J Exp Bot*, *66*(6), 1607–1616.

Charron, G., Zhang, M. M., Yount, J. S., Wilson, J., Raghavan, A. S., Shamir, E., & Hang, H. C. (2009). Robust fluorescent detection of protein fatty-acylation with chemical reporters. *J Am Chem Soc*, *131*(13), 4967–4975.

de Vries, J. S., Andriotis, V. M. E., Wu, A.-J., & Rathjen, J. P. (2006). Tomato *Pto* encodes a functional N-myristoylation motif that is required for signal transduction in *Nicotiana benthamiana*. *Plant J*, *45*(1), 31–45.

Dean, P. (2011). Functional domains and motifs of bacterial type III effector proteins and their roles in infection. *FEMS Microbiol Rev*, *35*(6), 1100–1125.

Dodds, P. N., & Rathjen, J. P. (2010). Plant immunity: towards an integrated view of plant-pathogen interactions. *Nat Rev Genet*, *11*(8), 539–548.

Dou, D., & Zhou, J.-M. (2012). Phytopathogen effectors subverting host immunity: different foes, similar battleground. *Cell Host Microbe*, *12*(4), 484–495.

Dowen, R. H., Engel, J. L., Shao, F., Ecker, J. R., & Dixon, J. E. (2009). A family of bacterial cysteine protease type III effectors utilizes acylation-dependent and -independent strategies to localize to plasma membranes. *J Biol Chem*, *284*(23), 15867–15879.

Drisdel, R. C., & Green, W. N. (2004). Labeling and quantifying sites of protein palmitoylation. *BioTechniques*, *36*(2), 276–285.

Dutilleul, C., Ribeiro, I., Blanc, N., Nezames, C. D., Deng, X. W., Zglobicki, P., Palacio Barrera, A. M., Atehortùa, L., Courtois, M., Labas, V., Giglioli-Guivarc'h, N., & Ducos, E. (2016). ASG2 is a farnesylated DWD protein that acts as ABA negative regulator in *Arabidopsis*. *Plant Cell Environ*, *39*(1), 185–198.

Farnsworth, C., Casey, P., Howald, W., Glomset, J., & Gelb, M. (1990). Structural characterization of prenyl groups attached to proteins. *Methods*, *1*(3), 231–240.

Felix, G., Duran, J. D., Volko, S., & Boller, T. (1999). Plants have a sensitive perception system for the most conserved domain of bacterial flagellin. *Plant J*, *18*(3), 1–12.

Feng, F., & Zhou, J.-M. (2012). Plant-bacterial pathogen interactions mediated by type III effectors. *Curr Opin Plant Biol*, *15*(4), 469–476.

Frederick, R. D., Thilmony, R. L., Sessa, G., & Martin, G. B. (1998). Recognition specificity for the bacterial avirulence protein AvrPto is determined by Thr-204 in the activation loop of the tomato Pto kinase. *Mol Cell*, *2*(2), 241–245.

Gao, Z., Gao, Z., Chung, E.-H., Eitas, T. K., & Dangl, J. L. (2011). Plant intracellular innate immune receptor Resistance to *Pseudomonas syringae* pv. *maculicola* 1 (RPM1) is activated at, and functions on, the plasma membrane. *Proc Natl Acad Sci*, *108*(18), 7619–7624.

Geissler, B. (2012). Bacterial toxin effector-membrane targeting: outside in, then back again. *Front Cell Infect Microbiol*, *2*, 75.

Göhre, V., Spallek, T., Häweker, H., Mersmann, S., Mentzel, T., Boller, T., de Torres, M., Mansfield, J. W., & Robatzek, S. (2008). Plant pattern-recognition receptor FLS2 is directed for degradation by the bacterial ubiquitin ligase AvrPtoB. *Curr Biol*, *18*(23), 1824–1832.

Gómez-Gómez, L., & Boller, T. (2000). FLS2: an LRR receptor-like kinase involved in the perception of the bacterial elicitor flagellin in *Arabidopsis*. *Mol Cell*, *5*(6), 1003–1011.

Gutierrez, J. R., Balmuth, A. L., Ntoukakis, V., Mucyn, T. S., Gimenez-Ibanez, S., Jones, A. M. E., & Rathjen, J. P. (2010). Prf immune complexes of tomato are oligomeric and contain multiple Pto-like kinases that diversify effector recognition. *Plant J*, *61*(3), 507–518.

Hannoush, R. N. (2012). Profiling cellular myristoylation and palmitoylation using ω-alkynyl fatty acids. *Methods Mol Biol*, *800*, 85–94.

Hannoush, R. N., & Sun, J. (2010). The chemical toolbox for monitoring protein fatty acylation and prenylation. *Nat Chem Biol*, *6*(7), 498–506.

Hauck, P., Thilmony, R., & He, S. Y. (2003). A *Pseudomonas syringae* type III effector suppresses cell wall-based extracellular defense in susceptible *Arabidopsis* plants. *Proc Natl Acad Sci*, *100*(14), 8577–8582.

He, P., Shan, L., Lin, N.-C., Martin, G. B., Kemmerling, B., Nürnberger, T., & Sheen, J. (2006). Specific bacterial suppressors of MAMP signaling upstream of MAPKKK in *Arabidopsis* innate immunity. *Cell*, *125*(3), 563–575.

Hellens, R., Mullineaux, P., & Klee, H. (2000). A guide to *Agrobacterium* binary Ti vectors. *Trends Plant Sci*, *5*(10), 446–451.

Helvig, C., Alayrac, C., Mioskowski, C., Koop, D., Poullain, D., Durst, F., & Salaün, J. P. (1997). Suicide inactivation of cytochrome P450 by midchain and terminal acetylenes. A mechanistic study of inactivation of a plant lauric acid ω-hydroxylase. *J Biol Chem*, *272*(1), 414–421.

Hemsley, P. A. (2015). The importance of lipid modified proteins in plants. *New Phytol*, *205*(2), 476–489.

Hemsley, P. A., Taylor, L., & Grierson, C. S. (2008). Assaying protein palmitoylation in plants. *Plant Methods*, *4*(1), 2–7.

Hemsley, P. A., Weimar, T., Lilley, K., Dupree, P., & Grierson, C. (2013). Palmitoylation in plants: new insights through proteomics. *Plant Signal Behav*, *8*(8).

Hemsley, P. A., Weimar, T., Lilley, K. S., Dupree, P., & Grierson, C. S. (2012). A proteomic approach identifies many novel palmitoylated proteins in Arabidopsis. *New Phytol*, *197*(3), 805–814.

Hicks, S. W., Charron, G., Hang, H. C., & Galán, J. E. (2011). Subcellular targeting of *Salmonella* virulence proteins by host-mediated S-palmitoylation. *Cell Host Microbe*, *10*(1), 9–20.

Hicks, S. W., & Galán, J. E. (2013). Exploitation of eukaryotic subcellular targeting mechanisms by bacterial effectors. *Nat Rev Microbiol*, *11*(5), 316–326.

Hurst, C. H., & Hemsley, P. A. (2015). Current perspective on protein S-acylation in plants: more than just a fatty anchor? *J Exp Bot*, *66*(6), 1599–1606.

Ivanov, S. S., & Roy, C. (2013). Host lipidation: a mechanism for spatial regulation of *Legionella* effectors. *Curr Top Microbiol Immunol*, *376*, 135–154.

Jones, J. D. G., & Dangl, J. L. (2006). The plant immune system. *Nature*, *444*(7117), 323–329.

Kaschani, F., Verhelst, S. H. L., van Swieten, P. F., Verdoes, M., Wong, C.-S., Wang, Z., Kaiser, M., Overkleeft, H. S., Bogyo, M., & van der Hoorn, R. A. L. (2009). Minitags for small molecules: detecting targets of reactive small molecules in living plant tissues using 'click chemistry'. *Plant J*, *57*(2), 373–385.

Kim, M. G., da Cunha, L., McFall, A. J., Belkhadir, Y., DebRoy, S., Dangl, J. L., & Mackey, D. (2005). Two *Pseudomonas syringae* type III effectors inhibit RIN4-regulated basal defense in *Arabidopsis*. *Cell*, *121*(5), 749–759.

Martin, B. R. (2013). Nonradioactive analysis of dynamic protein palmitoylation. *Curr Protoc Protein Sci*, *73*, Unit 14.15.

Martin, B. R., & Cravatt, B. F. (2009). Large-scale profiling of protein palmitoylation in mammalian cells. *Nat Methods*, *6*(2), 135–138.

Martin, D. D. O., Beauchamp, E., & Berthiaume, L. G. (2011). Post-translational myristoylation: fat matters in cellular life and death. *Biochimie*, *93*(1), 18–31.

Martin, D. D. O., Vilas, G. L., Prescher, J. A., Rajaiah, G., Falck, J. R., Bertozzi, C. R., & Berthiaume, L. G. (2008). Rapid detection, discovery, and identification of post-translationally myristoylated proteins during apoptosis using a bio-orthogonal azidomyristate analog. *FASEB J*, *22*(3), 797–806.

Martin, G. B., Bogdanove, A. J., & Sessa, G. (2003). Understanding the functions of plant disease resistance proteins. *Annu Rev Plant Biol*, *54*(1), 23–61.

Martin, G. B., Brommonschenkel, S. H., Chunwongse, J., Frary, A., Ganal, M. W., Spivey, R., Wu, T., Earle, E. D., & Tanksley, S. D. (1993). Map-based cloning of a protein kinase gene conferring disease resistance in tomato. *Science*, *262*(5138), 1432–1436.

Martinez, A., Traverso, J. A., Valot, B., Ferro, M., Espagne, C., Ephritikhine, G., Zivy, M., Giglione, C., & Meinnel, T. (2008). Extent of N-terminal modifications in cytosolic proteins from eukaryotes. *Proteomics*, *8*(14), 2809–2831.

Mathieu, J., Schwizer, S., & Martin, G. B. (2014). Pto kinase binds two domains of AvrPtoB and its proximity to the effector E3 ligase determines if it evades degradation and activates plant immunity. *PLoS Pathog*, *10*(7), e1004227.

Mathieu, J., Warthmann, N., Küttner, F., & Schmid, M. (2007). Export of FT protein from phloem companion cells is sufficient for floral induction in *Arabidopsis*. *Curr Biol*, *17*(12), 1055–1060.

Maurer-Stroh, S., Eisenhaber, B., & Eisenhaber, F. (2002). N-terminal N-myristoylation of proteins: prediction of substrate proteins from amino acid sequence. *J Mol Biol*, *317*(4), 541–557.

Maurer-Stroh, S., & Eisenhaber, F. (2004). Myristoylation of viral and bacterial proteins. *Trends Microbiol*, *12*(4), 178–185.

Méresse, S. (2011). Is host lipidation of pathogen effector proteins a general virulence mechanism? *Front Microbiol*, *2*, 73.

Mucyn, T. S., Clemente, A., Andriotis, V. M. E., Balmuth, A. L., Oldroyd, G. E. D., Staskawicz, B. J., & Rathjen, J. P. (2006). The tomato NBARC-LRR protein Prf interacts with Pto kinase in vivo to regulate specific plant immunity. *Plant Cell*, *18*(10), 2792–2806.

Nakagawa, T., Suzuki, T., Murata, S., Nakamura, S., Hino, T., Maeo, K., Tabata, R., Kawai, T., Tanaka, K., Niwa, Y., Watanabe, Y., Nakamura, K., Kimura, T., & Ishiguro, S. (2007). Improved Gateway binary vectors: high-performance vectors for creation of fusion constructs in transgenic analysis of plants. *Biosci Biotechnol Biochem*, *71*(8), 2095–2100.

Nimchuk, Z., Marois, E., Kjemtrup, S., Leister, R. T., Katagiri, F., & Dangl, J. L. (2000). Eukaryotic fatty acylation drives plasma membrane targeting and enhances function of several type III effector proteins from *Pseudomonas syringae*. *Cell*, *101*(4), 353–363.

Oh, C.-S., & Martin, G. B. (2011). Effector-triggered immunity mediated by the Pto kinase. *Trends Plant Sci*, *16*(3), 132–140.

Pedley, K. F., & Martin, G. B. (2003). Molecular basis of *Pto*-mediated resistance to bacterial speck disease in tomato. *Annu Rev Phytopathol*, *41*, 215–243.

Pierre, M., Traverso, J. A., Boisson, B., Domenichini, S., Bouchez, D., Giglione, C., & Meinnel, T. (2007). N-myristoylation regulates the SnRK1 pathway in *Arabidopsis*. *Plant Cell*, *19*(9), 2804–2821.

Podell, S., & Gribskov, M. (2004). Predicting N-terminal myristoylation sites in plant proteins. *BMC Genomics*, *5*(1), 37.

Qi, D., DeYoung, B. J., & Innes, R. W. (2012). Structure-function analysis of the coiled-coil and leucine-rich repeat domains of the RPS5 disease resistance protein. *Plant Physiol*, *158*(4), 1819–1832.

Qi, D., & Innes, R. W. (2013). Recent advances in plant NLR structure, function, localization, and signaling. *Front Immunol*, *4*, 348.

Qi, Q., Rajala, R. V., Anderson, W., Jiang, C., Rozwadowski, K., Selvaraj, G., Sharma, R., & Datla, R. (2000). Molecular cloning, genomic organization, and biochemical characterization of myristoyl-CoA:protein N-myristoyltransferase from *Arabidopsis thaliana*. *J Biol Chem*, *275*(13), 9673–9683.

Renna, L., Stefano, G., Majeran, W., Micalella, C., Meinnel, T., Giglione, C., & Brandizzi, F. (2013). Golgi traffic and integrity depend on N-myristoyltransferase 1 in *Arabidopsis*. *Plant Cell*, *25*(5), 1756–1773.

Resh, M. D. (1999). Fatty acylation of proteins: new insights into membrane targeting of myristoylated and palmitoylated proteins. *Biochim Biophys Acta*, *1451*(1), 1–16.

Robert-Seilaniantz, A., Shan, L., Zhou, J.-M., & Tang, X. (2006). The *Pseudomonas syringae* pv. *tomato* DC3000 type III effector HopF2 has a putative

myristoylation site required for its avirulence and virulence functions. *Mol Plant Microbe Interact*, *19*(2), 130–138.

Roth, A. F., Wan, J., Bailey, A. O., Sun, B., Kuchar, J. A., Green, W. N., Phinney, B. S., Yates, J. R., & Davis, N. G. (2006). Global analysis of protein palmitoylation in yeast. *Cell*, *125*(5), 1003–1013.

Scofield, S., Tobias, C., Rathjen, J., Chang, J., Lavelle, D., Michelmore, R., & Staskawicz, B. (1996). Molecular basis of gene-for-gene specificity in bacterial speck disease of tomato. *Science*, *274*(5295), 2063–2065.

Shahinian, S., & Silvius, J. R. (1995). Doubly-lipid-modified protein sequence motifs exhibit long-lived anchorage to lipid bilayer membranes. *Biochemistry*, *34*(11), 3813–3822.

Shan, L., He, P., Li, J., Heese, A., Peck, S. C., Nürnberger, T., Martin, G. B., & Sheen, J. (2008). Bacterial effectors target the common signaling partner BAK1 to disrupt multiple MAMP receptor-signaling complexes and impede plant immunity. *Cell Host Microbe*, *4*(1), 17–27.

Shan, L., Thara, V. K., Martin, G. B., Zhou, J. M., & Tang, X. (2000). The *Pseudomonas* AvrPto protein is differentially recognized by tomato and tobacco and is localized to the plant plasma membrane. *Plant Cell*, *12*(12), 2323–2338.

Smotrys, J. E., & Linder, M. E. (2004). Palmitoylation of intracellular signaling proteins: regulation and function. *Annu Rev Biochem*, *73*(1), 559–587.

Sorek, N., Bloch, D., & Yalovsky, S. (2009). Protein lipid modifications in signaling and subcellular targeting. *Curr Opin Plant Biol*, *12*(6), 714–720.

Sorek, N., Poraty, L., Sternberg, H., Bar, E., Lewinsohn, E., & Yalovsky, S. (2007). Activation status-coupled transient S acylation determines membrane partitioning of a plant Rho-related GTPase. *Mol Cell Biol*, *27*(6), 2144–2154.

Sorek, N., & Yalovsky, S. (2010). Analysis of protein S-acylation by gas chromatography-coupled mass spectrometry using purified proteins. *Nat Protoc*, *5*(5), 834–840.

Takemoto, D., & Jones, D. A. (2005). Membrane release and destabilization of *Arabidopsis* RIN4 following cleavage by *Pseudomonas syringae* AvrRpt2. *Mol Plant Microbe Interact*, *18*(12), 1258–1268.

Takemoto, D., Rafiqi, M., Hurley, U., Lawrence, G. J., Bernoux, M., Hardham, A. R., Ellis, J. G., Dodds, P. N., & Jones, D. A. (2012). N-terminal motifs in some plant disease resistance proteins function in membrane attachment and contribute to disease resistance. *Mol Plant Microbe Interact*, *25*(3), 379–392.

Tang, X., Frederick, R., Zhou, J., Halterman, D., Jia, Y., & Martin, G. B. (1996). Initiation of plant disease resistance by physical interaction of AvrPto and Pto kinase. *Science*, *274*(5295), 2060–2063.

Thinon, E., & Hang, H. C. (2015). Chemical reporters for exploring protein acylation. *Biochem Soc Trans*, *43*(2), 253–261.

Tobimatsu, Y., Van de Wouwer, D., Allen, E., Kumpf, R., Vanholme, B., Boerjan, W., & Ralph, J. (2014). A click chemistry strategy for visualization of plant cell wall lignification. *Chem Commun*, *50*(82), 12262–12265.

Traverso, J. A., Meinnel, T., & Giglione, C. (2008). Expanded impact of protein N-myristoylation in plants. *Plant Signal Behav*, *3*(7), 501–502.

van der Hoorn, R. A. L., & Kamoun, S. (2008). From guard to decoy: a new model for perception of plant pathogen effectors. *Plant Cell*, *20*(8), 2009–2017.

Wessel, D., & Flügge, U. I. (1984). A method for the quantitative recovery of protein in dilute solution in the presence of detergents and lipids. *Anal Biochem*, *138*(1), 141–143.

Wright, M. H., Heal, W. P., Mann, D. J., & Tate, E. W. (2010). Protein myristoylation in health and disease. *J Chem Biol*, *3*(1), 19–35.

Wu, F.-H., Shen, S.-C., Lee, L.-Y., Lee, S.-H., Chan, M.-T., & Lin, C.-S. (2009). Tape-*Arabidopsis* sandwich - a simpler *Arabidopsis* protoplast isolation method. *Plant Methods*, *5*(1), 16–10.

Xiang, T., Zong, N., Zou, Y., Wu, Y., Zhang, J., Xing, W., Li, Y., Tang, X., Zhu, L., Chai, J., & Zhou, J.-M. (2008). *Pseudomonas syringae* effector AvrPto blocks innate immunity by targeting receptor kinases. *Curr Biol*, *18*(1), 74–80.

Yap, M. C., Kostiuk, M. A., Martin, D. D. O., Perinpanayagam, M. A., Hak, P. G., Siddam, A., Majjigapu, J. R., Rajaiah, G., Keller, B. O., Prescher, J. A., Wu, P., Bertozzi, C. R., Falck, J. R., & Berthiaume, L. G. (2010). Rapid and

selective detection of fatty acylated proteins using ω-alkynyl-fatty acids and click chemistry. *J Lipid Res*, *51*(6), 1566–1580.

Yoo, S.-D., Cho, Y.-H., & Sheen, J. (2007). *Arabidopsis* mesophyll protoplasts: a versatile cell system for transient gene expression analysis. *Nat Protoc*, *2*(7), 1565–1572.

Yount, J. S., Zhang, M. M., & Hang, H. C. (2011). Visualization and identification of fatty acylated proteins using chemical reporters. *Curr Protoc Chem Biol*, *3*(2), 65–79.

Zhou, B., An, M., Freeman, M. R., & Yang, W. (2014a). Technologies and challenges in poteomic analysis of protein S-acylation. *J Proteomics Bioinform*, *7*(9), 256–263.

Zhou, J., Wu, S., Chen, X., Liu, C., Sheen, J., Shan, L., & He, P. (2014b). The *Pseudomonas syringae* effector HopF2 suppresses *Arabidopsis* immunity by targeting BAK1. *Plant J*, *77*(2), 235–245.

Zipfel, C. (2014). Plant pattern-recognition receptors. *Trends Immunol*, *35*(7), 345–351.

CHAPTER 5

WHERE TO GO FROM HERE?

5.1 Future directions

We have shown that the tomato Pti1 kinases mediate flagellin-induced production of reactive oxygen species (ROS) and contribute to pattern-triggered immunity (PTI) against the bacterial speck pathogen *Pseudomonas syringae* pv. *tomato* (*Pst*). However, our current results do not shed light on the molecular mechanism by which the Pti1 proteins function. Given that the two proteins contain predicted S-acylation sites and localize to the cell periphery, we speculate that they might be part of the FLS2/BAK1 receptor complex or associate with the NADPH oxidases RBOHB responsible for the ROS burst in tobacco and, presumably, tomato (Yoshioka et al., 2003; Segonzac et al., 2011). Preliminary data indicate that the Pti1 proteins do not associate with the FLS2 complex in the plant cell environment either before or after flagellin treatment, however, these findings need to be substantiated. We have not tested if the Pti1 proteins interact with and possibly phosphorylate RBOHB, which would immediately suggest a mechanism for their function. If such phosphorylation is observed, it would be interesting to map the phosphorylation sites and compare them with the residues of RBOHD known to be phosphorylated by BIK1 and calcium-dependent protein kinases in Arabidopsis (Boudsocq et al., 2010; Dubiella et al., 2013; Kadota et al., 2014).

While ROS production is diminished in tomato hairpin-Pti1 (hpPti1) plants with reduced *Pti1* expression, mitogen-activated protein kinase (MAPK) phosphorylation, another early defense readout, is not affected. It is known that influx of calcium into the plant cell is a prerequisite for both ROS production and MAPK phosphorylation (Segonzac et al., 2011), therefore we do not expect Ca^{2+} influx to

be affected in these plants. Nevertheless, establishing whether or not our transgenic hpPti1 plants have normal Ca^{2+} influx would help to confirm the functional placement of Pti1 in the hierarchy of PTI responses.

It is possible that the Pti1 proteins are involved in other signaling pathways in addition to those induced by flagellin perception. We did not explore this possibility due to the limited number of PTI inducers that reliably trigger ROS production in tomato, although peptides derived from bacterial cold shock protein can induce the oxidative burst and should be tested in the future (Felix & Boller, 2003; Hann & Rathjen, 2007). Maybe more interestingly, we observed increased susceptibility of hpPti1 plants to accidental powdery mildew infection compared to wild-type plants. We have not experimentally tested for enhanced powdery mildew disease development, but we made this observation on two distinct occasions. This would suggest that Pti1 serves a broader role in promoting PTI responses and is not limited to flagellin-mediated resistance, although with respect to *Pst* infection that would likely be its main contribution (Chakravarthy et al., 2010; Rosli et al., 2013). In addition to powdery mildew, the hpPti1 plants could be tested for enhanced susceptibility to infection with *Xanthomonas campestris* pv. *vesicatoria* which causes bacterial spot disease and *Phytophthora infestans*, the causal agent of late blight, two economically important tomato pathogens.

Of course, the hpPti1 plants we developed are not useful in the field as they are more susceptible to *Pst* and possibly other pathogens. However, transgenic plants overexpressing one or both of the *Pti1* genes might have improved resistance if they generate increased ROS production upon pathogen detection. Another possibility would be to mutationally enhance the activities of the Pti1 kinases which would eliminate the need for overexpression. In Arabidopsis, the plasma membrane-localized receptor-like cytoplasmic kinase (RLCK) MRI was found to act down-

stream of FER, a receptor-like kinase (RLK) of the *Catharanthus roseus* RLK1-like family (Boisson-Dernier et al., 2015). A single amino acid substitution (R240C) in the core catalytic domain of MRI enhanced its ability to activate downstream responses, possibly by enhancing kinase activity. MRI belongs to the same group of RLCKs as tomato Pti1 and the corresponding R234C mutation might enhance its activity (Boisson-Dernier et al., 2015). However, enhanced resistance can come at a cost and in order to maximize their reproductive success plants have to carefully tune their defense responses. In agricultural settings, immune systems that are hypersensitive can lead to reduced plant growth and negatively impact yield.

If Pti1 is an important immune regulator it might be targeted by pathogen effectors, which are important virulence determinants that promote pathogen fitness. We tested more than 20 *Pst* effectors for interaction with the two Pti1 proteins in a yeast two-hybrid system but found no valid interactors (In-Sun Hwang and Gregory Martin, unpublished data). However, it is possible that effector proteins from other pathogens might target the Pti1 proteins to suppress plant immune responses and thus promote disease development. If interacting effectors from agronomically important tomato pathogens are found that contribute significantly to pathogenesis, one could attempt to engineer the Pti1 proteins so that they no longer interact with or are modified by those effectors but still fulfill their function in plant immunity in an attempt to promote disease resistance in the field. It was recently shown that COI1, a constituent of the jasmonate receptor complex that is targeted by the *Pst* toxin coronatine (Xin & He, 2013), can be modified such that it still binds jasmonate but the interaction with coronatine is greatly reduced, thus promoting disease resistance (Zhang et al., 2015).

We identified two RLKs, Mal1 and Mal2, with extracellular malectin-like domains that might function in monitoring cell wall integrity. The role of these

putative receptors in plant immunity should be further explored as they might constitute novel and important receptors contributing to defense against *Pst* and other pathogens. Towards this end, our laboratory is developing CRISPR/Cas9 lines with mutations in both *Mal1* and *Mal2* that are currently being evaluated. If a function in disease resistance is confirmed it would shed light on another piece of the complex plant immune system and might enable enhanced resistance in the field by transferring these receptors to plant species that might lack them or that recognize different types of cell wall damage. Moreover, the interaction between the Pti1 proteins and Mal1/2 should be further explored. If these interactions can be confirmed in the plant cell environment it would explain why Pti1 was originally identified as an interactor of Pto and tie the Pti1 proteins into a PTI signaling pathway.

5.2 Bibliography

Boisson-Dernier, A., Franck, C. M., Lituiev, D. S., & Grossniklaus, U. (2015). Receptor-like cytoplasmic kinase MARIS functions downstream of CrRLK1L-dependent signaling during tip growth. *Proc Natl Acad Sci*, *112*(39), 12211–12216.

Boudsocq, M., Willmann, M. R., McCormack, M., Lee, H., Shan, L., He, P., Bush, J., Cheng, S.-H., & Sheen, J. (2010). Differential innate immune signalling via Ca^{2+} sensor protein kinases. *Nature*, *464*(7287), 418–422.

Chakravarthy, S., Velásquez, A. C., Ekengren, S. K., Collmer, A., & Martin, G. B. (2010). Identification of *Nicotiana benthamiana* genes involved in pathogen-associated molecular pattern-triggered immunity. *Mol Plant Microbe Interact*, *23*(6), 715–726.

Dubiella, U., Seybold, H., Durian, G., Komander, E., Lassig, R., Witte, C.-P., Schulze, W. X., & Romeis, T. (2013). Calcium-dependent protein kinase/NADPH oxidase activation circuit is required for rapid defense signal propagation. *Proc Natl Acad Sci*, *110*(21), 8744–8749.

Felix, G., & Boller, T. (2003). Molecular sensing of bacteria in plants. The highly conserved RNA-binding motif RNP-1 of bacterial cold shock proteins is recognized as an elicitor signal in tobacco. *J Biol Chem*, *278*(8), 6201–6208.

Hann, D. R., & Rathjen, J. P. (2007). Early events in the pathogenicity of *Pseudomonas syringae* on *Nicotiana benthamiana*. *Plant J*, *49*(4), 607–618.

Kadota, Y., Sklenar, J., Derbyshire, P., Stransfeld, L., Asai, S., Ntoukakis, V., Jones, J. D., Shirasu, K., Menke, F., Jones, A., & Zipfel, C. (2014). Direct regulation of the NADPH oxidase RBOHD by the PRR-associated kinase BIK1 during plant immunity. *Mol Cell*, *54*(1), 1–13.

Rosli, H. G., Zheng, Y., Pombo, M. A., Zhong, S., Bombarely, A., Fei, Z., Collmer, A., & Martin, G. B. (2013). Transcriptomics-based screen for genes induced by flagellin and repressed by pathogen effectors identifies a cell wall-associated kinase involved in plant immunity. *Genome Biol*, *14*(12), R139.

Segonzac, C., Feike, D., Gimenez-Ibanez, S., Hann, D. R., Zipfel, C., & Rathjen, J. P. (2011). Hierarchy and roles of pathogen-associated molecular pattern-induced responses in *Nicotiana benthamiana*. *Plant Physiol*, *156*(2), 687–699.

Xin, X.-F., & He, S. Y. (2013). *Pseudomonas syringae* pv. *tomato* DC3000: a model pathogen for probing disease susceptibility and hormone signaling in plants. *Annu Rev Phytopathol*, *51*, 473–498.

Yoshioka, H., Numata, N., Nakajima, K., Katou, S., Kawakita, K., Rowland, O., Jones, J. D. G., & Doke, N. (2003). *Nicotiana benthamiana* gp91^{phox} homologs *NbrbohA* and *NbrbohB* participate in H_2O_2 accumulation and resistance to *Phytophthora infestans*. *Plant Cell*, *15*(3), 706–718.

Zhang, L., Yao, J., Withers, J., Xin, X.-F., Banerjee, R., Fariduddin, Q., Nakamura, Y., Nomura, K., Howe, G. A., Boland, W., Yan, H., & He, S. Y. (2015). Host target modification as a strategy to counter pathogen hijacking of the jasmonate hormone receptor. *Proc Natl Acad Sci*, *112*(46), 14354–14359.